RECENT AND MIOCENE CARBONATE SEDIMENTS FROM INDONESIA

(IN TWO VOLUMES)

BY

PENELOPE JANE LOOPUYT-TURNER

Submitted for the degree of
Doctor of Philosophy
to
Aston University
Department of Geological Sciences

March 1986

VOLUME II

LIST OF PLATES

1. Physiographical zonation of a typical reef.

2. Islands selected for detailed study.

3. Variation in reef anatomy.

4. Features of cay marginal zones.

5. Sediment structures in the intertidal zone.

6. Features of mangrove mudflats and early colonisers of the cay.

7. Characteristics of coral growth and supratidal-intertidal zones.

8. Sand flat and algal zones.

9. Biota of algal zone and outer colonised moat.

10. Outer reef flat biota.

11. Lagoons and ramparts.

12. Characteristics and constituents of the shingle rampart.

13. Reef margin sediments and Callianassa.

14. Shallow reef crest and slope communities.

15. Reef crest.

16. Reef slope biota.

17. Deep forereef environments.

18. Bored grains examined by SEM.

19. Borings and encrustations on Recent grains.

20. Microborings & encrustations.

21. Reefrock.

22. Reefrock.

23. Reefrock.

24. Microfauna from Recent unconsolidated reef flat samples.

25. Characteristics of northern and southern reefs in the Pulau Seribu.

26. Reef types illustrating hypothesised evolution of the Pulau Seribu.

27. Textures of the coral intraclastic floatstone-rudstone facies.

28. Textures of the coral intraclastic floatstone-rudstone facies.

29. Textures of the coral intraclastic floatstone-rudstone facies.

30. Textures of the foraminiferal-skeletal packstone-wackestone facies.

31. Textures of the algally bound floatstone facies.

32. Textures of the impure sandy grainstone facies.

33. Textures of the sparsely fossiliferous wackestone-lime mudstone facies.

34. Textures of the foraminiferal floatstone-rudstone facies and mottled floatstones.

35. Microtextures from the Batu Raja limestones.

36. Microtextures from the Batu Raja limestones.

37. Microtextures from the Rajamandala limestones.

38. Outcrops of the Rajamandala limestone.

39. Microtextures from the Sengkang Basin limestones.

40. Microtextures from the Sengkang Basin limestones.

41. Outcrops of the Parigi limestone and mounds in the Sengkang Basin.

42. Microtextures from the Parigi limestones.

43. Textures associated with micritisation.

44. Bladed and granular cements.

45. Neomorphosed early cements.

46. Fibrous cements.

47. Preferential dolomitistion of the matrix.

48. Textures of matrix micrite.

49. Porous and non-porous dolomitised intervals.

50. Dolomite textures under SEM.

51. Dolomite textures under SEM.

52. Authigenic clays in dolomitised intervals, under SEM.

53. Luminescent characteristics of dolomite crystals.

54. Dolomite lining and replacing allochems.

55. Dolomitisation of allochems.

56. Dolomite pseudomorphing selenite, and replacement of sparry calcite.

57. The occurrence and distribution of ferroan and nonferroan calcite.

58. The occurrence and distribution of ferroan and nonferroan calcite.

59. Mouldic solution porosity.

60. Neomorphic textures in allochems.

61. Selective dissolution textures.

62. Solution-infilling and micrite neomorphism.

63. Pore types and compactional textures visible in core slabs.

64. Cathodoluminescence characteristics of micrite and neomorphic spar.

65. Intraskeletal porosity and matrix textures under SEM.

66. Inter- and intraskeletal pore-filling calcite cement and syntaxial rims.

67. Cathodoluminescence characteristics of syntaxial rims.

68. SEM textures of calcite cement and microspar.

69. Calcite occluding primary and secondary porosity.

70. Sparry calcite under SEM.

71. Cathodoluminescence characteristics of sparry calcite cement and neomorphic spar.

72. Calcite cement textures and silicification.

73. Silicification textures.

74. Textures associated with pyrite growth.

75. Compactional features.

76. Fracturing & pressure solution

77 Diagenetic fabrics

LIST OF APPENDICES

			Page
1.		Sample Location Map; Pulau Seribu	77
2.	(a)	List of Miocene Wells and Core Samples	78
	(b)	Localities of Miocene Outcrop Samples.	80
3.		Key to Lithological Symbols used in the Carbonate Core Summary Charts.	83
4.		Carbonate Core Summary Charts.	85 - 91
		ZU-3	
		ZU-4	
		ZZZ-2	
		Duma-2	
		Duma-3	
		Duma-5	
		Duma-9	
		Duma-11	
		Nurbani-3	
		Nurbani-4	
		Nurbani-5	
		Nurbani-6	
		Nurbani-10	

Plate 1 - Physiological Zonation of a Typical Reef

Pulau Belanda looking North

Schematic representation of reef zones


cay asymmetrically developed on western side of reef flat.

i — intertidal sands

sand flat; coarse coral-Halimeda-mollusc debris

algal flat

outer colonised moat

well-developed wave-built rampart

prolific living coral on crest. Note relatively wide crest developed on eastern flank

reef wall

reef base gorgonian community

sand-rubble fall

ch — channel

The east-west axis of the cay is approximately 40 m.

PLATE 1

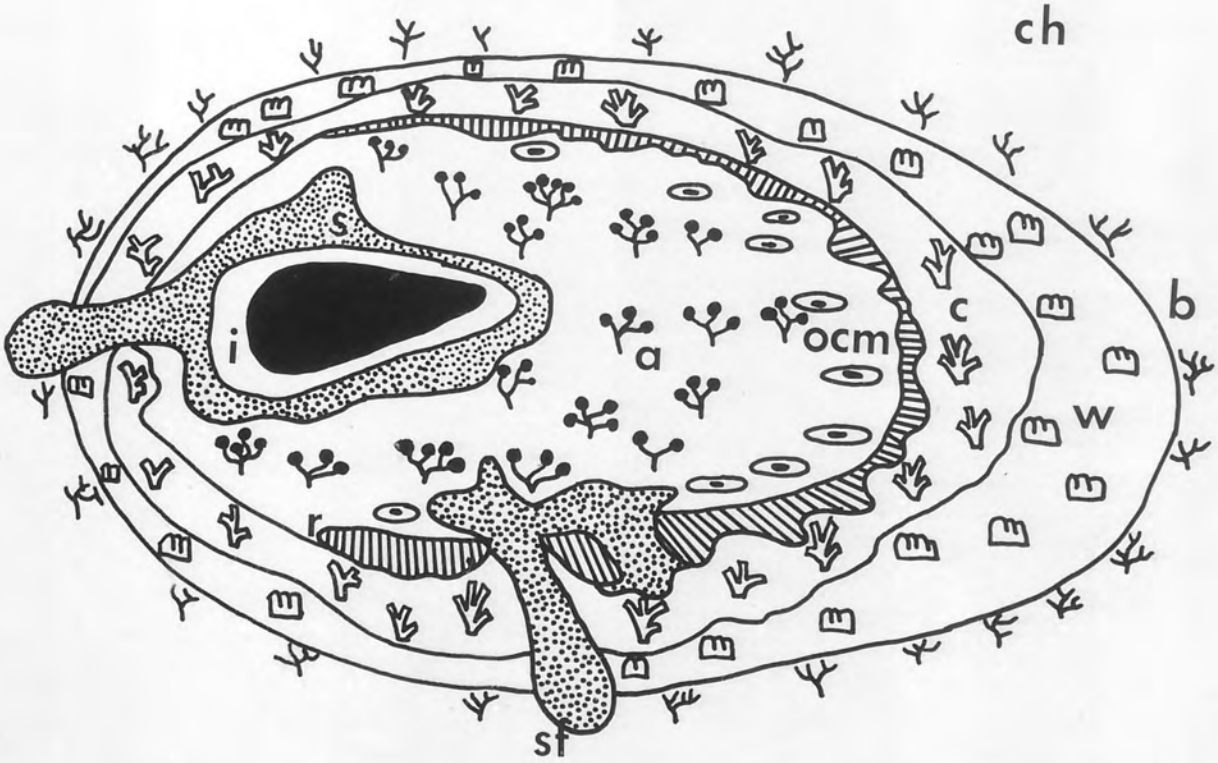

Plate 2 - Islands selected for detailed study

A. Pulau Pari complex; in the foreground is Pulau Tikus, large island in the background is Pari cay. Dark line bordering the reef on northern margin is a discontinuous shingle rampart. Photograph taken looking east.

B. Group of patch reefs in the extreme north of the Pulau Seribu. Pulau Ringit in far distance, Pulau Pabeasan in middle distance centre of photograph. Photograph taken looking north-east.

C. Pulau Petundang Kecil in foreground. Photograph taken looking north-west.

D. Foreground; the east-west elongated double reef of Pulau Kotok Kecil. Background; Pulau Kotok Besar. Photograph looking SSW, (Courtesy R. Cook, P.T. Bessindo).

PLATE 2

Plate 3 - Variation in reef anatomy

A. Islands in the northern part of the Pulau Seribu; note large size of cay relative to the reef as a whole. Pulau Kelor Barat in foreground, Pulau Kelor Timor in middle distance and Pulau Satu in far distance.

B. Pulau Madaum in the south of the Pulau Seribu. The cay is very small relative to the area represented by the reef flat. The reef edge is irregular, prograding outward in a series of lobes. Pale whitish-buff is unconsolidated sand; purplish-blue is live coral patch reef. Photograph taken looking WNW.

C. Gosong Pulau Bira: an embryonic sandbody-type cay which is flooded at high tide. Photograph taken looking north-east.

PLATE 3

Plate 4 - Features of cay marginal zones

A. A bank semi-stabilised by rhizomal vegetation borders the intertidal zone, south-east cay margin, Pulau Ringit.

B. Storm-constructed coral shingle berms create step-like features on intertidal zones, Pulau Bira Besar.

C. Burrowed lower intertidal zone on the south-western shore of Pulau Pari. The habitat is densely colonised and burrowed by cerithiids. A greenish-brown slimy algal film coats the sediment surface in the shallow flooded pools. Width of photograph approx 1·2m.

D. Tracks left by the starfish Marthasterias glacialis which inhabits the shallow intertidal margins. Pulau Pari, southern intertidal zone. Width of photograph approx 1·5m.

PLATE 4

Plate 5 - Sediment structures in the intertidal zone

A. Looking south from the south-west shore of Pari cay over the extensive intertidal zone on spring lows. Dark brown hummocks in middle distance are clumps of algae that can withstand periodic emergence.

B. A sand pit in the lower intertidal zone displaying a blue-grey anoxic zone. Marker pen is 18 cm. long. Pulua Pari, southern intertidal zone.

C. Flat-topped ripples in the intertidal zone at Pulau Pari.
Width of photograph 1·5m.

D. Rippled or decapitated burrows are a common feature of the lower intertidal zone. Isolated pools occur in between exposed patches within which water temperatures of upto 39°C have been recorded, Pulau Pari, southern intertidal zone.
Width of photograph 1·8m.

PLATE 5

Plate 6 - Features of mangrove mudflats and early colonisers of the cay

A. Prop roots of the mangrove Avicennia baffle fine sediment in the intertidal mudflat zone to the north-west of Pari cay.

B. Gas holes and a thin greenish algal scum on the surface of mud flats. Marker pen is 18 cm. long, Pulau Pari.

C. Rootletted, burrow-mottled, unsorted, muddy silty sands of the mangrove-colonised mudflat, Pulau Pari.

D. The first colonisers of the emergent cay are lateral creepers which bind the sediment. The nutrient layer is of negligible thickness and so rootlets do not penetrate deeply, Pulau Ringit.

PLATE 6

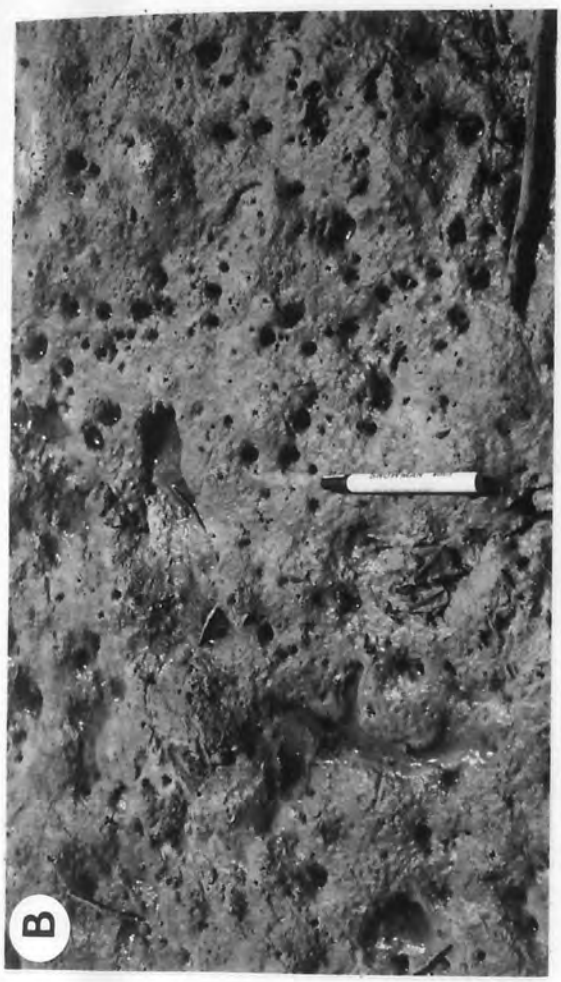

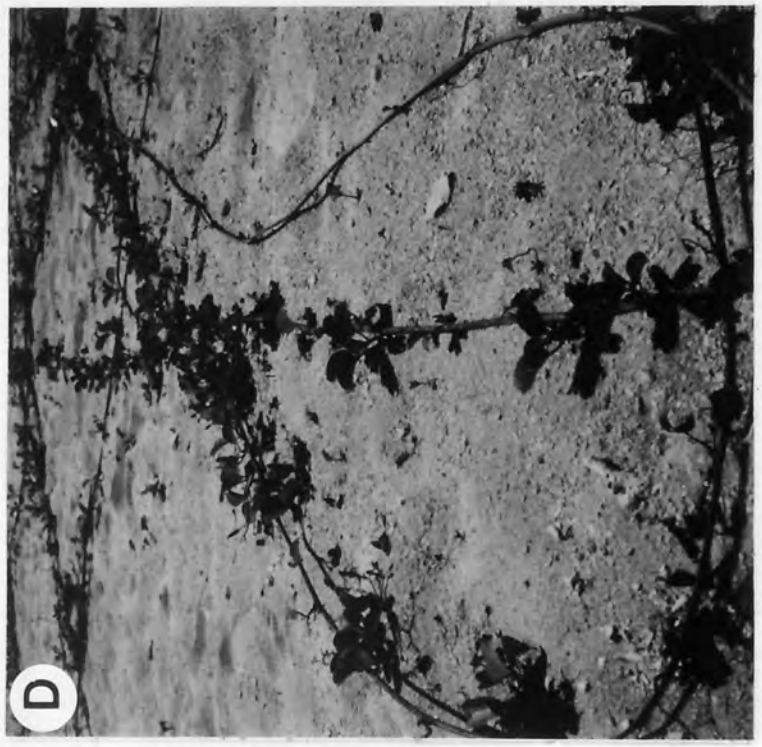

Plate 7 - Characteristics of coral growth and supratidal-intertidal zones

A. Coral growth on the reef flat occurs in a distinctive radial pattern.

pale whitish buff = unconsolidated sand
tongues of brown speckled with green = shingle bars colonised by Avicennia
radial streaks of purplish brown = live coral patch reefs
pale creamy brown border to the reef flat = periodically emergent shingle rampart.
speckled outer margin = reef slope

Pulau Petondang Kecil looking south.

B. Pulau Putri Besar. The cay is situated on the extreme northern margin of the reef flat. Photograph taken looking north-east.

C. Avicennia with pneumatophores prograding out across the southern intertidal mud-flat, Pulau Pari.

PLATE 7

Plate 8 - Sand flat and algal zones

A. Biota of the algal zone including Caulerpa (c), Thallassia (x) and Sargassum (s). Several sergeant major fishes. Pulau Pari.

B. The brown algae Turbinaria racemosa (t) and Padina (p) encrusting dead coral rubble. Biota that require hard substrates colonise such rubble. In this manner a small encrusted clump develops and new microatolls might be initiated. Pulau Pari.

C. Thallassia stabilises unconsolidated sediment on the sand flat. The black rope-like object on the right hand side of the photograph is the holothurian Holothuria atra. The mounds are constructed by Callianassa. Width of photograph 1·8m

D. A large faviid boulder coral on the high energy eastern reef flat at Pulau Petundang Kecil. Abundant coral rubble and small scattered Halimeda (h) fronds. Width of photograph 1·5m

PLATE 8

Plate 9 - Biota of the algal zone and outer colonised moat

A. An algal assemblage from the reef flat on Pulau Kotok Kecil includes Padina, Turbinaria and Caulerpha.
Width of photograph 1·2m

B. The outer colonised zone on the western margin of the reef flat on Pulau Kotok Kecil. Corals include Porites digitalis, Favia and Meandroidea. The rubble carpet is colonised and hence semi-stabilised by Caulerpha and Thallassia.
Width of photograph 1·6m

C. The outer colonised moat on the high energy reef flank at Pulau Belanda. The green alga Caulerpha is typical of high energy zones. Corals include Heliopora and Montastrea.
Width of photograph 1·2m

D. A microatoll on the southern outer reef flat of Pulau Pari. Living coral forms the margins of the colony but the top is dead and encrusted by Turbinaria. Width of photograph 1·6m.

PLATE 9

Plate 10 - Outer reef flat biota

A. Ledges of dead coral encrusted by new live colonies of Favia and Porites and the brown alga Padina, Pulau Pari.
Width of photograph 1m

B. Coral rock substrate. Embedded within it is a giant clam; Tridacna and a variety of algae and corals encrust it. The pale vermicular objects near to the clams are holothurian faecal strings composed of skeletal detritus. Pulau Pari.
Width of photograph 1m

C. Thallassia and Padina colonising the inter-ledge zone, Pulau Pari.
Width of photograph 80cm

D. A multi-layered sand rosette found in association with Callianassa mounds. The layers are composed of gummed sand. Gosong Cungka.
Diameter of coin 2¼ cm

E. Callianassa mounds on Gosong Cungka. The slopes of the mounds here are not so unstable as to prevent colonisation of the sands by such biota as Padina and Thallassia.
Width of photograph 80cm

F. Diadema setosum colonise unconsolidated sand flats, Pulau Kotok Kecil.
Width of photograph 50cm.

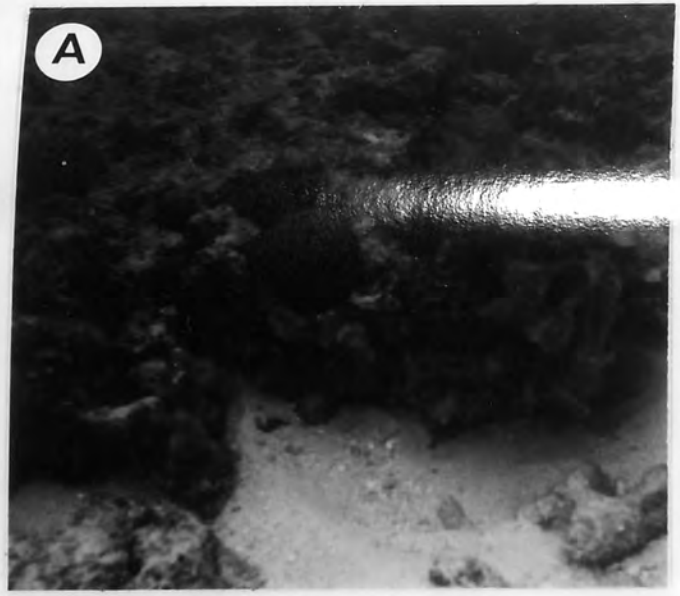

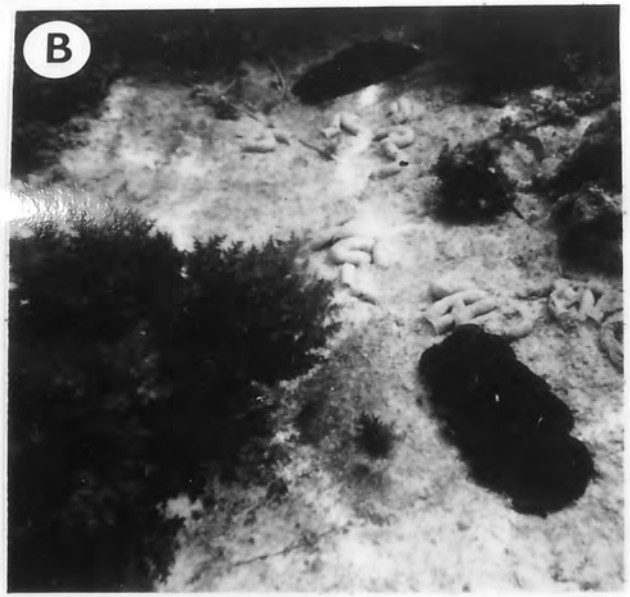

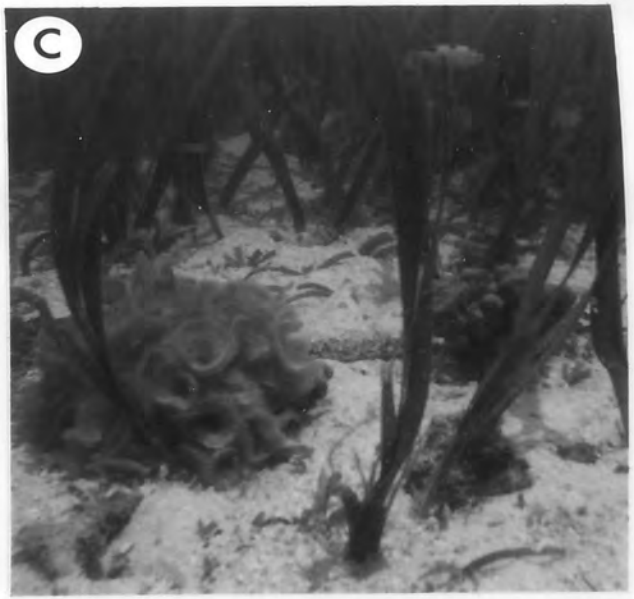

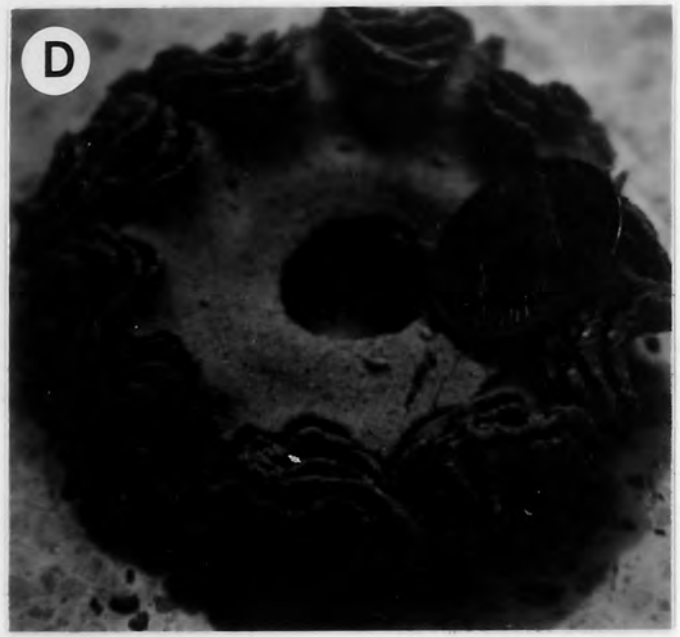

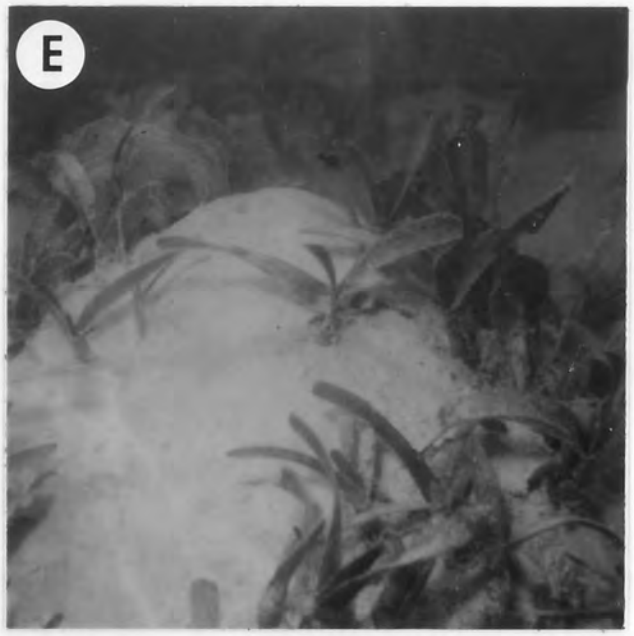

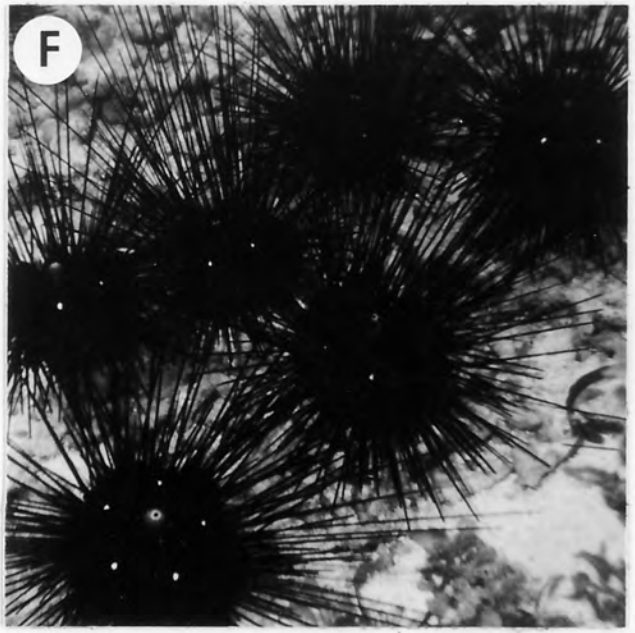

PLATE 10

Plate 11 - Lagoons and ramparts

A. Interlinked shallow lagoons on Gosong Cungka. Sediments from the reef flat and from lagoon margin patch reefs are rapidly filling these basins.

B. Reticulate pattern of patch reefs surrounding small shallow lagoons on Gosong Cungka. Photograph width 125m at base

C. Massive coral species lining sand flats on the outer reef flat. The sand patches may represent filled-in lagoons. Pulau Madaum.
Photograph width 75m

D. An emergent shingle rampart is present on the reef flat of Pulau Ayer well within an outer submergent rampart.
Photograph taken looking north.

E. Filled in lagoonal basins on Karang Bongko. The lagoon margin patch reefs have also been engulfed by sediment. In the background, live marginal patch reefs and shallow lagoonal basins are visible.
Photograph width 80m.

F. Photograph taken looking south-east and showing the east-west elongation of most patch reefs. Pulau Jukung is in the foreground right-hand side. The submerged island in the foreground is Gosong Kelor and the pale coloured plume is a sand fall.

PLATE 11

Plate 12 - Characteristics and constituents of the shingle rampart

A. The submerged wave surge part of the shingle rampart. The coral rubble is bound by the alga Caulerpa Pulau Petundang Kecil, depth 0.5m. Photograph width 1m.

B. The steep cayward slip face of the shingle rampart. Rubble is moved across the reef flat during periods of high storm activity. Pulau Pari outer reef flat.

C. Platy Acropora hyacinthus is easily dislodged from its slender base and thrown up by waves to form the rampart zone. Acropora sp. in background, Porites astreoides in foreground and branching Porites porites are also present. Pulau Pari, northern crest, 3 m. depth.

D. Close-up of the submerged cayward slipface of the rampart showing the main components; the table-like Acropora hyacinthus and branching Acropora sp. Pulau Pari, northern reef flat. Photograph width 1m.

PLATE 12

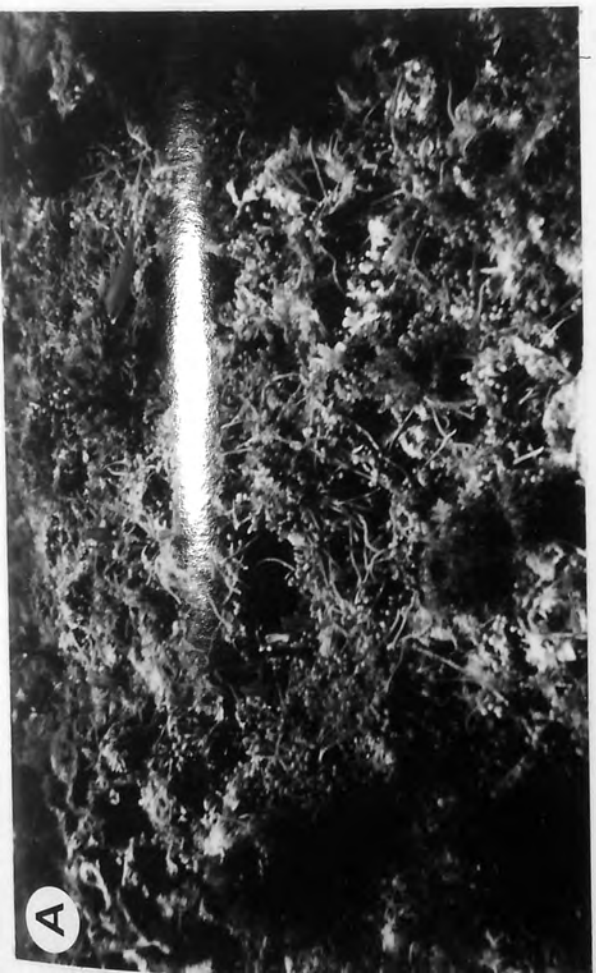

Plate 13 - Reef margin sediments and Callianassa

A. The emergent portion of the shingle rampart at Pulau Pari at low tide.

B. A burrowing stromatopod which preys on Callianassa

C. A sand and rubble fall on Pulau Ringit composed largely of coral branches and conspicuous white gravelly plates from the alga Halimeda. Padina colonises the margins of the debris patch. Depth, 8m.

D. Live and dead Halimeda; the live fronds are green and the dead ones, white. Dead Halimeda plates form a large proportion of the sediment of reef slope sand falls. The yellow organism is a sponge. Photograph is life size. Pulau Pari, eastern flank, depth 3m.

PLATE 13

Plate 14 - Shallow reef crest and slope communities

A. Porites lutea forms large butresses at a depth of approximately 4 m. This colony is bored by brightly coloured Sabellastarte indica, and encrusted by a large black sponge. The dead base of the colony forms a suitable substrate for the growth of new coral colonies. Pulau Kotok Kecil, 4m. depth.

B. A wave-exposed shallow reef top colonised almost exclusively by Halimeda. Pulau Petundang Besar, eastern crest, 1 m. depth.

C. Sabellastarte indica boring Porites lutea. Photograph width 1m.

D. A forereef slope environment dominated by Acropora. Note the cavernous irregular profile of the framework. Pulau Kotok Kecil, northern slope, 8m. depth. Photograph width 2m.

PLATE 14

Plate 15 - Reef Crest

A. A shallow crest community including Acropora species, leather coral and stinging hydroid. Upward growth is constrained by the level of low tide. Pulau Ringit, northern flank, depth 1m.

B. A platy colony of Acropora hyacinthus in shallow water where it is vulnerable to breakage and detachment during storms. Pulau Pari, northern flank, 1m. depth.

C. A narrow chute orientated at a high angle to the reef edge. Porites, leather coral and anemones are among the members of the biotic community. Pulau Pari, northern flank, 3 m. depth.

D. Agaricia and Acropora colonise the break in slope between the reef crest and reef wall environments. Pulau Petundang Kecil, northern flank, 4 m. depth.

PLATE 15

Plate 16 - Reef slope biota

A. White scrape marks from the rasping action of parrot fish. Pulau Kotok Kecil, western slope, 5 m. depth.

B. A variety of sponges feather stars and rhodolithic algae encrust dead coral. Pulau Ringit, eastern flank, 16 m. depth.

C. 'Bleached' Acropora sp. encrusted by algae. Pulau Petundang Kecil, southern slope, 11 m. depth.

D. Sea fans and seawhips, both of the order Gorgonacea, and soft coral in a sheltered reef slope environment. Pulau Kotok Kecil, southern flank, 12 m. depth.

PLATE 16

Plate 17 - Deep forereef environments

A. A slope community incuding sponges, leather coral, soft corals, feather stars and Acropora hyacinthus. Pulau Pari, eastern flank, 15 m. depth.

B. Octocorallines, sponges, feather stars and soft coral in a sheltered deep slope environment. Pulau Kotok Kecil, eastern flank, 20 m. depth.

C. Dead encrusted coral and numerous feather stars in a reef base environment. Pulau Ringit, southern slope, 21 m. depth.

D. Feather stars clinging to a tree-like antipatharian. Pulau Pari, eastern flank, 28 m. depth.

PLATE 17

Plate 18 - Bored grains examined by SEM

A. Small indeterminate borings with a circular cross-section mainly result from the activity of bivalves.
Sample PT 13, Magnification X350.

B. A high density of bores on the surface of a coral. Some bores are clogged with fine sand. Small entrances to bores open up into a network of enlarged cavities within the host fragment.
Sample PT 12, Magnification X100.

C. An organic filament penetrating into the coral by weakening and detaching chips of the substrate.
Sample 30, Magnification X350.

D. Sorted subround coral sand welded into a shallow cavity on the surface of a bored coral fragment.
Sample PT 13, Magnification X100.

E. Borings in a fractured mollusc.
Sample 30, Magnification X400.

F. Interconnected macro- and microborings partially filled with fine sediment.
Sample PT 13, Magnification X350.

PLATE 18

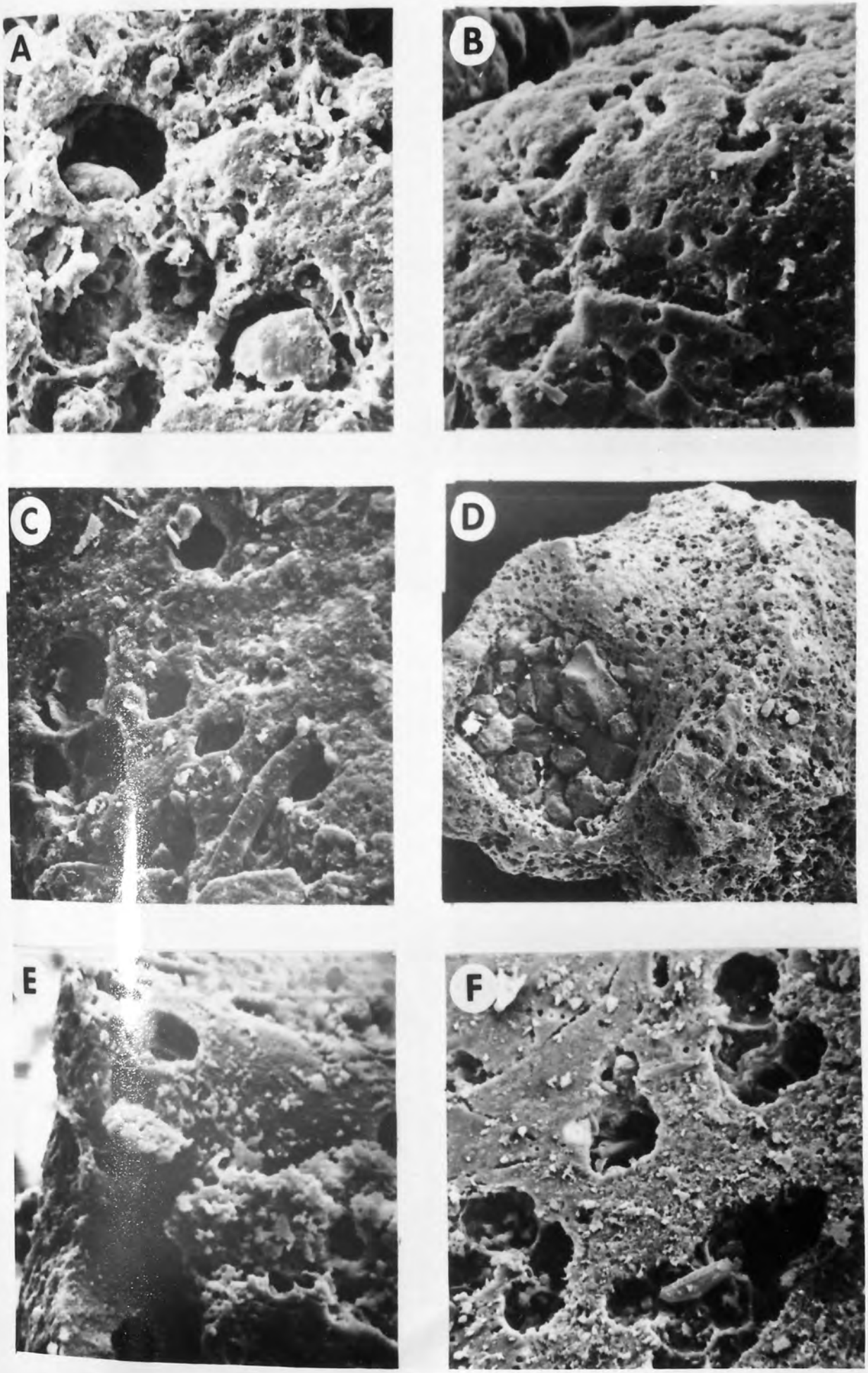

Plate 19 - Borings and encrustations on Recent grains

A. Coral surface is beyond the field of view in bottom right hand side of photograph. A sharply defined micritised layer is present beneath a less bored clearer outer layer of coral (in extreme lower right). An inner coral zone and the micritised layer have been penetrated by bulbous-shaped macrobores. The substance impregnating the macrobores is resin from thin-section preparation.
Sample K2, Magnification X42.

B. Large secondary cavities in coral. Note the scalloped margins to the bores. Dark coloured organic residue partly lines the bore cavities.
Sample K2, Magnification X42.

C. A high intensity of borings near to the encrusted coral surface diminishes inwards (upwards in the photograph). An increasingly uniform orientation of microboring is also apparent in this direction. The encrusting alga has the laminated structure and characteristic retilinear cell shape of Lithothamnion.
Sample K2, Magnification X42.

D. Multiple algal and serpulid encrustations on a coral. The serpulid displays the typical multi-laminated walls and the algal layers are dense and largely amorphous looking. Some encrustations have been secondarily bored.
Sample K2, Magnification X42.

E. Numerous round-ended parallel-sided microbores probably due to cyanophytes. Few bores bifurcate though the boring pattern exhibits no relation to the coral surface (not shown) or microarchitecture. Many of the fine bores are blocked by organic residue.
Sample P10, Magnification X167.

F. Cavities within a bored coral are filled with sand and mud. Fine sand has also adhered to the encrusting algae. Acids produced by such algae produce a corrosive microenvironment further weakening the coral surface.
Sample K21, Magnification X42.

PLATE 19

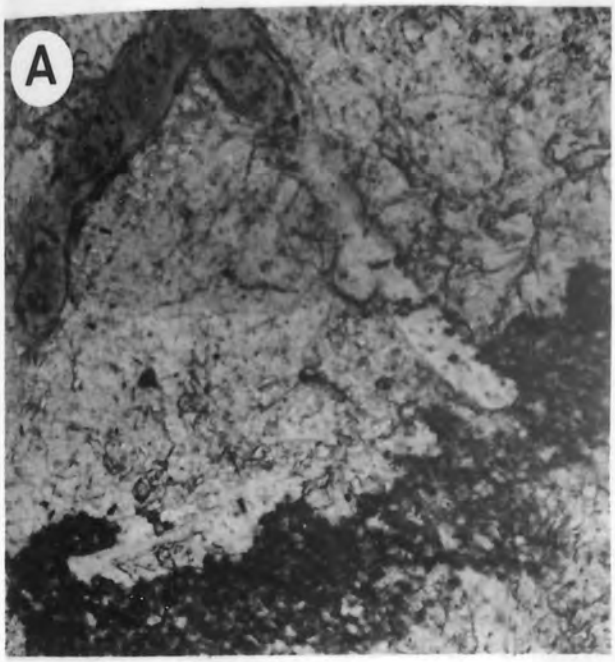

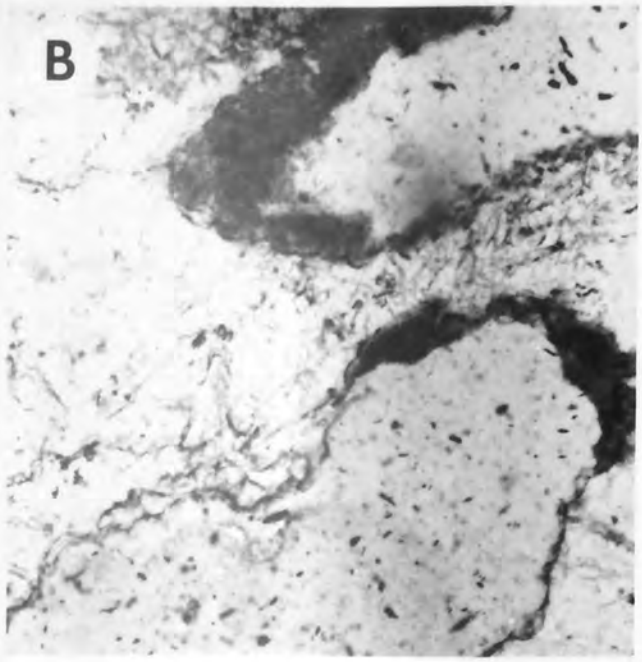

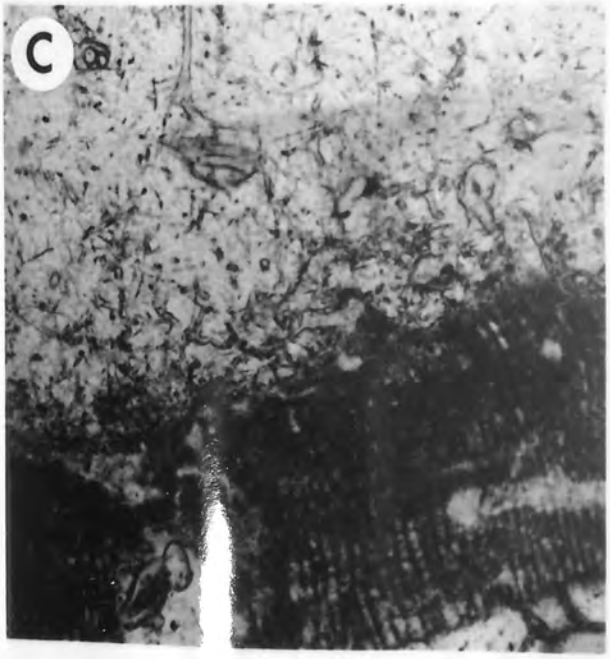

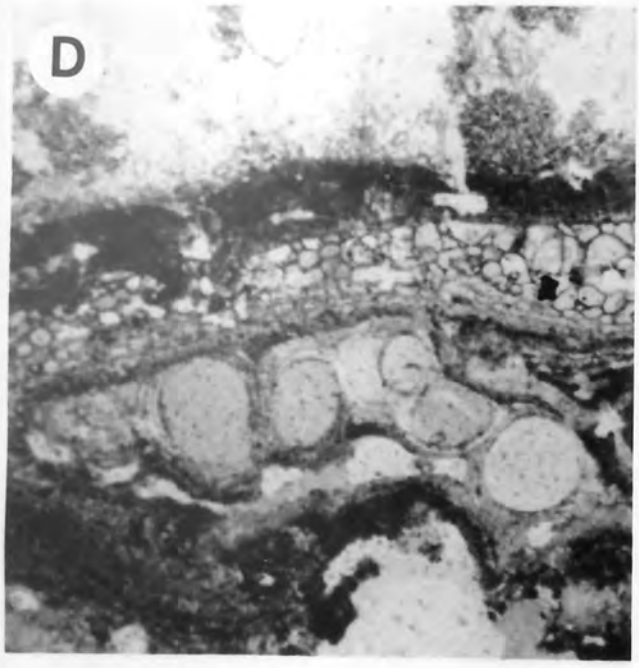

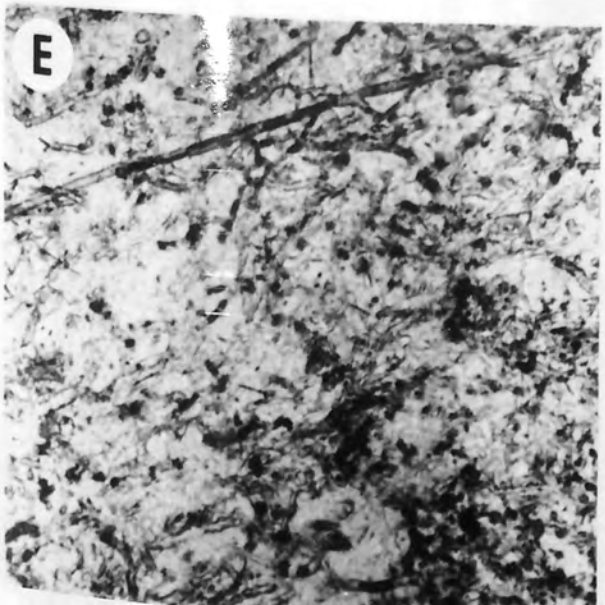

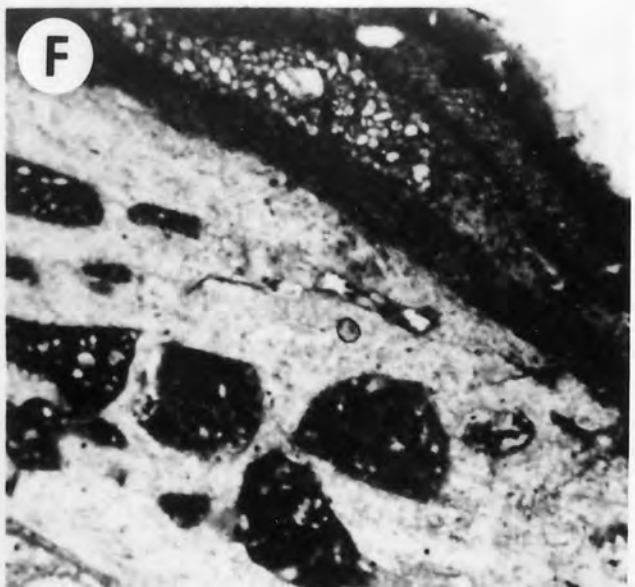

Plate 20 - Microborings, encrustations and needle cement examined under SEM

A. Radial stellate patterns of microborings on the surface of a coral.
Sample 8, Magnification X550.

B. Cross-sections and long-sections of microborings on the surface of a mollusc.
Sample 8, Magnification X550.

C. The porous cellular structure of Lithothamnian partly blocked with fine sediment or reproductive sporangia.
Magnification X800.

D. The surface of an encrusting alga clogged with fine pore-filling sediment.
Magnification X350.

E. Fine needle aragonite in a protected cavity.
Sample K3, Magnification X1500.

F. Tapering acicular aragonite crystals partly filling and obstructing a cavity and trpping fine sediment.
Sample K21, Magnification X2000.

PLATE 20

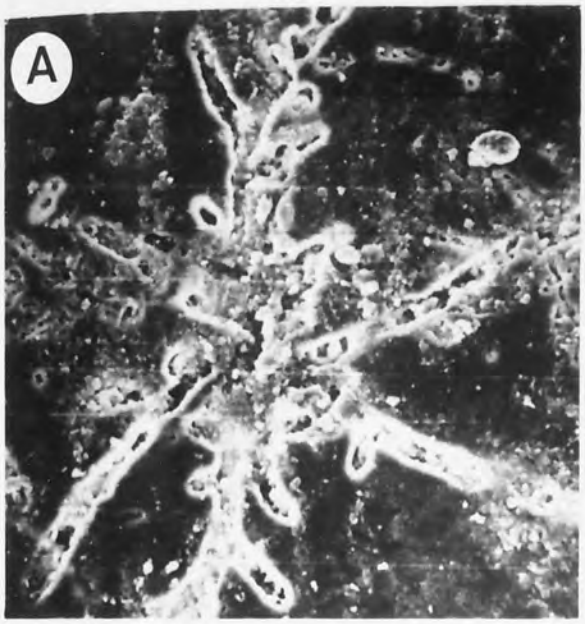

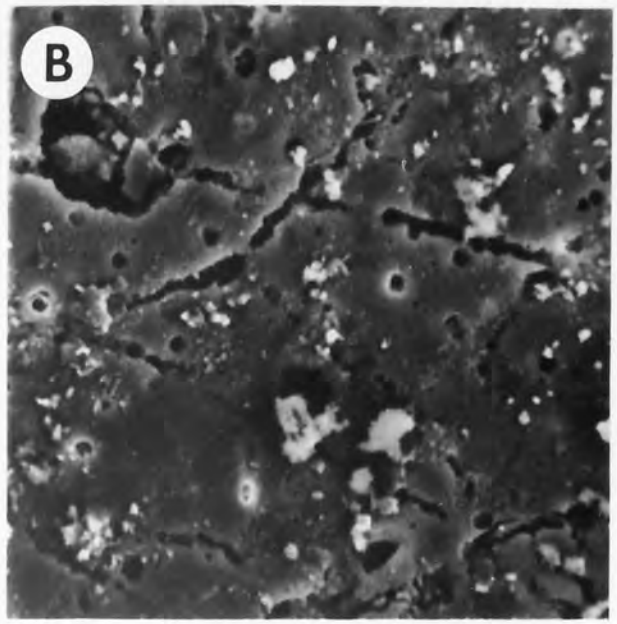

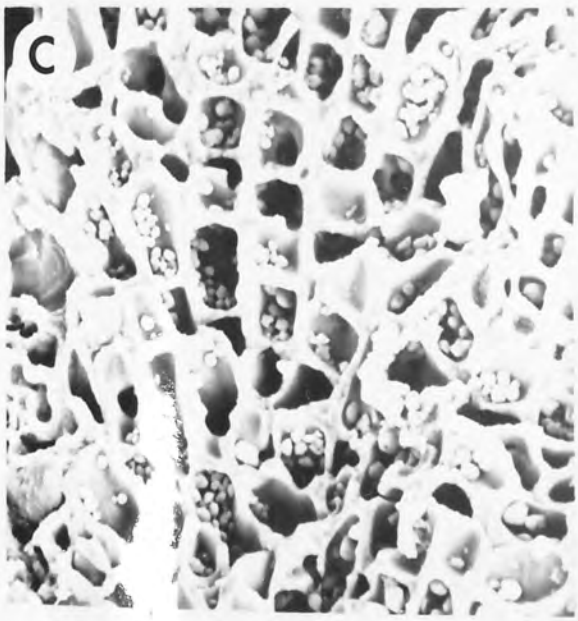

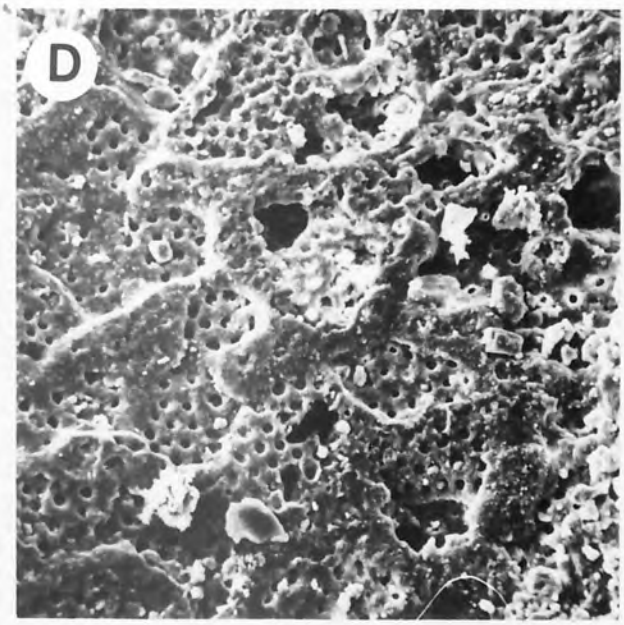

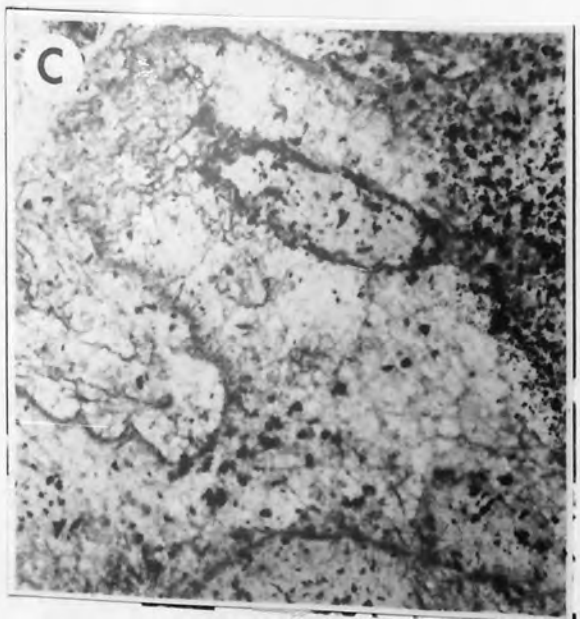

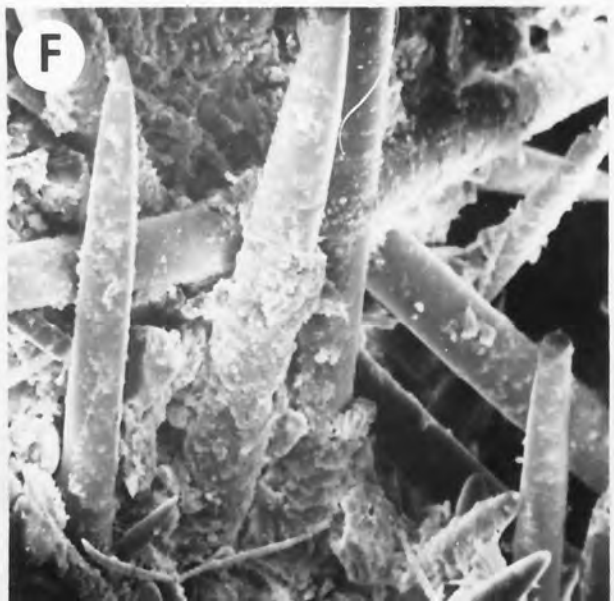

Plate 21

A. A ridge of reefrock rimming the shore at Pulau Pari.

B. Emergent reefrock in the intertidal zone. Pulau Kotok Kecil.


A


B

Plate 22

Intensive boring in a coral head embedded in the reefrock. Pulau Pari.
Width of photograph approximately 5cm.

Plate 23

Reefrock with floatstone texture, the main component of which is fragmented branched coral. Pulau Kǫtok Kecil.
Width of photograh approximately 10cm.

Plate 24 - Microfauna from Recent unconsolidated reef flat samples

A. Indeterminate gastropod.
Magnification X120.

B. Loxoconcha cf. gramanni.
Magnification X150.

C. Calcarina spengleri.
Magnification X120.

D. Cymbaloporetta squammosa.
Magnification X100.

E. ? Bryozoan fragment.
Magnification X75.

F. ? Cymbaloporetta squammosa.
Magnification X350.

G. Calcarina spengleri.
Magnification X200.

H. ? Operculinella venosa.
Magnification X150.

I. Indeterminate gastropod.
Magnification X100.

PLATE 24

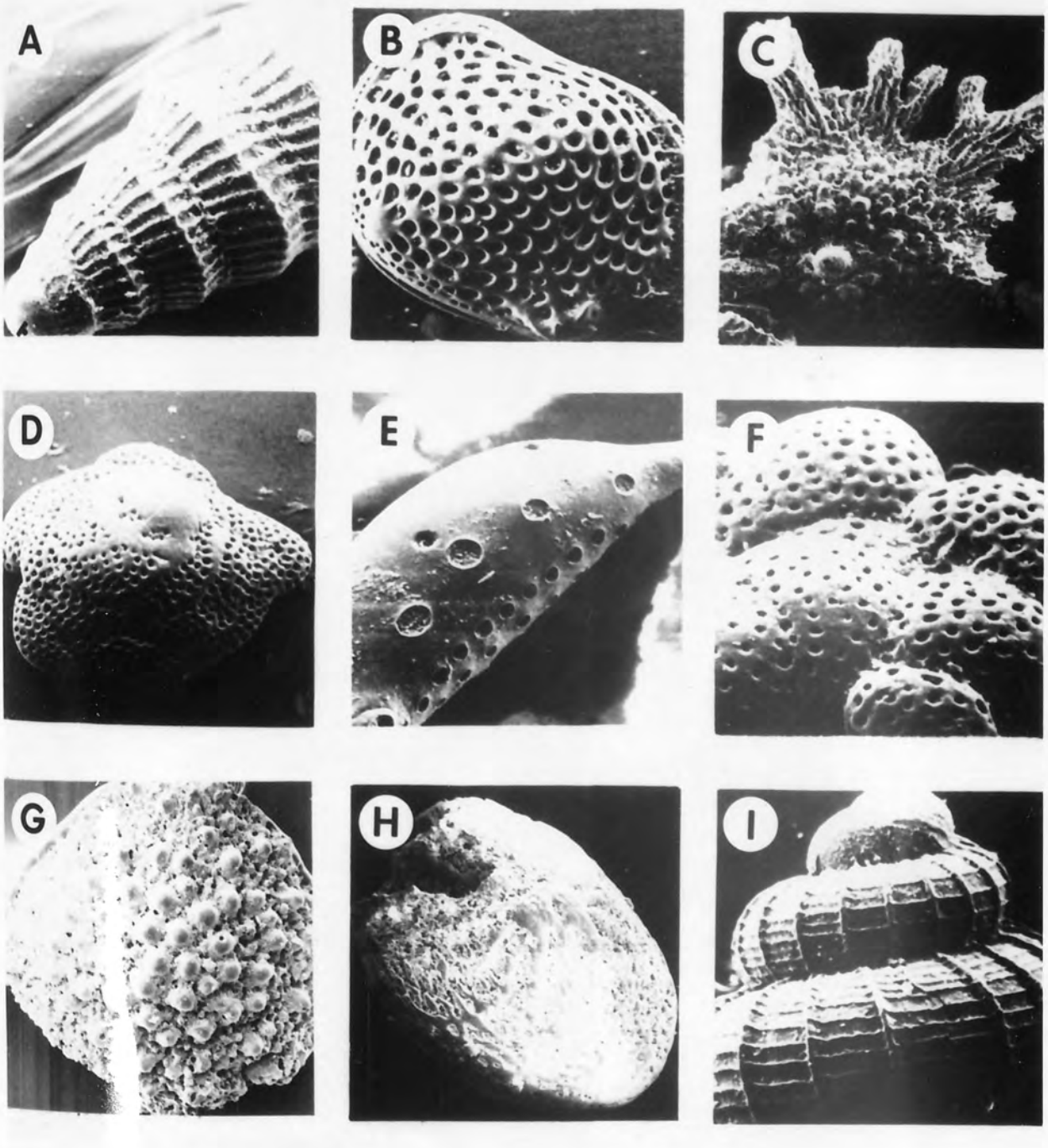

Plate 25 - Characteristics of northern and southern type reefs in the Pulau Seribu

A. In the northern part of the Pulau Seribu the size of the cay is large relative to the reef flat area, and islands are closely spaced. Left foreground; Pulau Melintang and Tangkin, middle distance; Pulau Putri Besar and Putri Kecil, far distance; Pulau Petundang Besar and Petundang Kecil. Photograph taken looking ESE.

B. An extensive reef flat and lagoon to the east of the cay. Pulau Ayer looking NW.

C. The large reef flat and lagoon of Gosong Cungka. The boundary between northern- and southern-type islands lies in the middle distance just to the north of this lagoonal-cay platform reef.

D. A type I reef; Gosong Bira.

PLATE 25

Plate 26 - Reef types illustrating hypothesised evolution of the Pulau Seribu

A. A deep lagoon on Pulau Simpit rimmed by a relatively narrow reef flat. Such a lagoon might result from enclosure of a shallow inter-reef channel through merging of adjacent reefs.

B. Pulau Putri Besar. On the extreme right hand side of the photograph the reef flat of Pulau Putri Kecil is visible. Continued growth might result in merging of these islands.

C. Pulau Pamagaran. The 'neck' in the cay might result from the merging of two islands. The narrow ribbon of sand extending across the reef flat suggests that the cay is continuing to grow. The submerged reef on the left of the photograph might soon weld onto this island. Photograph taken looking west.

PLATE 26

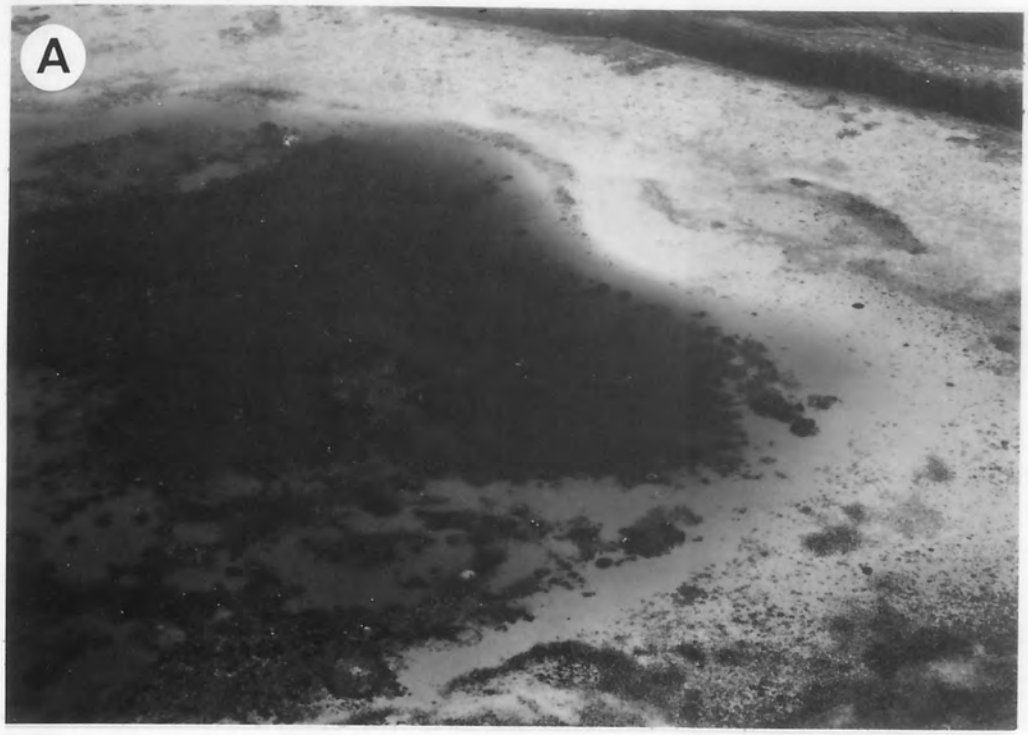

Plate 27 - Textures of the coral intraclastic floatstone rudstone facies

A. Nurbani 4 1677'. Coral rudstone texture with recrystallised Favites-type (top centre) and Lobophyllia-type (bottom right) corals in a packstone matrix. The corallites are oil stained.

B. Nurbani 4 1767' Coral floatstone. Oil stained detrital corals in an unsorted packstone matrix. Corals are alga-encrusted and unabraded molluscs are common.

C. Nurbani 4 1755'. Robust massive and branched detrital corals in a rhodolith-foraminiferal-mollusc rudstone matrix.

D. Nurbani 4 1770'. Leached and partly collapsed micritised foliose corals. The fabric is unstratified and orientation is haphazard. The appearance of the detrital coral results from aragonite leaching prior to matrix lithification with resultant collapse of the void.

E. Nurbani 4 1849'8. Detrital scleractinian coral filled with cream algal-rich mud.

PLATE 27

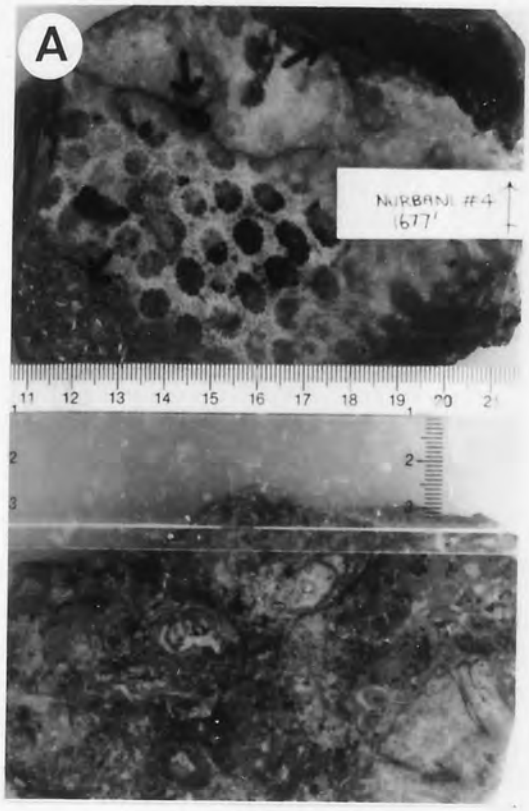
A
NURBANI #4
1677'


B
NURBANI #4
1767'

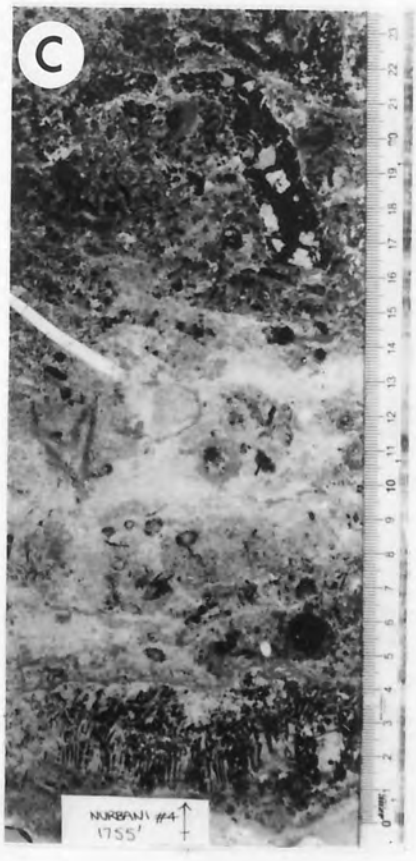
C
NURBANI #4
1755'

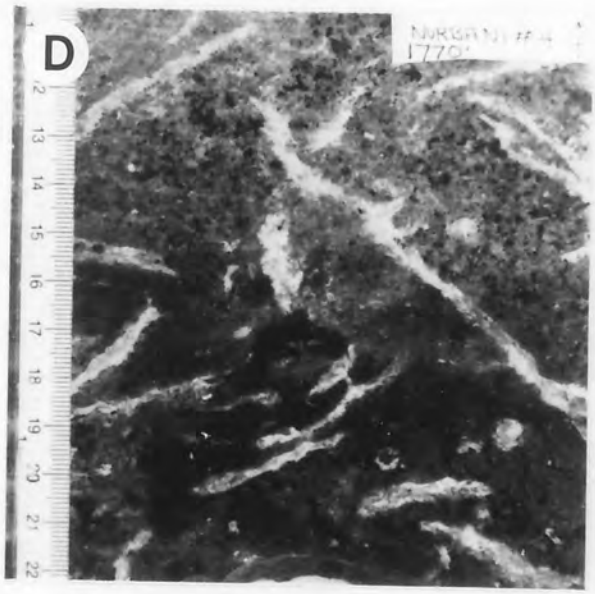
D
1770'

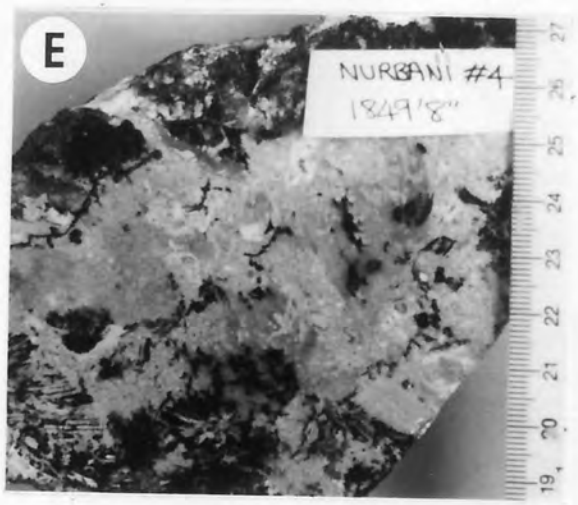
E
NURBANI #4
1849'8"

Plate 28 - Textures of the coral intraclastic floatstone-rudstone facies

A. Duma 11 2345'6. Mud-rich wispy-layered algal-encrusted coral floatstone. Wispy layering is a result of the partial solution of tabular corals and subsequent collapse of the void, as in Plate 27d.

B. Duma 5 2500'. Mouldic vugs from leached tabular corals from a connected pore network. The substrate displays irregular-undulose lamination and is rich in foraminifera.

C. Duma 5 2524'6. Numerous thin foliose corals interlayered with laminated algae in a mottled mudstone matrix.

D. Duma 5 2514'. Broken foliose corals in a muddy matrix.

E. Duma 5 2527'. Well sorted detrital coral rudstone. Fragments of branched coral are abraded and uniformly gravel sized. Leaching has resulted in high mouldic porosity.

PLATE 28


A
DUMA #11
2345'6"

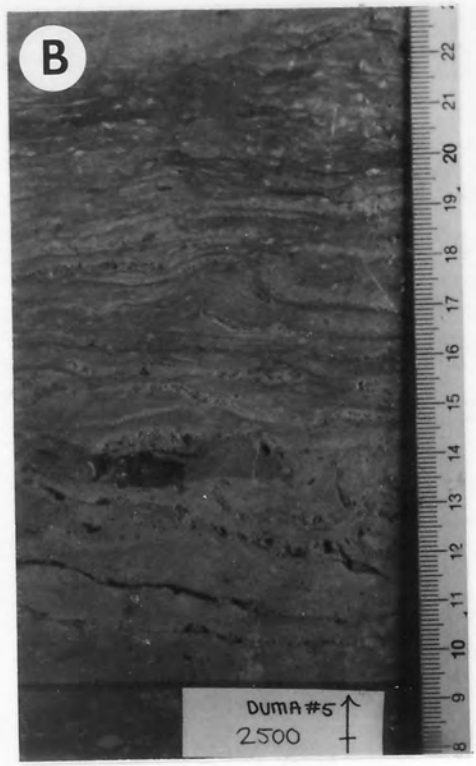
B
DUMA #5
2500

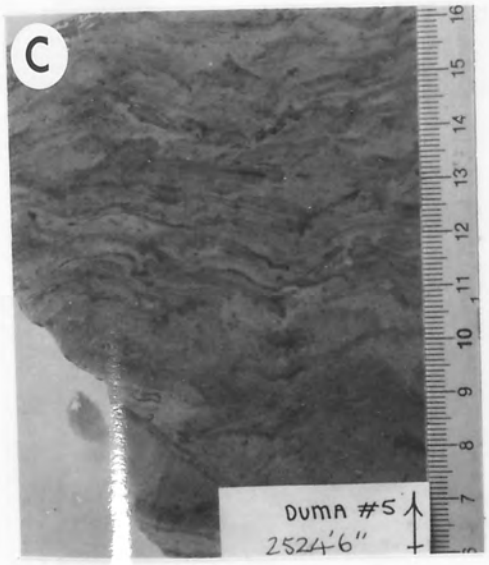
C
DUMA #5
2524'6"


D
DUMA #5
2514'


E
DUMA #5
2527'

Plate 29 - Textures of the coral intraclastic floatstone-rudstone facies

A. Duma 11 2335'. Sandy argillaceous matrix with irregularly shaped packstone intraclasts. Algal nodules are common. Intergranular porosity moderate.

B. Duma 11 2339'. Very porous rudstone with a leached matrix and abundant rounded rhodoliths.

C. Duma 11 2320'. Tight floatstone texture with common white nodular rhodoliths and abraded corals. The vertical solution channel at the top is filled with dark coloured leached impure grainstone.

D. Duma 11 2350'. Rhodolith-intraclast rudstone with a foraminiferal skeletal matrix. Bimodal sorting of allochems.

E. Duma 5 2457'. Mollusc-algal floatstone-rudstone. Unabraded gastropods, thin shelled disarticulated bivalves, recrystallised blue-grey mud intraclasts and irregular-ellipsoidal rhodoliths in a bioclastic packstone matrix.

F. Duma 11 2346'. Unsorted conglomeratic texture composed of well-rounded rhodoliths and irregular dark coloured packstone intraclasts.

G. Duma 11 2346'6. Conglomeratic intraclast-rhodolith rudstone. Several shallow oblique fractures occluded by coarse brown calcite.

PLATE 29

A
DUMA #11
2335'
B
DUMA #11
2339'
C
DUMA #11
2330'
D
DUMA #11
2350'
E
DUMA #5
2457'
F
DUMA #11
2346'
G
DUMA #11
2346'6"

Plate 30 - Textures of the foraminiferal skeletal packstone-wackestone facies

A. Duma 5 2494'6. Leached foraminiferal mollusc packstone. The matrix has been preferentially removed resulting in high secondary intergranular porosity.

B. Duma 5 2334'6. Slightly impure well-sorted packstone with shallow oblique leached zones.

C. Duma 5 2493'. Bioclastic packstone containing leached tabular corals and subhorizontally orientated larger foraminifera concentrated near to the base of the slab. The matrix also displays wispy lamination near to the base.

D. Duma 5 2401'6. A well-sorted speckled fine sand matrix with scattered cobbles of abraded coral and irregularly shaped intraclasts. Subhorizontal leached zone.

E. Duma 5 2455'. Burrow-mottled well-sorted packstone.

F. Duma 5 2409'6. Irregular blotchy oil stain may be related to bioturbation. Note the thin parallel tabular corals at the bottom right of photograph. Matrix is biomicritic.

G. Duma 11 2338'. Foraminiferal packstone with common rounded rhodoliths.

PLATE 30

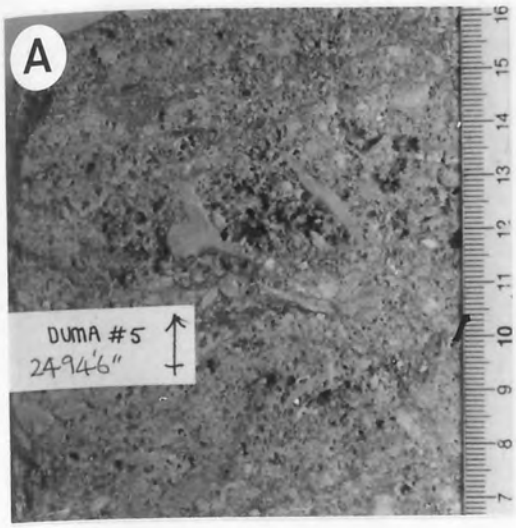
A
DUMA #5
2494'6"

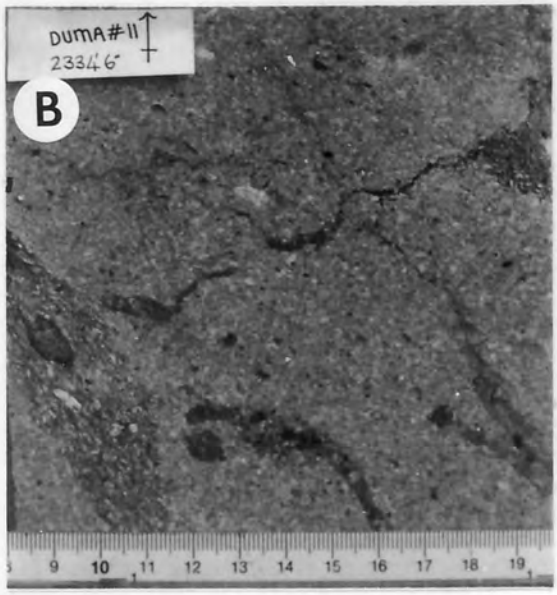
DUMA#11
2334'6"
B


C
DUMA #5
2493'

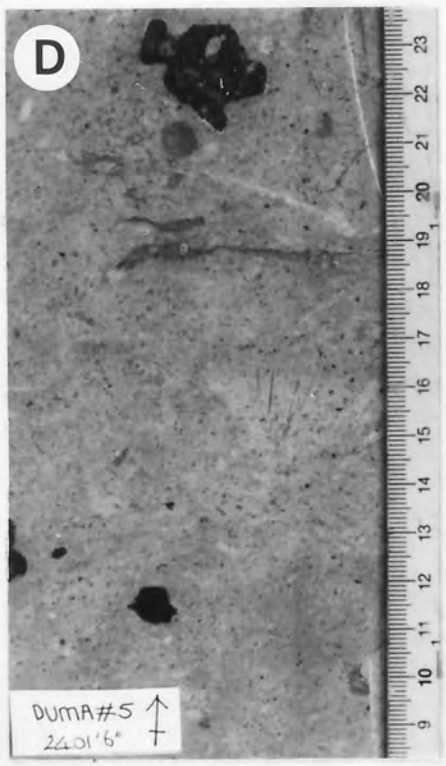
D
DUMA#5
2401'6"


E
DUMA#5
2455'

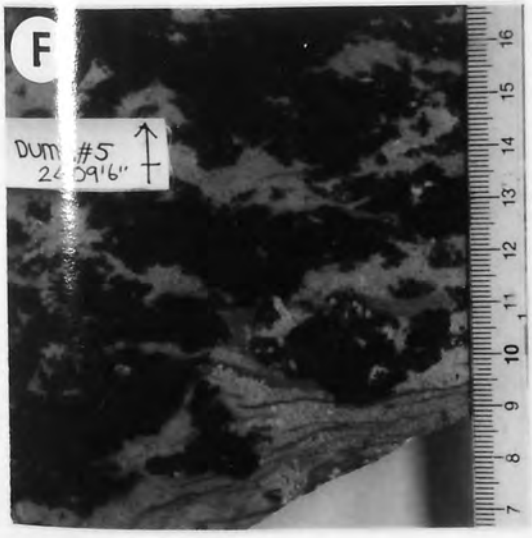
F
DUM #5
2 09'6"

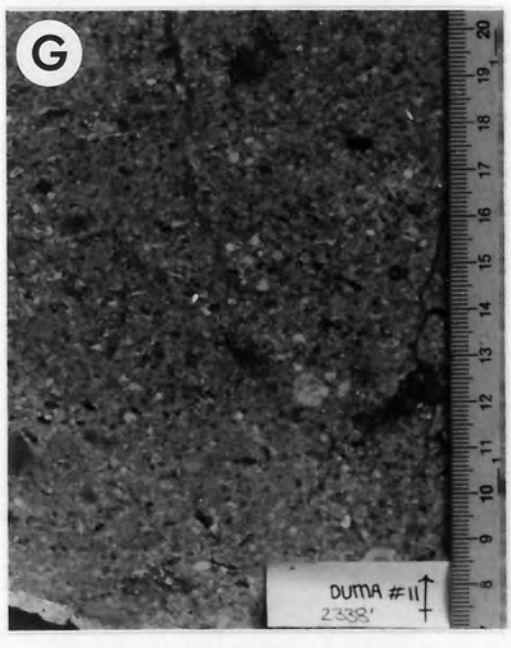
G
DUMA #11
2338'

Plate 31 - Textures of algal boundstones and algal-rich lithologies

A. Duma 5 2526'. Creamy-buff algal-layered lime mudstone. Laminae are contorted and subhorizontal.

B. Duma 5 2459'10. Irregular convolute layering of algal muds.

C. Duma 11 2362'. Unstratified coral-foraminiferal floatstone-packstone with blue-grey algal mottling near the base associated with a lens of foliose coral rudstone.

D. Duma 5 2464'. Conglomeratic mottling in an algal-foraminiferal mudstone. Recrystallisation of the matrix causes the mottles and generally initiates around an allochem. Streaky leached zone are visible between the mottles.

E. Nurbani 4 1826'6. Foraminiferal packstone matrix with abundant algal encrustations on grains. Matrix is highly leached. Rhodoliths and alga-encrusted coral fragments are common.

PLATE 31

A
DUMA #5
2526'
B
DUMA #5
2459'10"
C
DUMA #1
2362'
D
DUMA #5
2464'
E
NURBANI #4
1826'6"

Plate 32 - Textures of the impure sandy grainstone facies

A. Duma 11 2302'. Horizontally-stratified grainstone rich in pyrite, glauconite and impurities.

B. Duma 11 2309'. Unstratified homogeneous grainstone. Pale brown layer at top of photograph is fibrous calcite.

C. Duma 11 2306'. Common thin subparallel. Unfractured foliose corals define a subhorizontal layering. Fibrous calcite layer at the top of the photograph.

D. Duma 11 2307'4. Common almond-shaped mud lenticles, one of which is visible near the bottom of the core close to the calcite filled fracture. Sorting is poor and the streaky subhorizontal layering results from flattening of mud clasts and orientation of elongate fragments.

E. Duma 11 2314'6. Well-sorted horizontally-stratified grainstone. Layers are defined by concentrations of glauconite in the black speckled layers and concentrations of skeletal grains and micritic mud pellets in the pale layers.

PLATE 32

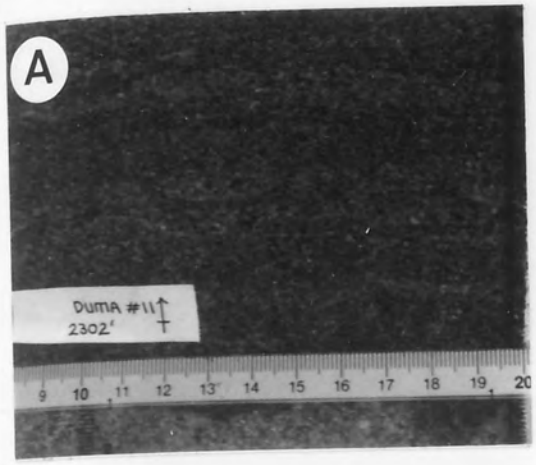

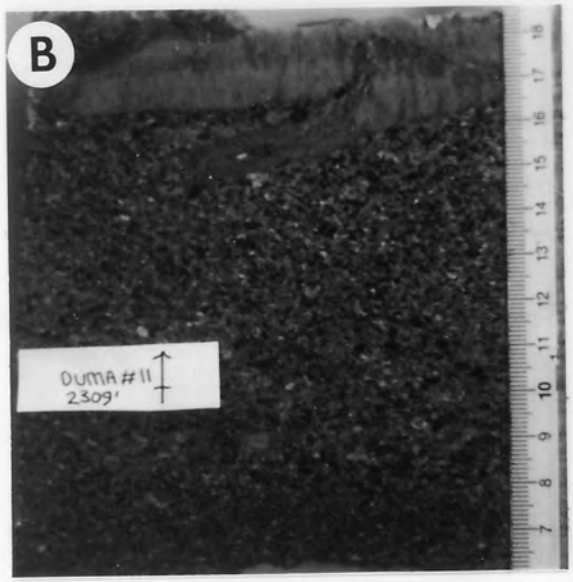

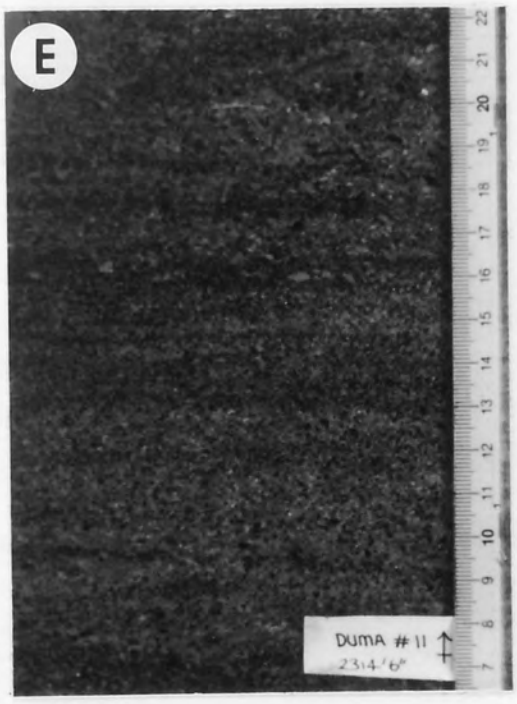

Plate 33 - Textures of the sparsely fossiliferous wackestone-lime mudstone facies

A. Duma 5 2406'. Pale lenticular to wispy-layered, mottled wackestone-lime mudstone with streaky algal wisps and common unabraded benthic foraminifera.

B. Duma 5 2419'. Pale coloured leached skeletal packstone lenses in mottled sparsely fossiliferous wackestone. The lenses may have been deposited as intraclasts and subsequently flattened.

C. Duma 5 2410'6. Merging of packstone lenticles and streaky layered wackestone matrix.

D. Duma 5 2447'. Slightly bioturbated lime mudstone. The pale micritic streaks might result from the dissolution of thin tabular corals.

PLATE 33

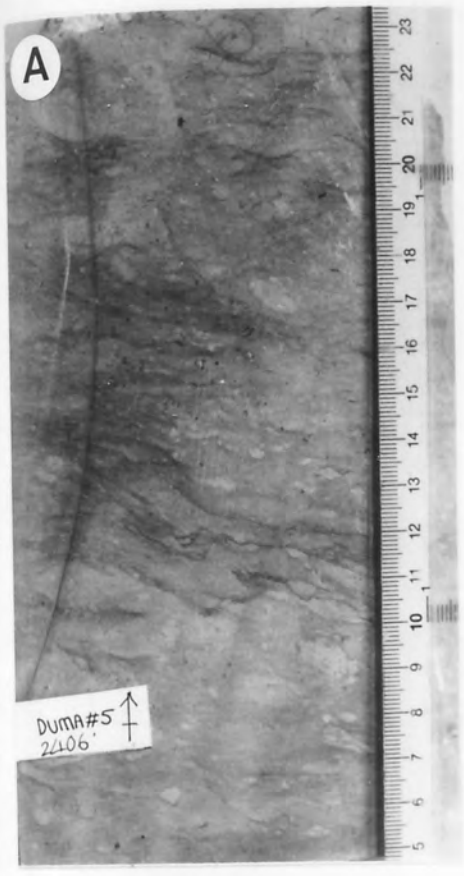

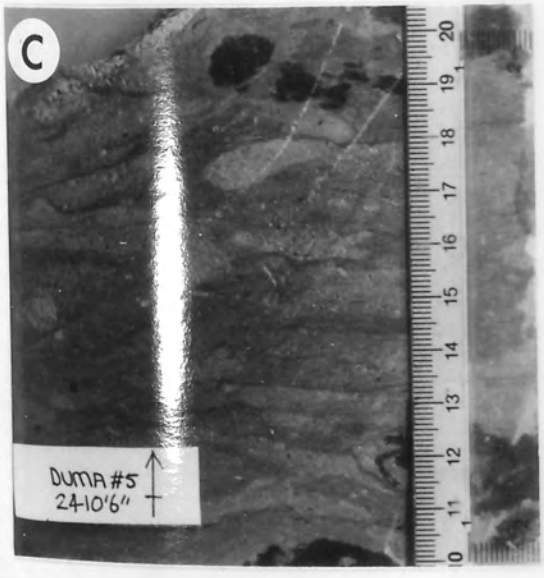

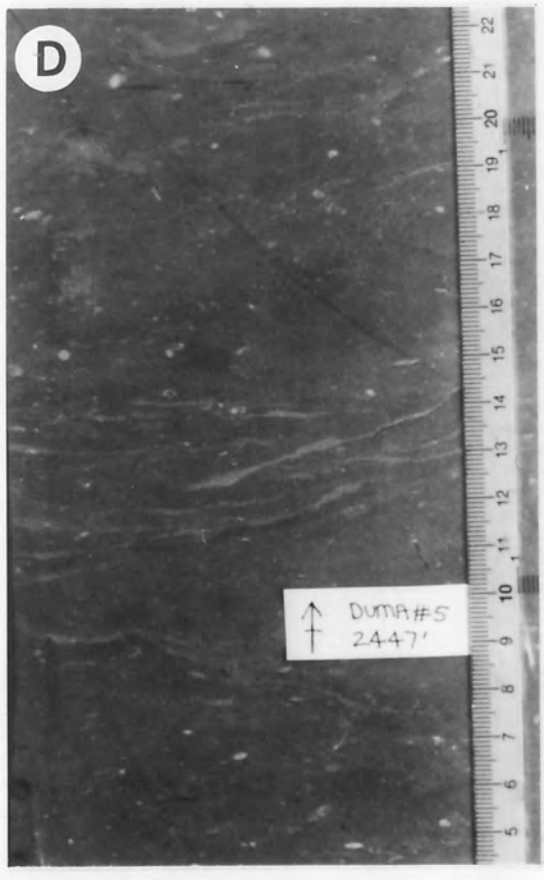

Plate 34 - Textures of the foraminiferal floatstone facies and mottled floatstones

A. Duma 5 2452'. Foraminiferal rudstone. In some patches the foraminifera are haphazardly orientated in a "cardhouse" fashion although towards the base of the slab orientation is subhorizontal defining a layering.

B. Duma 5 2440'6. Leached floatstone rudstone. Allochems are unsorted and float in wispy-laminated muds. Foraminifera, molluscs and abraded coral fragments are the main constituents.

C. Duma 5 2506'. Conglomeratic mottling of a wackestone lithology. Anastomosing solution zones are visible.

D. Duma 11 2345'. Lenticularly-layered wackestone with a layer of displacive calcite at the top of the slab. Layering is the result of anastomosing subhorizontal solution zones. Encrusting algae and foraminifera are common.

E. Duma 5 2414'. Stratified, reworked, mottled packstone wackestone. The cream micritic layers might result from flattening of lime mud lenticles.

F. Duma 5 2474'. Detrital tabular corals stacked in a haphazard fashion. The interstitial blue-grey patches are areas of recrystallised micritic mud.

PLATE 34

A
DUMA#5
2452'
B
DUMA#5
2440'
C
DUMA #5
2506'
D
DUMA#11
2345'
E
DUMA #5
2415'
F
DUMA #5
2474'

Plate 35 - Microtextures from the Batu Raja limestones

A. Mud-filled boring in a coral.
Sample N6 1782', Magnification X49.

B. Boring in a mud intraclast filled with calcite.
Sample N6 1759'11, Magnification X42.

C. Borings in a rhodolith. The borings exhibit the characteristic oval cross-section, horn-shaped long-section and blunt termination of bivalve borings.
Sample D11 2348', Magnification X42.

D. Impure sandy grainstone facies. Globigerinids/pellets and angular quartz grains are cemented by slightly ferroan calcite.
Sample D11 2307', Magnification X42.

E. An intraclast composed of coral and quartz silt and planktic foraminifera.
Sample D11 2307', Magnification X42.

F. The internal structure and composition of an intraclast showing the lack of sorting and fine muddy matrix. The identifiable constituents include a gastropod fragment, spines from benthic foraminifera and planktic foraminifera.
Sample N6 1759'11, Magnification X58.

PLATE 35

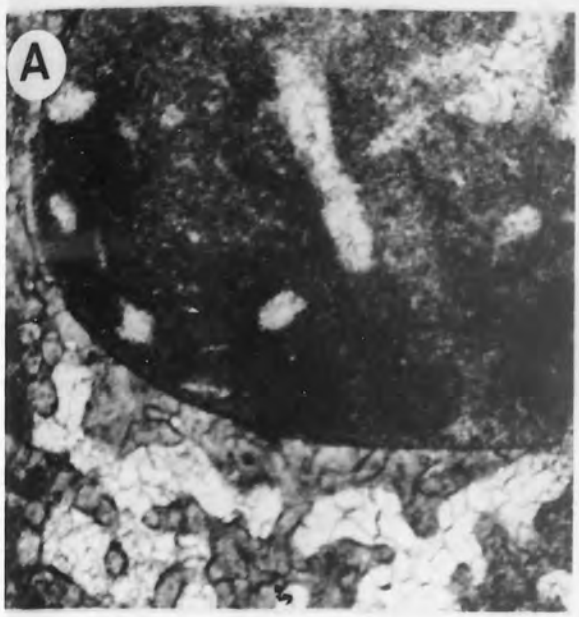

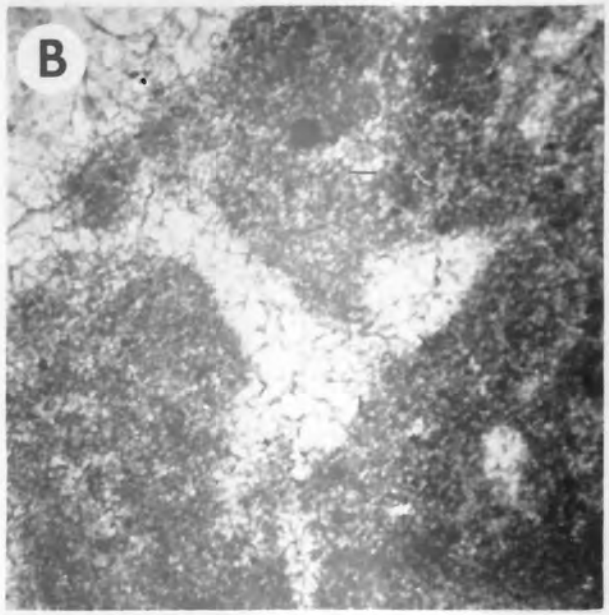

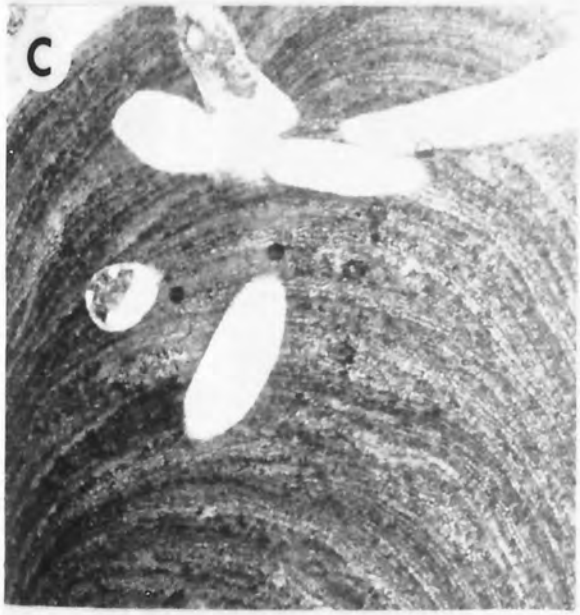

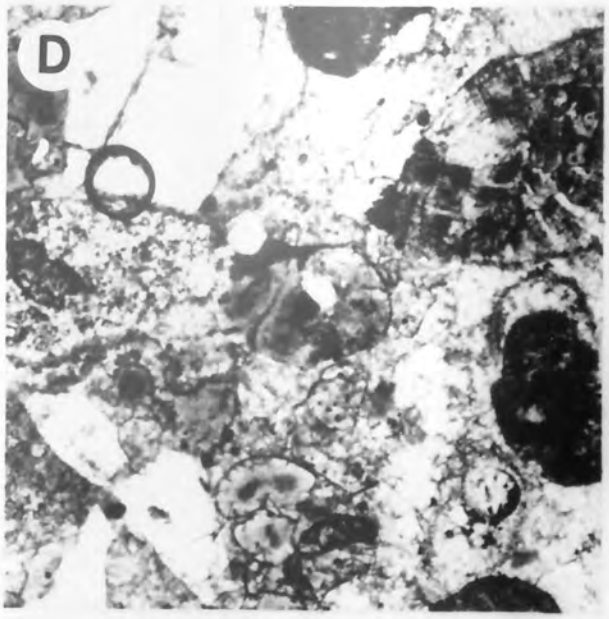

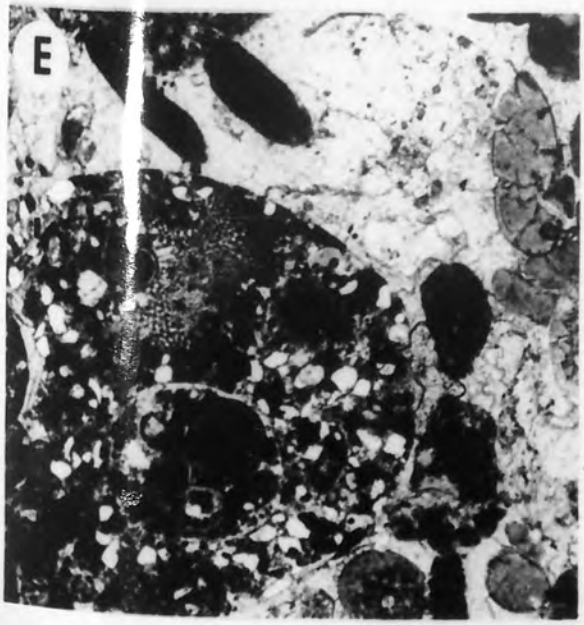

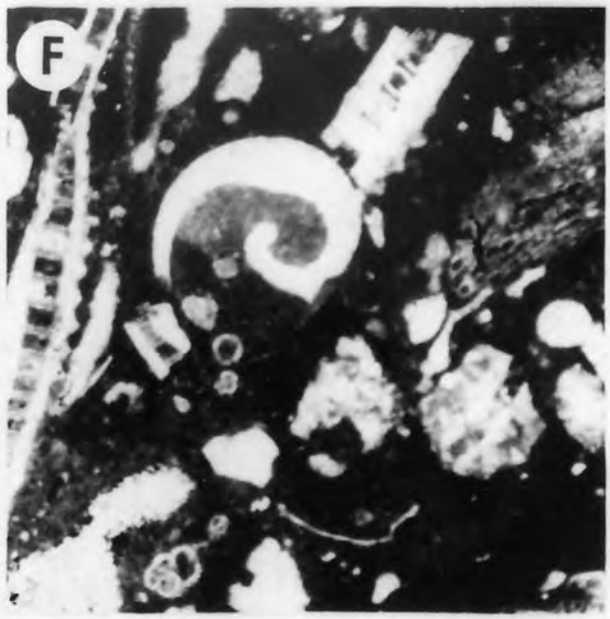

Plate 36 - Microtextures from the Batu Raja limestones

A. Delicate unfractured foraminifer spines in a silty micritic matrix. Sparsely fossiliferous lime mudstone facies.
Sample D11 2352'6, Magnification X42.

B. Section through a robust gastropod. Coral-intraclastic floatstone-rudstone facies.
Sample D11 2345', Magnification X42.

C. Strongly laminated highly impure sample with pronounced preferential horizontal permeability. The elongate fragments in the lower right are fossilised wood splinters.
Sample ZU-1 2626', Magnification X42.

D. Strongly laminated texture. Matrix very impure and rich in quartz silt. The cellular organism at the top of the photograph is an abraded benthic foraminifer. Sample is from the top of Nurbani-4 but due to the poor recovery there it is impossible to judge the precise depth.
Magnification X49.

E. Highly porous Nummulites packstone. Foraminiferal skeletal packstone-wackestone facies.
Sample ZU-1 2597'9, Magnification X42.

F. Foraminiferal packstone unit interlayered with coral floatstones. Foraminifera include Discocyclina and globogerinids.
Sample N4 1675', Magnification X42.

PLATE 36

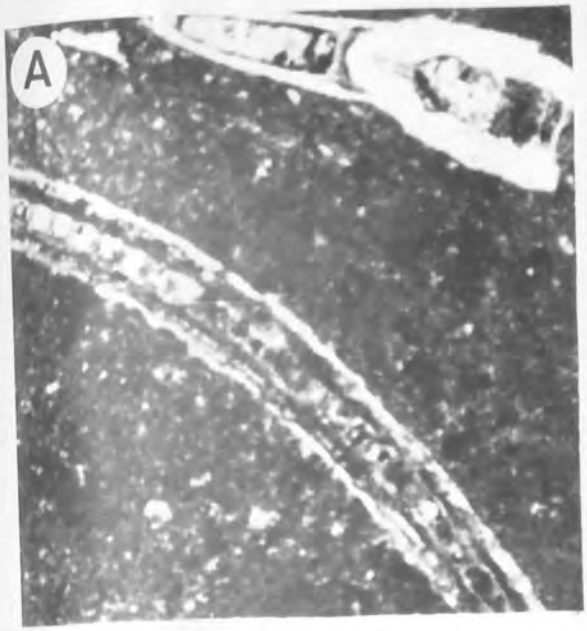

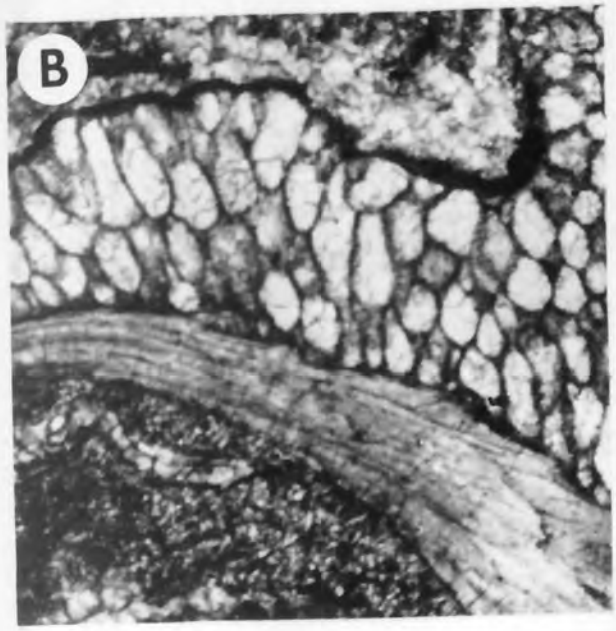

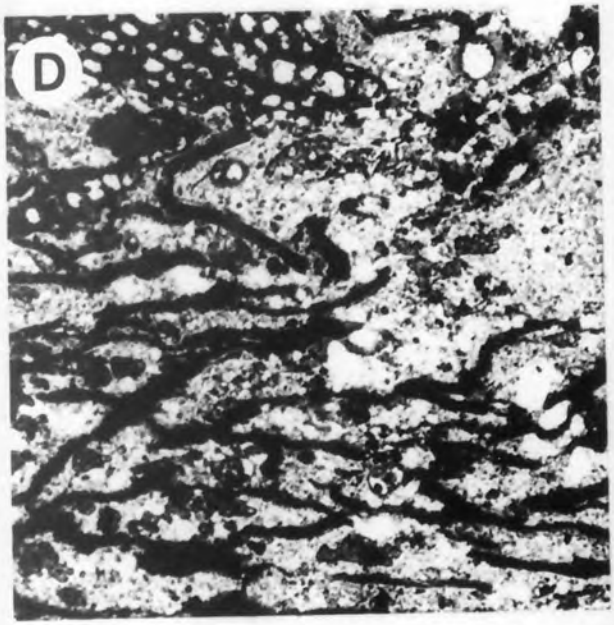

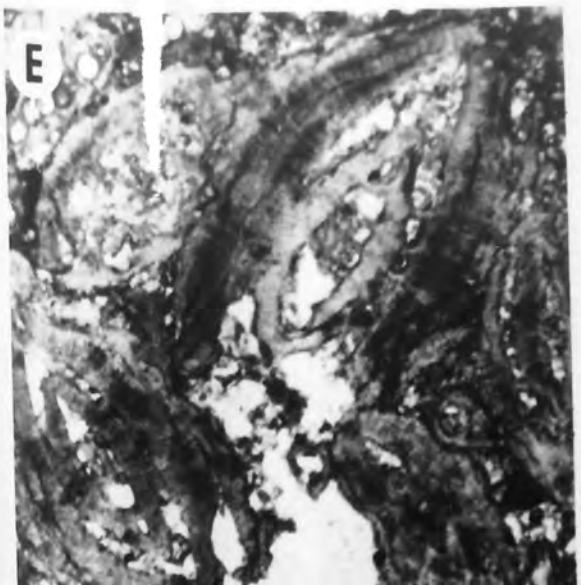

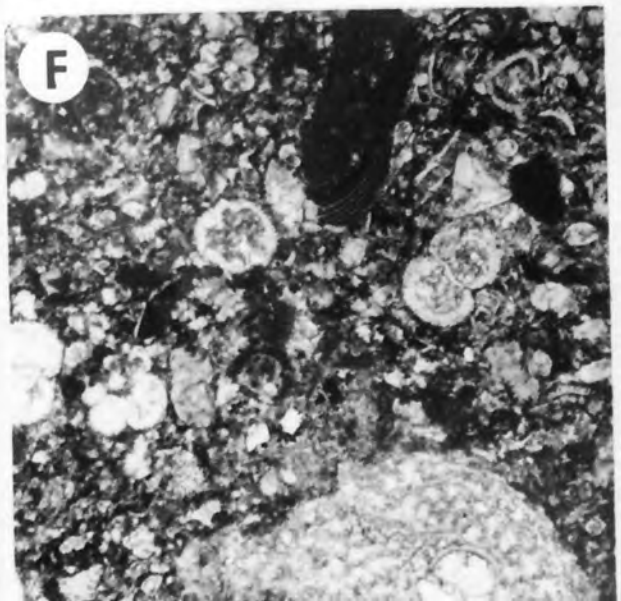

Plate 37 - Microtextures from the Rajamandala Limestones

A. An accumulation of benthic foraminifera in a wackestone matrix.
Sample GH3, Magnification X42.

B. Calcareous algae are the main component of the foraminiferal skeletal packstone-wackestone facies in the Sukabumi area. Note also the encrusting bryozoan to the extreme left of the photograph.
Sample BQ2, Magnification X42.

C. Foraminifera, pellets and abraded coral debris welded with isopachous rim cementse. Foraminiferal-skeletal packstone wackestone lithofacies.
Sample GH5, Magnification X42.

D. A mud-filled recrystallised coral from the coral framestone lithofacies in the Bandung area. The lithology is dense and nonporous.
Sample BQ3, Magnification X42.

E. Recrystallised foraminiferal-algal packstone with scattered detrital coral fragments. The opaque grains are micritised aglae.
Sample GP2, Magnification X42.

F. Moderately well-sorted packstone composed of recrystallised abraded unidentifiable grains and planktic foraminifera.
Sample TA2, Magnification X49.

PLATE 37

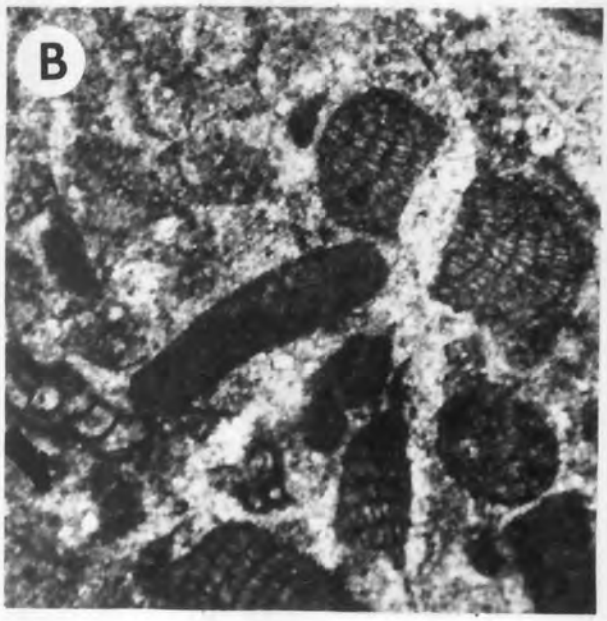

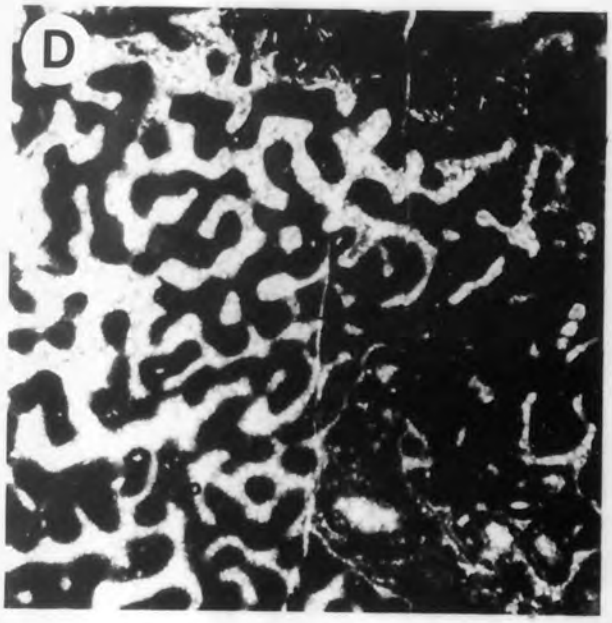

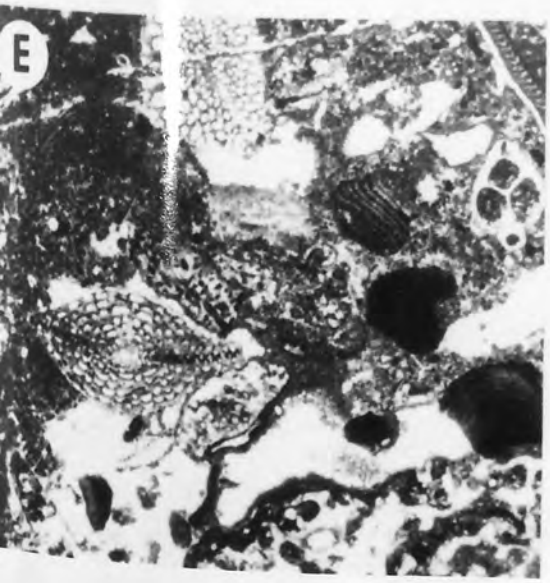

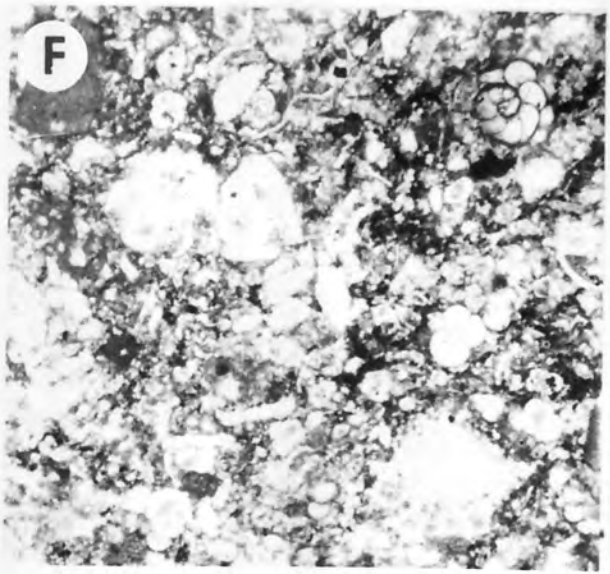

Plate 38 - Outcrops of the Rajamandala limestones

A. Gunung Walat quartzite from the Cibinong Cement works in Cibidak to the southwest of Sukabumi. The quartzite is thickly bedded and unfossiliferous. Note the presence of a coal bed beneath the figure.

B. Citatah Quarry on the eastern end of the Rajamandala Ridge. The coral framestones of this area are unstratified dense and non-porous.

C. Detrital abraded branched corals in a micrite matrix from an outcrop of coral debris floatstone rudstone at Tagog Apu.

D. A massive colony in a bed of coral framestone. Gunung Hawu.

PLATE 38

Plate 39 - Microtextures of the Sengkang Basinal area limestones

A. Globigerina packstone.
Sample ER9, Magnification X49.

B. Foraminiferal packstone. Tightly packed benthic and planktic foraminifera and echinoderm fragments.
Sample ER8, Magnification X42.

C. Foraminiferal-mollusc assemblage. The mollusc fragments are recrystallised to a structureless low-Mg calcite mosaic. Subsidiary grain types include encrusting bryozoa.
Sample ER3, Magnification X42.

D. Benthic foraminifera such as these are rare in the Eocene limestones of the Enrenkang-Rantepao region and absent in the Late Miocene limestones of the south Sengkang Basin.
Sample ER7, Magnification X49.

E. Unsorted foraminiferal-algal-mollusc-echinoid assemblage.
Sample BM4, Magnification X42.

F. Recrystallised limestone totally replaced by a coarse mosaic of non-ferroan and ferroan low-Mg calcite. Skeletal grains have been replaced by dark ferroan calcite around their margins and non-ferroan calcite in central parts and the matrix has been totally replaced by non-ferroan calcite. The distribution of ferrous iron in the crystal mosaic provides the only evidence of the former presence of allochems.
Sample W2, Magnification X42.

PLATE 39

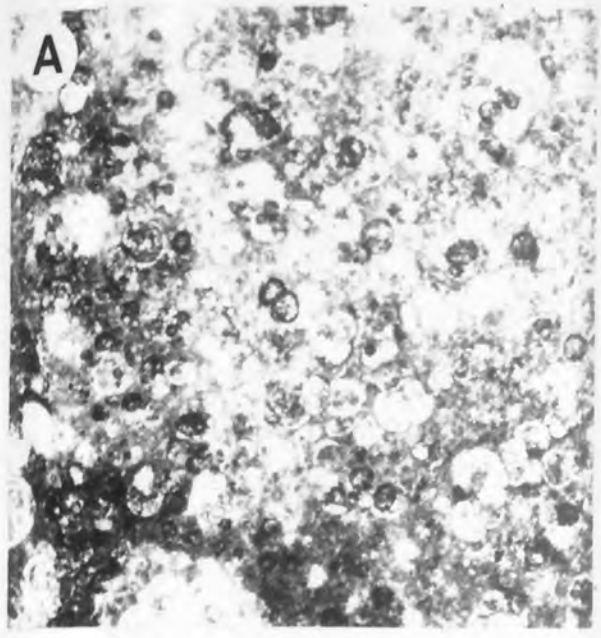

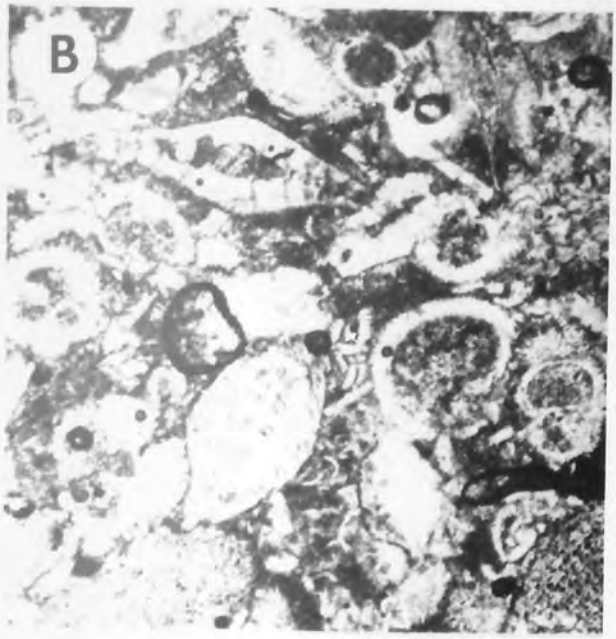

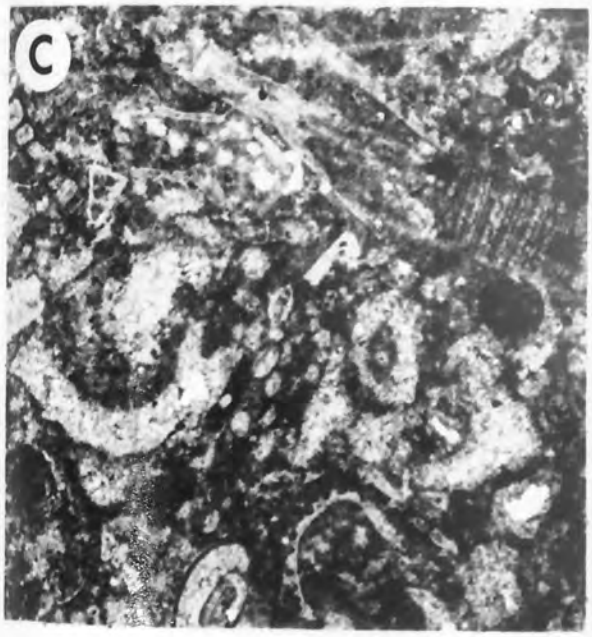

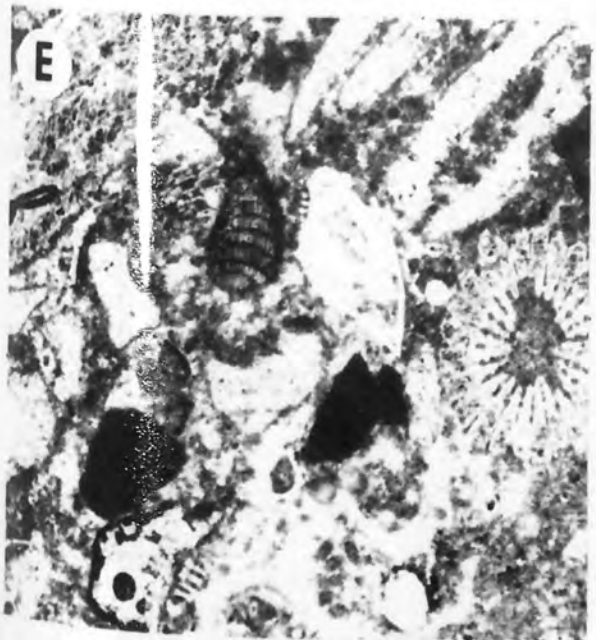

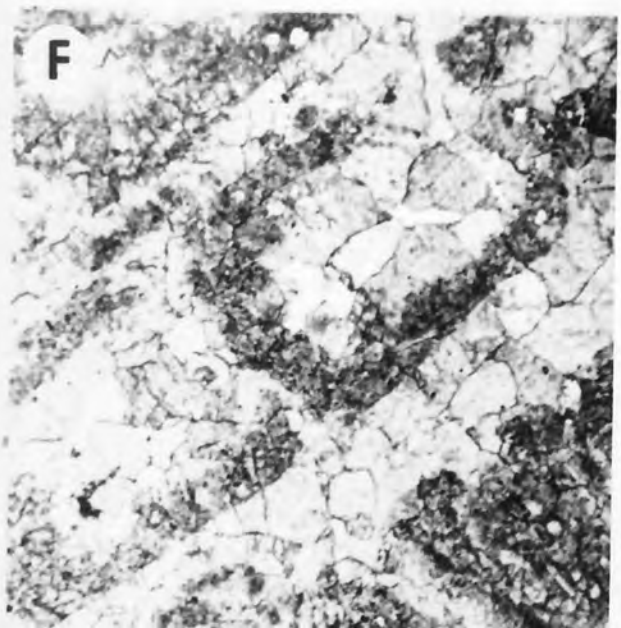

Plate 40 - Microtextures of the Sengkang Basinal limestones

A. Coral-foraminiferal assemblage. The coral has undergone solution-deposition. Foraminifera include benthic and planktic species.
Sample BL3, Magnification X42.

B. Highly leached skeletal packstone-wackestone. Secondary pores are mainly of vugular or mouldic type.
Sample LL2, Magnification X42.

C. Leached coral partly filled with non-ferroan spar.
Sample BL1, Magnification X42.

D. Well-sorted and tightly packed coarse sandy grainstone-packstone. Most of the original constituents have suffered recrystallisation or solution-deposition and are unidentifiable.
Sample LL2, Magnification X42.

E. Dolomite replacing zoned low-Mg calcite. Virtually none of the original texture of the sediment remains. Zones within the calcite spar are delineated by concentrations of impurities.
Sample BM4, Magnification X42.

F. Dolomitised coral. The original skeletal structure is faintly retained through preservation of micrite envelopes.
Sample BM5, Magnification X42.

PLATE 40

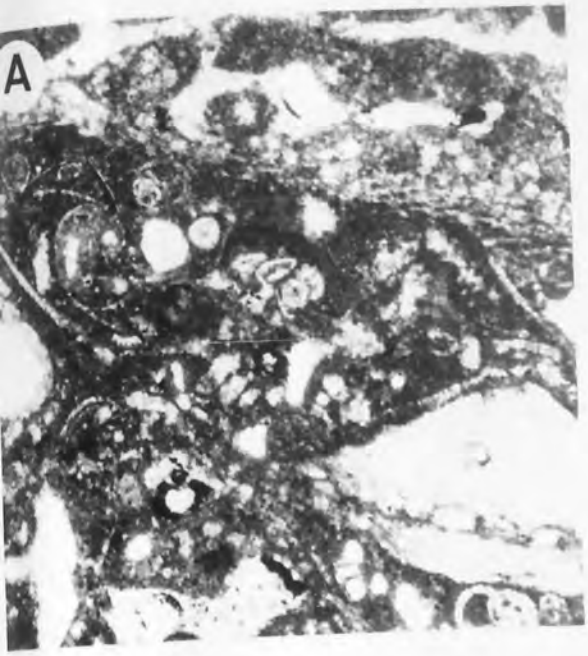

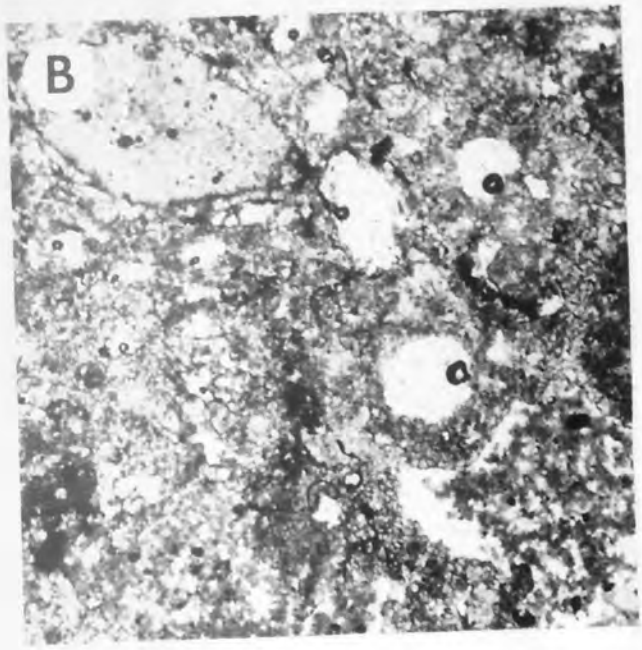

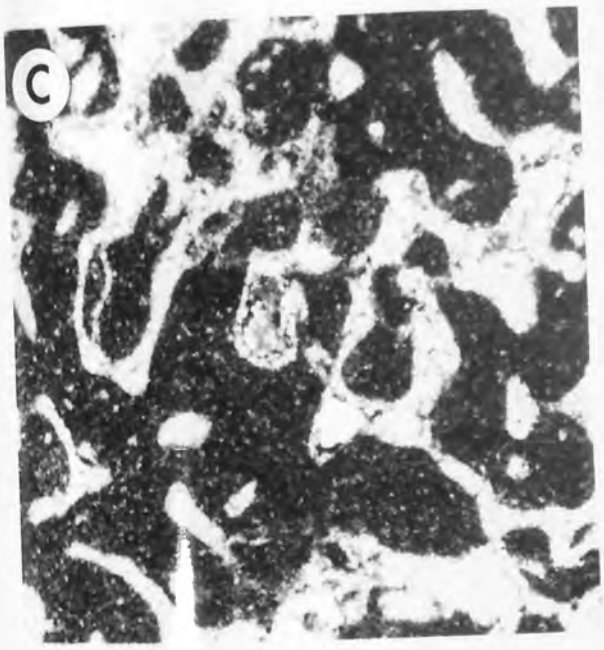

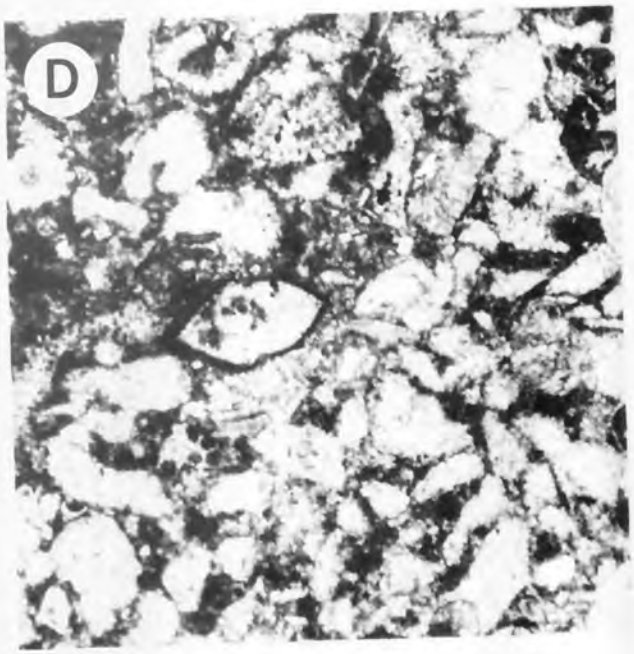

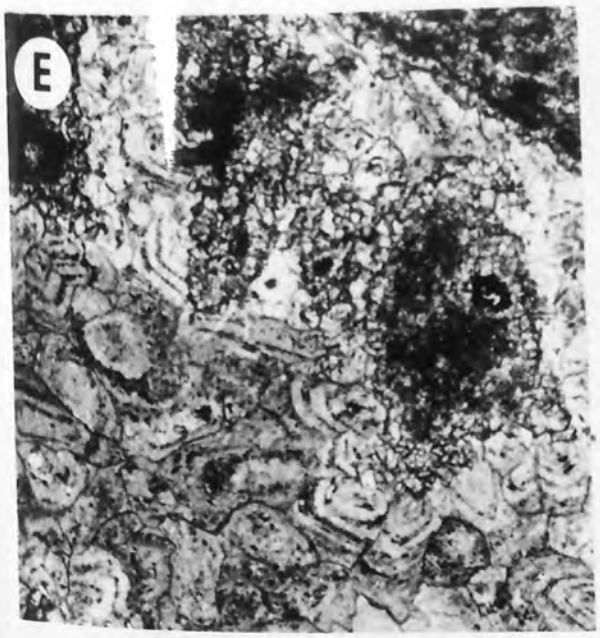

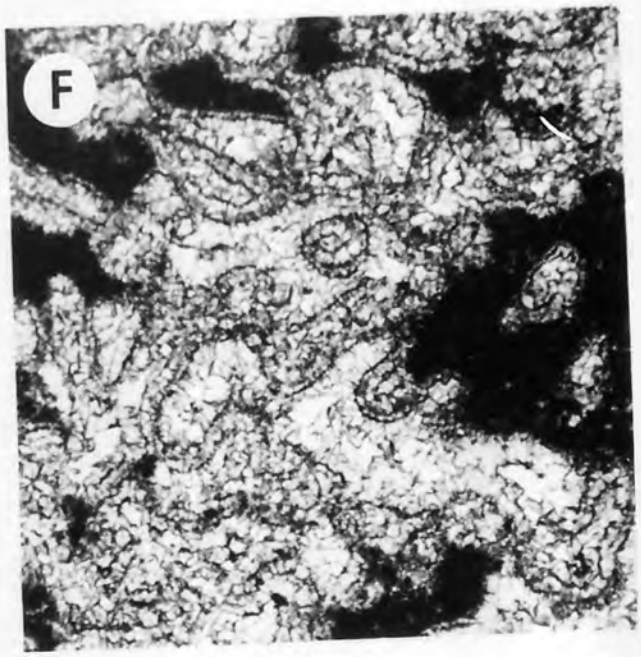

Plate 41 - Microtextures from the Sengkang Basinal area limestones

A. Articulated unfractured finely ribbed bivalve preserved in a sandy matrix. Locality; Wattansoppeng Quarry, South Sulawesi Lithofacies; Shelly floatstone-packstone.

B. Looking north-east from Bullo Loppo to the round topped reefal mound of Bullo Lebae and the flat topped West Sengkang Basin, South Sulawesi.

C. Reworked bioclastic foraminiferal packstone and lime mudstone. Locality; Cibinong Quarry, Bogor (Parigi Formation), Lithofacies; Interstitial sediment within the micritised shelly coral packstone-floatstone.

D. Thin parallel orientated unfractured foliose corals in a muddy matrix. Photograph taken on the northwest slope of Gunung Kamuning, Cibinong Quarry, Bogor (Parigi Formation). Lithofacies; Interbedded foliose coral framestone and foraminiferal floatstone.

PLATE 41

Plate 42 - Microtextures of the Parigi limestones

A. Foraminiferal-skeletal packstone sediment. The relatively insoluble rotalinid foraminifera resist solution-infilling and are the only readily identifiable component remaining in this sample.
Sample P1, Magnification X42,

B. Foraminifera in a quartz-rich muddy matrix. The depositional environment is interpreted as quiet-water due to the negligible fracturing of the fossils. Quartz grains are well-sorted and slightly etched.
Sample P13, Magnification X42,

C. Benthic and planktic foraminifera are the main components of the packstone interlayered with foliose coral limestone on the slopes of Gunung Kamuning.
Sample P12, Magnification X49.

D. Common globigerinids in an impure wackestone.
Lithofacies; coral skeletal floatstone interbedded with calcareous mudstone.
Sample P12, Magnification X49.

E. A finely preserved unfractured bivalve floating in a dolomitised planktic foraminifera-algal wackestone matrix.
Sample P12, Magnification X42.

F. Interstitial sediment within the micritised shelly coral packstone floatstone. The micritic matrix has a pelletal texture. Intraskeletal cavities are spar-filled.
Sample P3, Magnification X42.

PLATE 42

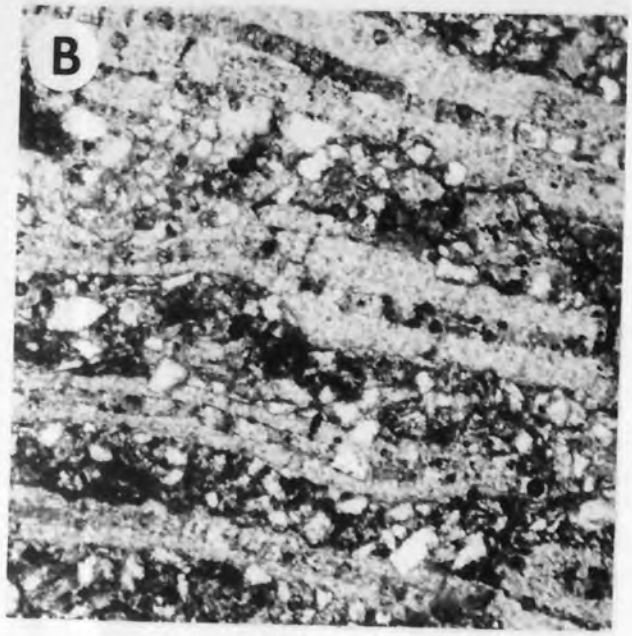

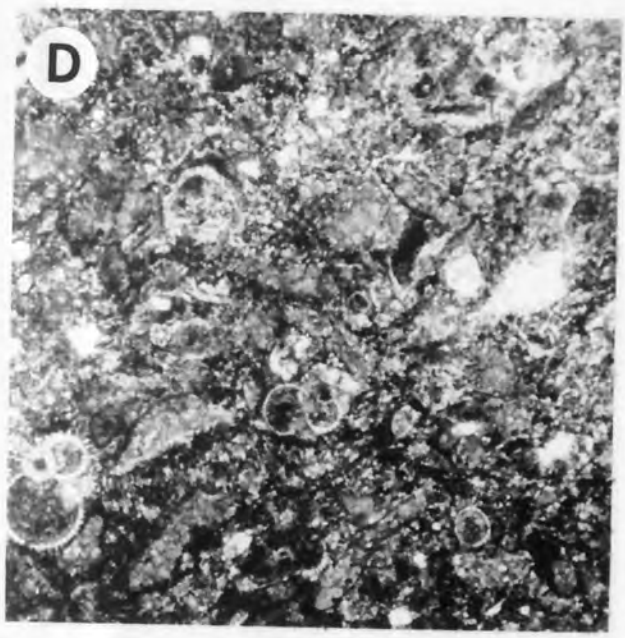

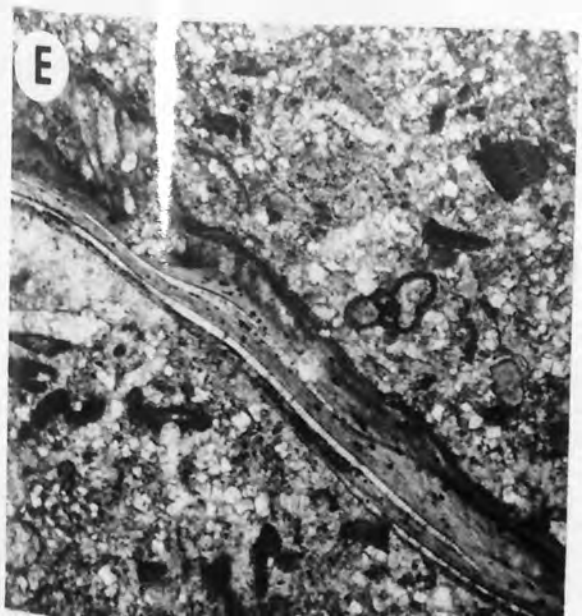

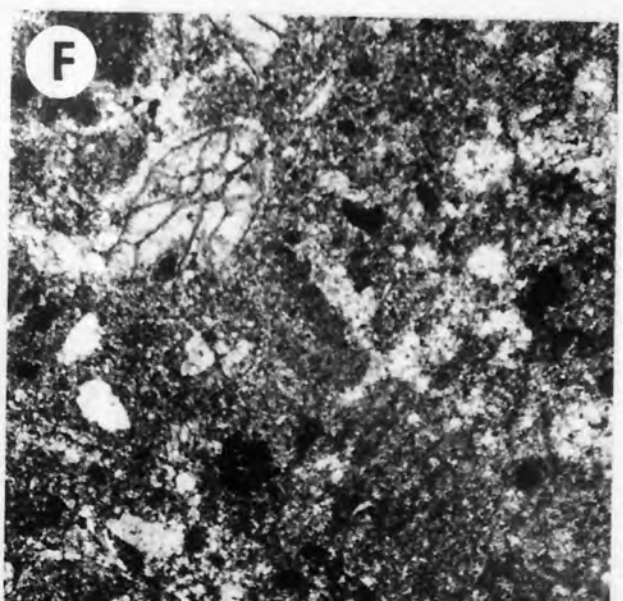

Plate 43 - Textures associated with micritisation

A. Chambered structure of micritised benthic foraminifer just discernible within the dark brown replacement. The surrounding formerly micritic matrix is neomorphosed to calcite spar.
Sample D5 2526'5 Magnification X42.

B. Micrite envelopes on grains which have undergone solution-infilling by low-Mg calcite. Intergranular porosity has been occluded by two generations of cement; the early generation is visible as a granular ragged crust lining the outer surface of the micrite envelopes.
Sample ZU-1 2588'4 Magnification X42.

C. Mollusc with microstructure vaguely preserved. Shell is bored and the outer rim is defined by a micrite envelope. Sparry calcite on inner (lower) margin, is a neomorphosed early cement fringe.
Sample D3 2403'6 Magnification X42.

D. Hydrozoan coral encrusted by a buckled algal mat. Microarchitecture of the algae is poorly preserved due to micritisation, although in places faint cellular structure is present between the coral and algae. The coral exhibits a tabular reticulate pattern of skeletal walls but the wall structure is obliterated due to the calcite-aragonite inversion. Intraskeletal porosity is filled with partially aggraded lime mud.
Sample D2 2802'2 Magnification X42.

E. Large calcareous algal fragment. Typical laminated and cellular structures is homogenised in patches to textureless dark micrite.
Sample N6 1759'11 Magnification X42.

F. Alga grading from a distinctly striated structure on left-hand margin of photograph, to structureless micrite on right-hand margin.
Sample D11 2345' Magnification X42.

PLATE 43

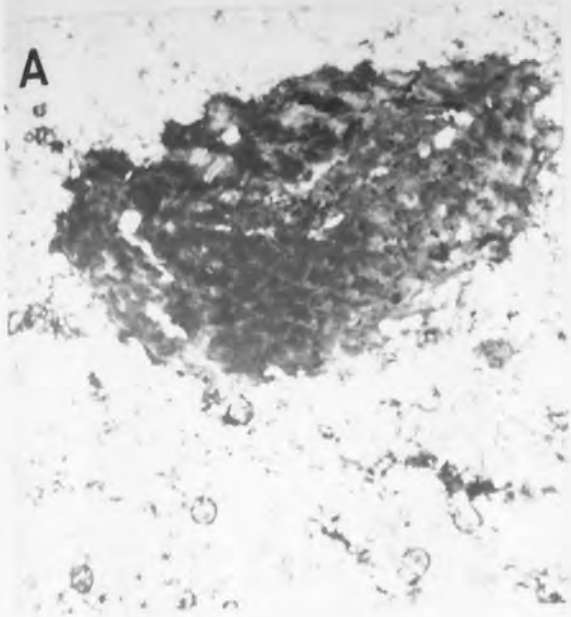

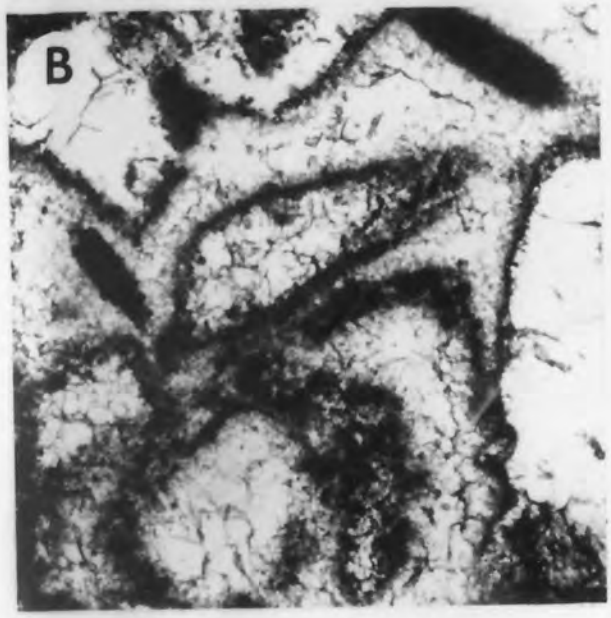

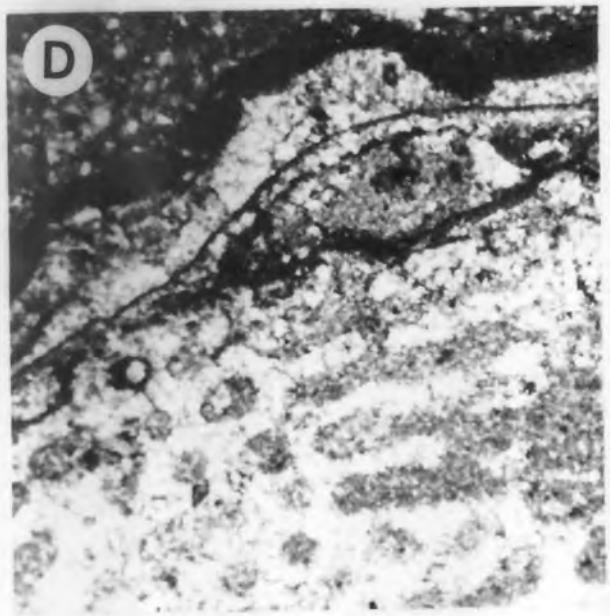

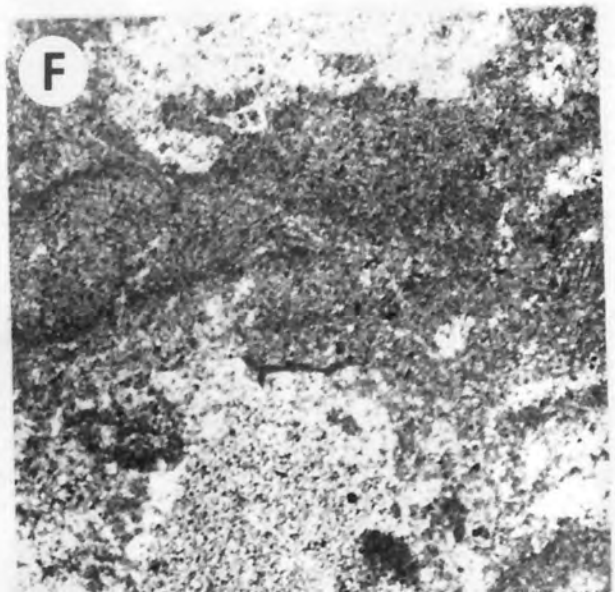

Plate 44 - Bladed and granular cements

A. Bladed cement on echinoid fragment.
Sample N6 1759'11 Magnification X42.

B. Granular cement lining chambers of a benthic foraminifer. This cement has been subsequently overlain and partially resorbed by equant low-Mg calcite. Wall structure of foraminifer is well preserved.
Sample D11 2349' Magnification X42.

C. Bladed granular fringe lining walls of foraminifer.
Sample D5 2421' Magnification X58.

D. Isopachous (neomorphosed fibrous) early cements. Elongate fragment in centre of photograph has been dissolved and infilled but the ghost cement rind and micrite envelope remain intact.
Sample ZU-1 2588'4 Magnification X42.

E. Precipitation of the cement around the foraminifer evidently preceded the dissolution of the foraminifer top centre. Irregular vuggy pores present in matrix.
Sample ZU-1 2588'4 Magnification X42.

F. Poikilotopic neomorphosed bladed cement on a benthic foraminifer. Cement grades outward into neomorphic matrix spar. In parts of this rock these cements weld adjacent grains and clearly formed a semi-rigid framework.
Sample N6 1759'11 Magnification X42.

PLATE 44

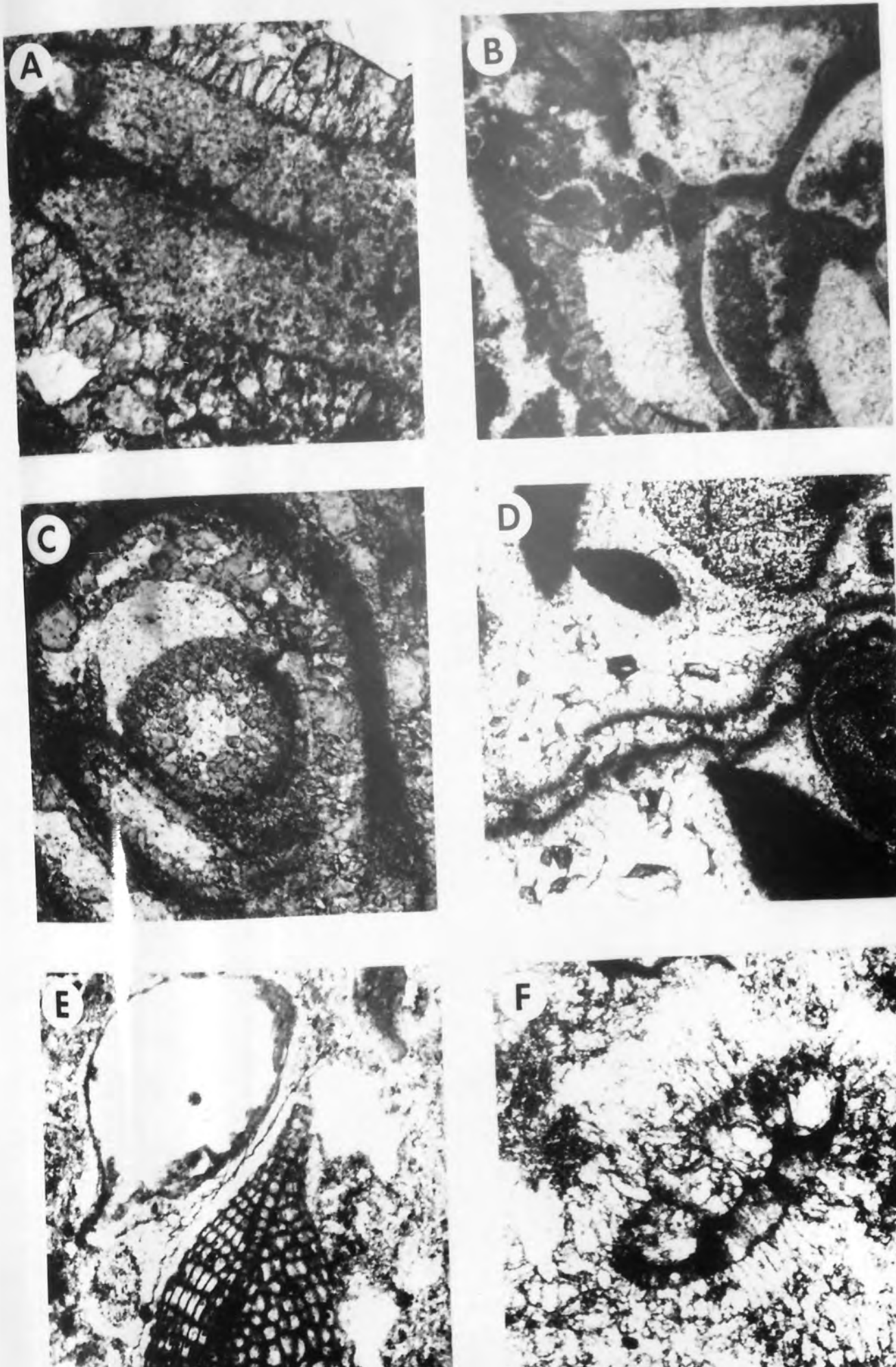

Plate 45 - Neomorphosed early cements

A. Two generations of cement on an echinoderm fragment. The early inclusion-rich neomorphosed fibrous cement is non-ferroan calcite and the later monocrystalline syntaxial overgrowth is ferroan calcite.
Sample ZU-1 12587'8 Magnification X42.

B. Ghost remnants of an early cement form a granular fringe lining foraminifera. A later mottled equant mosaic cement overlies it and the boundary between the generations is sharp. Right of centre is a ghosted foraminifer engulfed by sparry calcite.
Sample D9 2283'6 Magnification X42.

C. Isopachous cement rims on echinoderm grains and foraminifers.
Sample ZU-1 2588'4 Magnification X42.

D. Echinoderm grain (lower left) is encrusted with a fibrous cement fringe. Secondary pore (centre) has been lined with a marginal fine blocky cement and infilled with a coarse equant calcite mosaic.
Sample D11 2348' Magnification X42.

E. Part of a skeletal fragment is encrusted with equant ferroan calcite. Cement nucleation might be inhibited on the right-hand side by the presence of micrite. The cement sequence is similar to that described in A above.
Sample ZU-1 2587'8 Magnification X42.

F. Bladed cement on an indeterminate grain
Sample N6 1759'11 Magnification X42.

PLATE 45

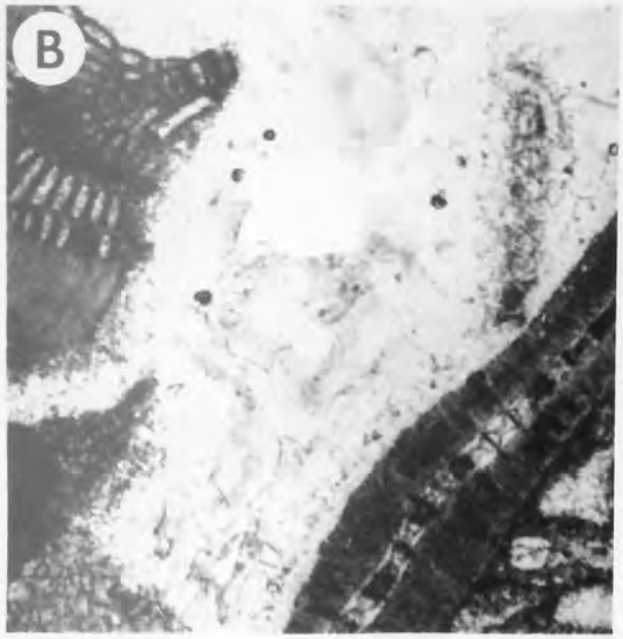

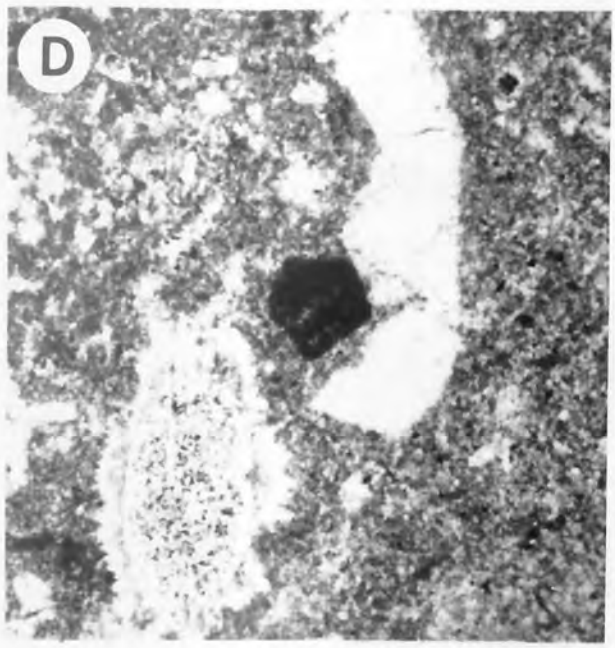

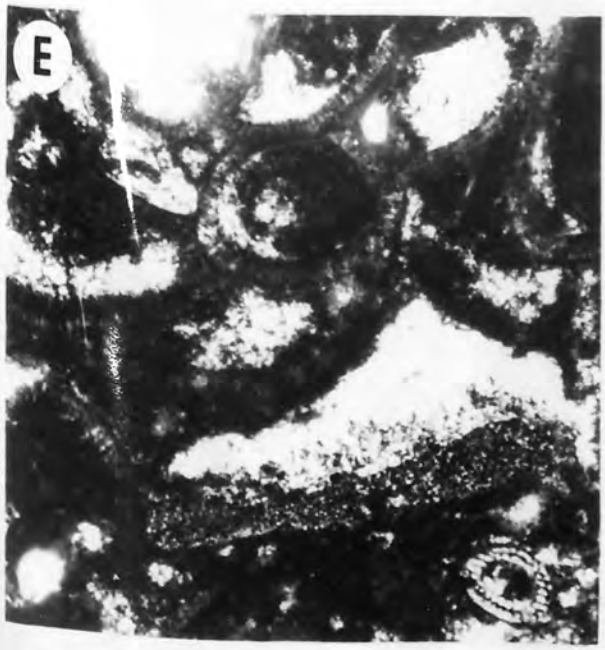

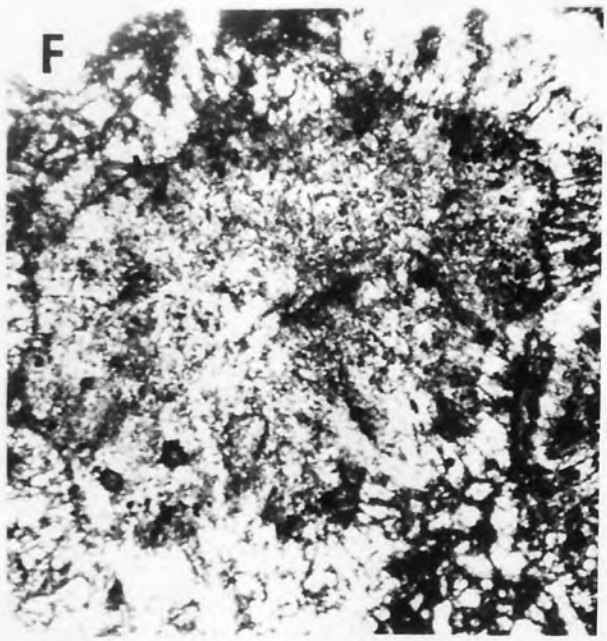

Plate 46 - Fibrous cements

A. Bladed-to-fibrous rim cement on an echinoderm grain.
Sample N6 1759' Magnification X42.

B. Ragged recrystallised fibrous cement rimming an echinoderm spine.
Sample N6 1735'6 Magnification X167.

C. Isopachous fibrous cement on foraminifer. Cross-polarised light.
Sample ZU-1 2588'4 Magnification X42.

D. Boring through fibrous isopachous fringe is filled with interlocking low-Mg calcite. Note dark micritic lower boundary of fibrous layer.
Sample D11 2345' Magnification X42.

E. Isopachous cement fringe on a micrite-filled coral. The fibrous texture is reminiscent of aragonite cement, and their oblique orientation with respect to the host substrate might result from overburden compaction.
Sample D11 2345' Magnification X42.

F. Poikilotopic syntaxial cement partly surrounds an echinoderm plate and grows into an open void.
Sample D9 2283'6 Magnification X58.

PLATE 46

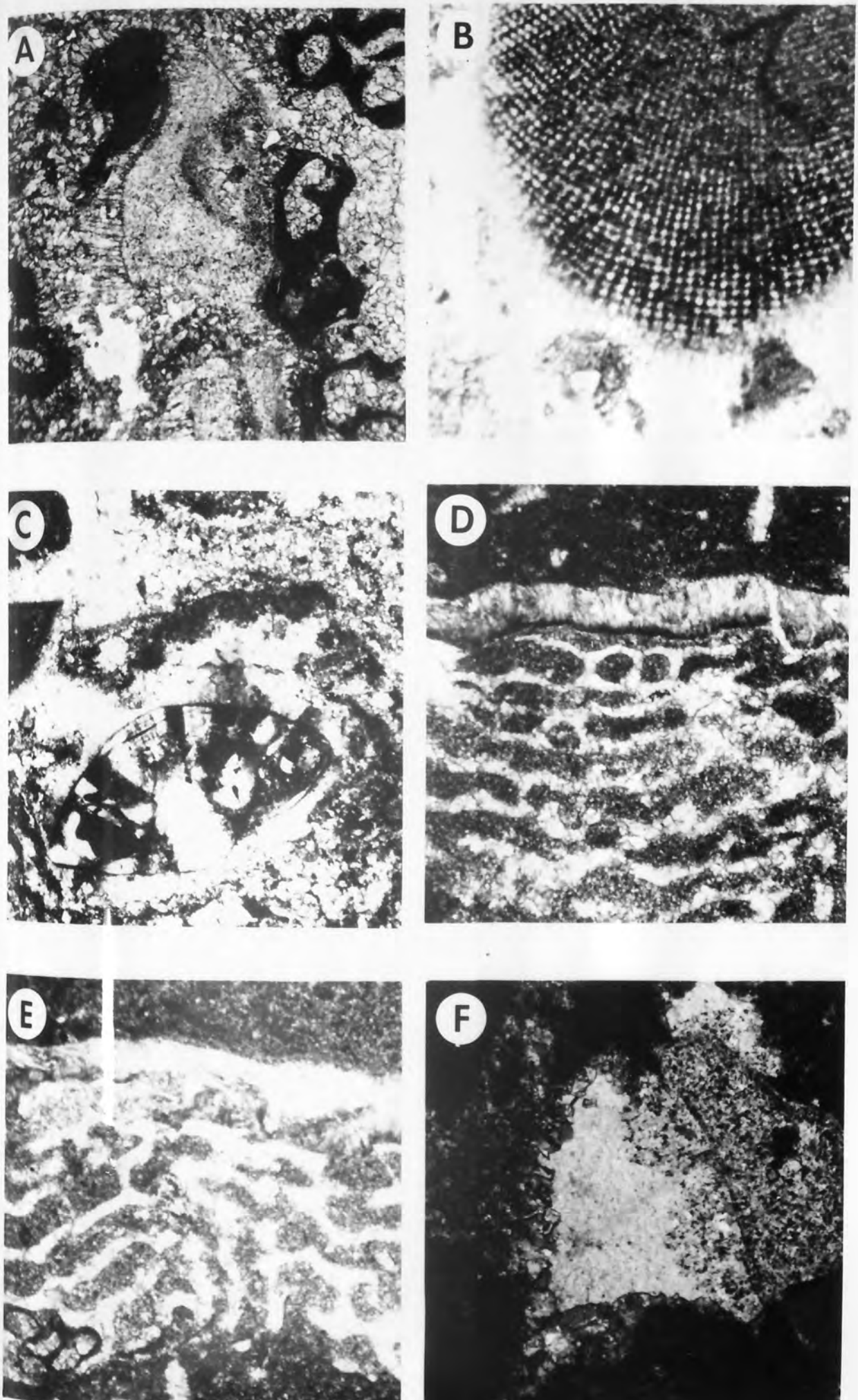

Plate 47 - Preferential dolomitisation of the matrix

A. Dolomite crystals in a matrix of microspar and residual micrite. Black grains are micritised algal fragments.
Sample D11 2320', Magnification X42.

B. Rhombs closely clustered in the matrix but do not form framework support. Altered skeletal grains are an abraded echinoderm and foraminifer.
Sample ZZZ2 2680', Magnification X42

C. Dolomitised matrix. Rhombs are closely packed and form framework support. Skeletal fragment is a recrystallised gastropod.
Sample N6 1755'6, Magnification X58.

D. Micritised bivalve floating in a dolomitised matrix. The cloudy fringe on the upper surface of the bivalve may be a neomorphosed early cement.
Sample N6 1755'6, Magnification X58.

E. Clear euhedral rhombic dolomite. Virtually no residual primary matrix. Foraminifera resist dolomitisation or micritisation.
Sample ZU-1 2597'9, Magnification X42.

F. Ribbed bivalve encrusted with a recrystallised early cement the margins of which are subsequently undergoing dolomitisation.
Sample N6 1755'6, Magnification X58.

PLATE 47

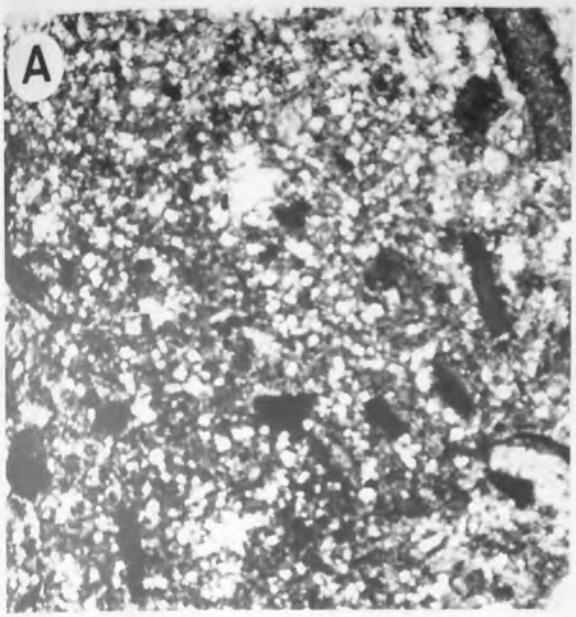

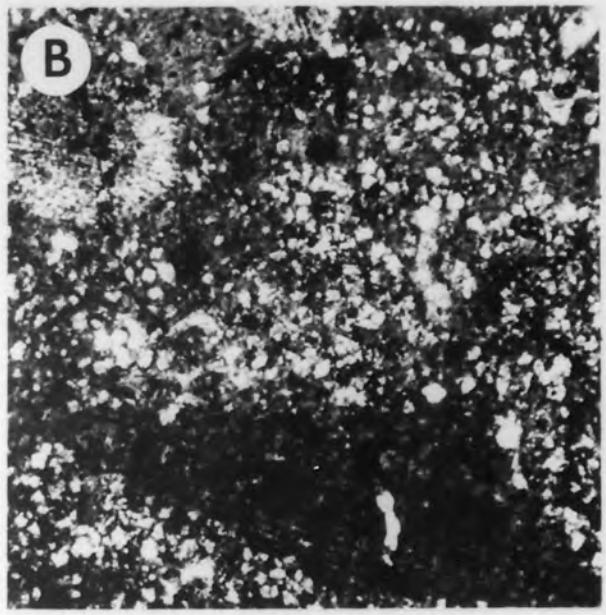

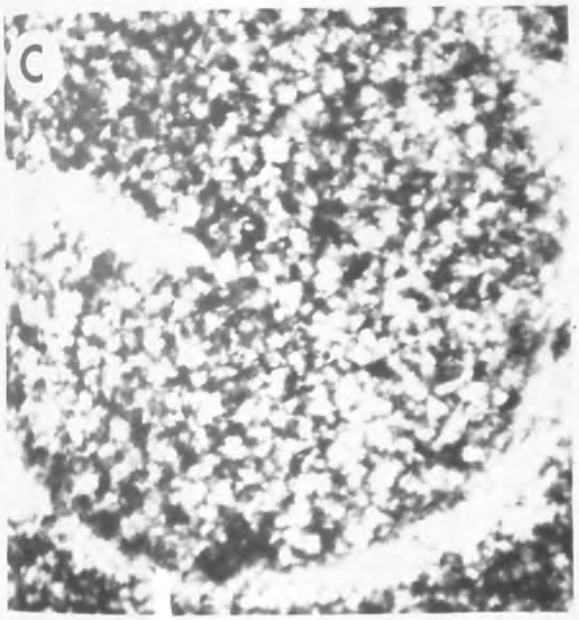

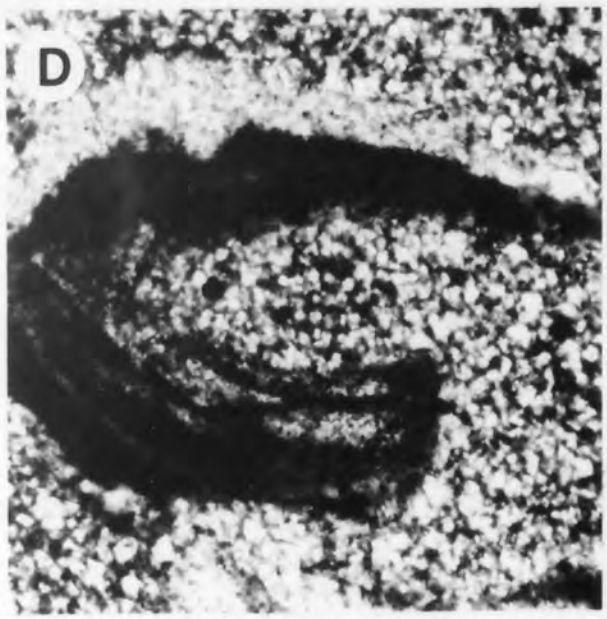

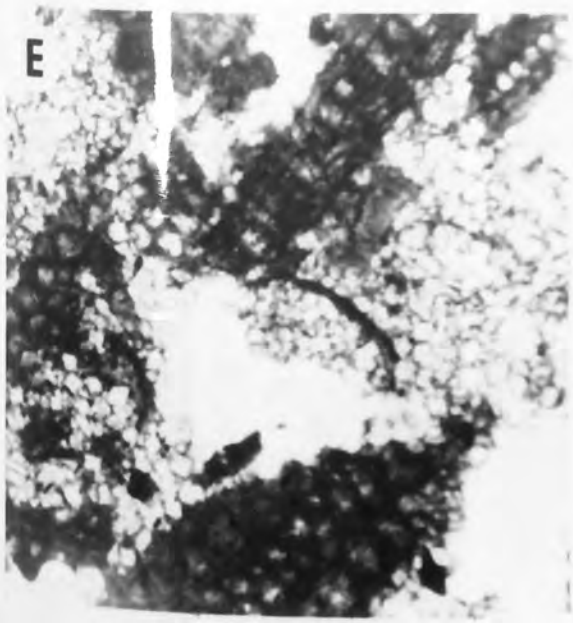

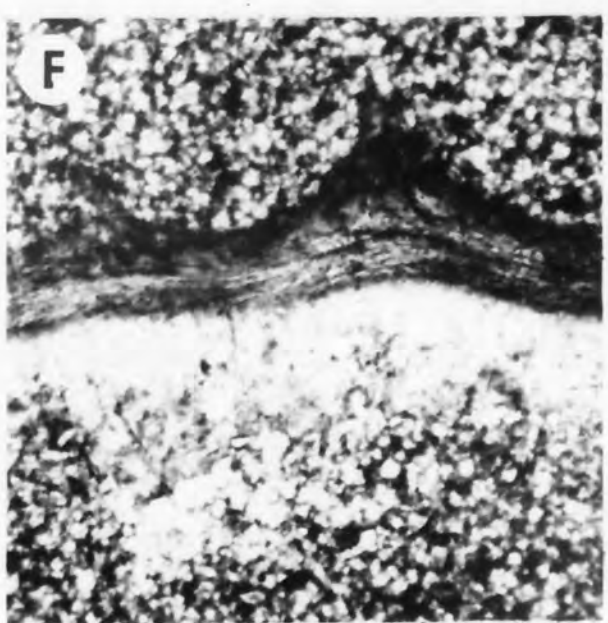

Plate 48 - Textures of matrix micrite

A. Interlocked dolomite with a very low intercrystalline porosity. A small amount of dark-coloured residual clayey matrix is present between the subhedral rhombs.
Sample ZZZ-2 2661', Magnification X58

B. Highly porous, leached dolomitised limestone. The original texture is indistinguishable; patches of residual matrix, microspar and micritised skeletal fragments float in the dolomitised matrix.
Sample ZU-4 2306'6, Magnification X42.

C. Clear euhedral dolomite rhombs replacing matrix and residing in skeletal interstices in a foraminiferal packstone.
Sample ZU-1 2635'6, Magnification X42.

D. Dolomite replacing microsparry matrix. Globogerinid (top left) is unaltered.
Sample ZZZ-2 2666', Magnification X42.

E. Rhombic dolomite completely replacing and obliterating primary depositional texture.
Sample ZU-1 2619'7, Magnification X42.

F. Dolomitised foraminiferal-algal wackestone. Dense black fragments are micritised algae.
Sample D11 2320', Magnification X42.

PLATE 48

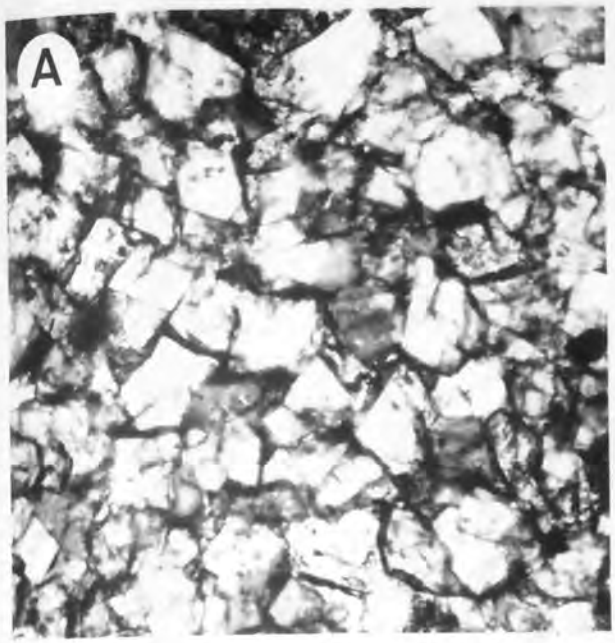

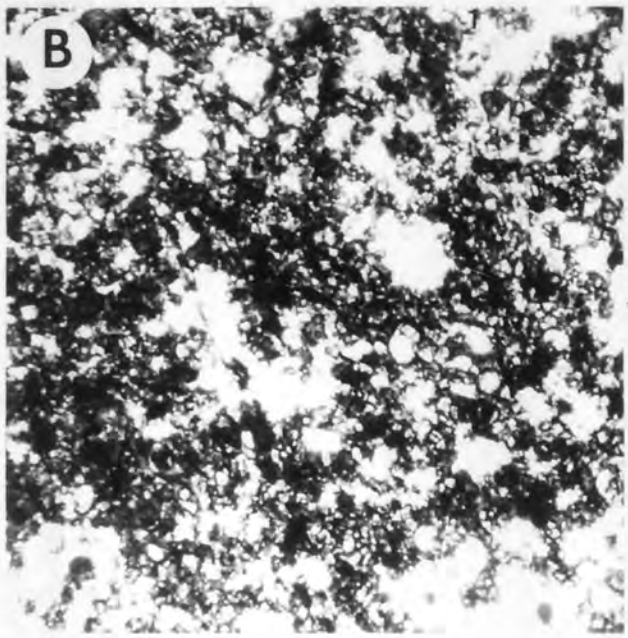

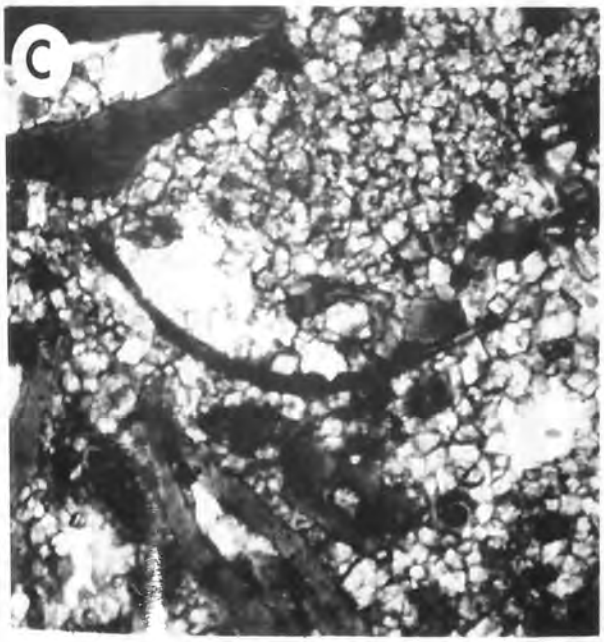

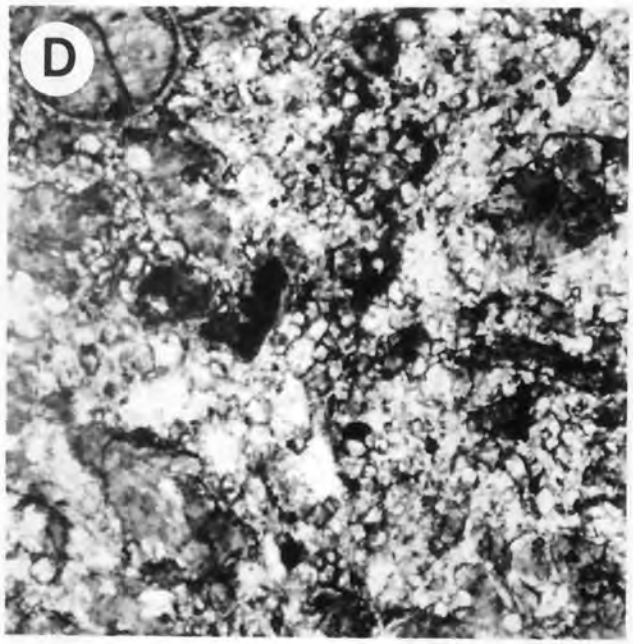

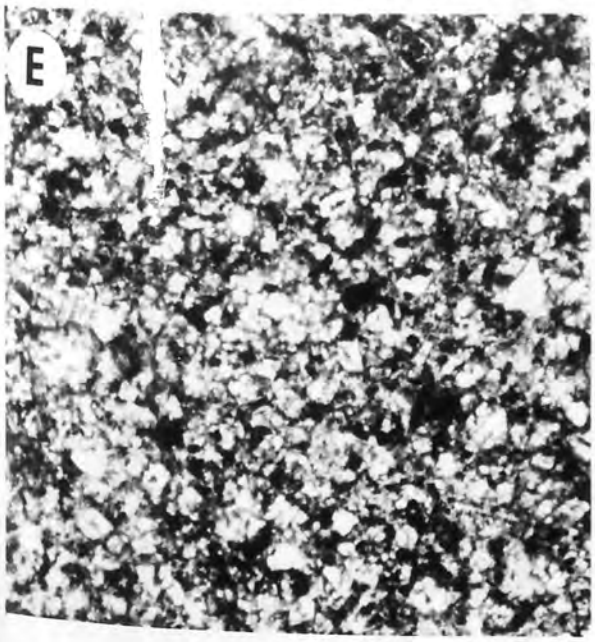

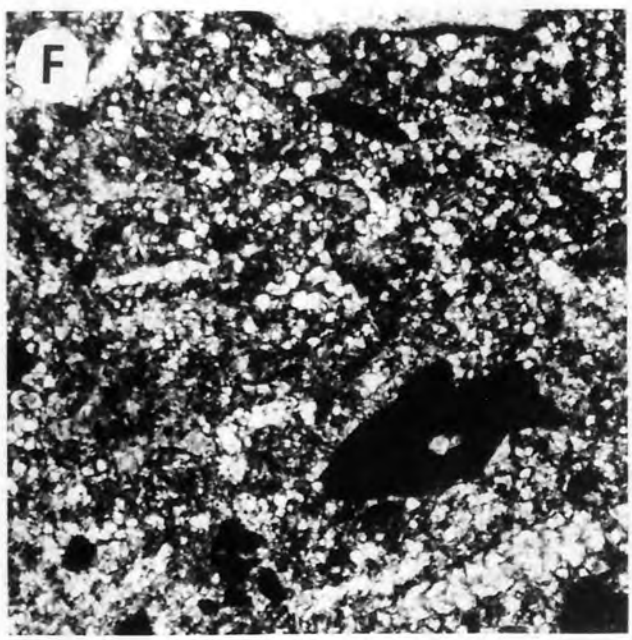

Plate 49 - Porous and non-porous dolomitised intervals

A. Dolomitised foraminiferal packstone-floatstone. The primary matrix is leached out resulting in a highly porous lithology.
Sample ZU-1 2597'9, Magnification X49.

B. Similar to A. The primary matrix must have been present prior to dolomitisation since it is clear that the foraminifera remaining do not support one another.
Sample ZU-1 2597'9, Magnification X49.

C. Leached dolomitised packstone. Some rhombs penetrate foraminifera walls.
Sample ZU-1 2623', Magnification X49.

D. A narrow leached zone in a tight micritic lithology has been selectively dolomitised. The oversized nature of the vug suggests that leaching also postdated dolomitisation.
Sample D11 2348', Magnification X42.

E. Dolomite in discrete clusters replacing microsparry matrix and recrystallised skeletal grains.
Sample D5 2414'6, Magnification X42.

F. Granular 'saccaroidal' dolomite in an oversized pore suggesting that leaching postdated dolomitisation.
Sample ZU-1 2592'3, Magnification X49.

PLATE 49

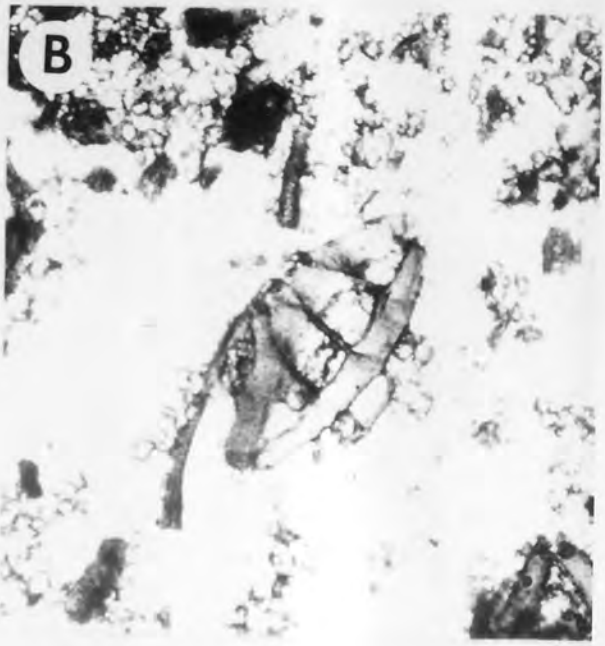

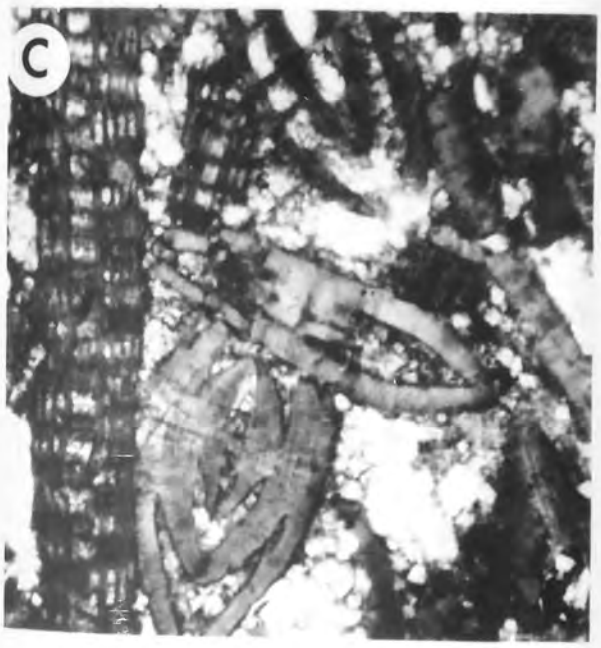

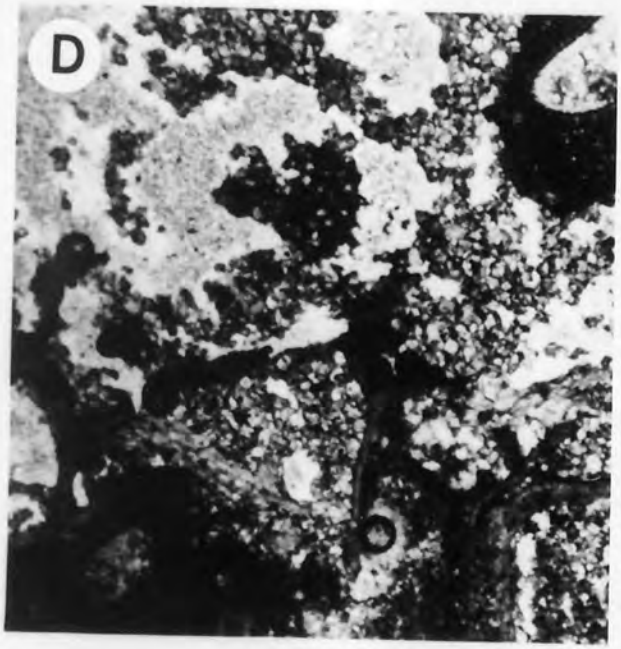

Plate 50 - Dolomite textures under SEM

A. A cluster of interlocked rhombic dolomite in a recrystallised microsparry matrix.
Sample ZU-4 2661', Magnification X350.

B. Clay coats and florets adhered to interlocked rhombic dolomite.
Sample N4 1675', Magnification X2800.

C. A sharp contact between a recrystallised skeletal fragment and the dolomitised matrix. The rhombs do not penetrate the walls of allochems unless the skeletal structure has been broken down by micritisation.
Sample N4 1675', Magnification X350.

D. A porous dolomitised limestone. The angular intercrystalline pores are partly clogged by fine residual micrite.
Sample ZZZ-2 2666', Magnification X2800.

E. Interlocked tight rhombic dolomite. The primary texture is entirely replaced.
Sample D5 2465, Magnification X300.

F. Clayey micritic slightly dolomitised matrix enveloping a skeletal grain.
Sample D11 2349', Magnification X350.

PLATE 50

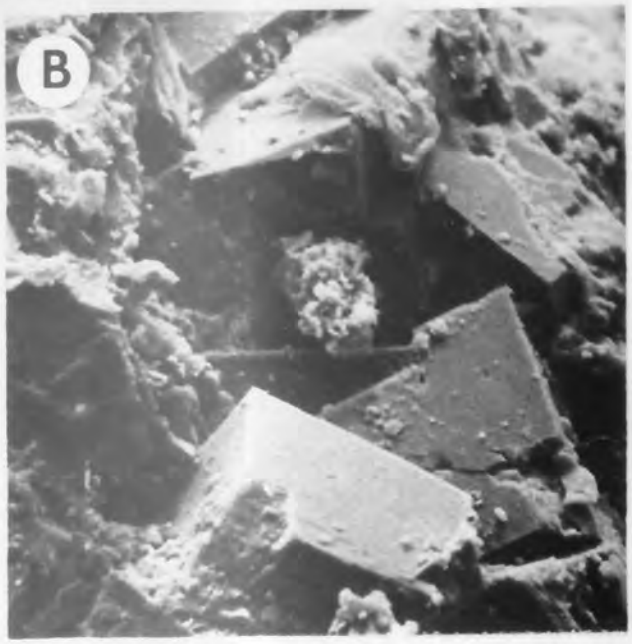

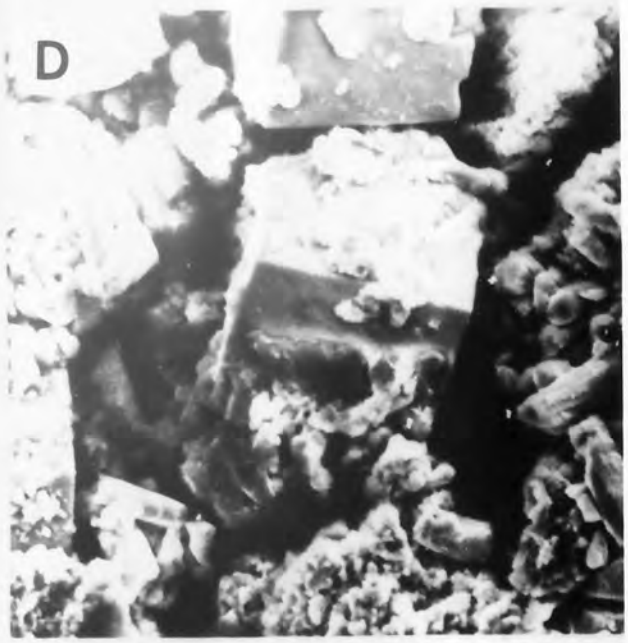

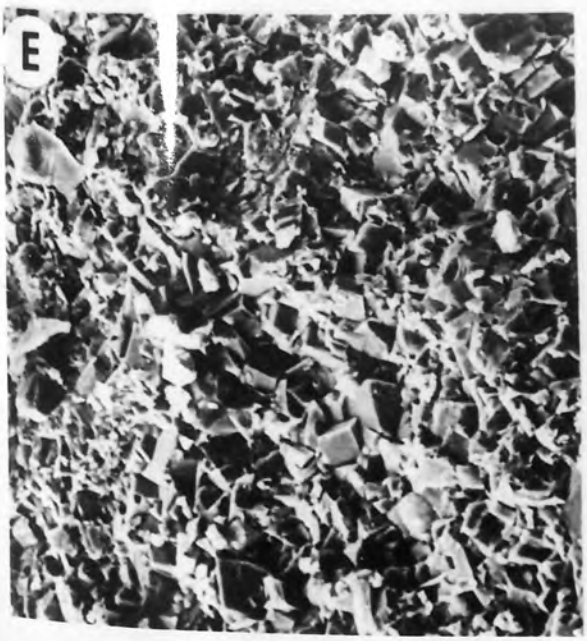

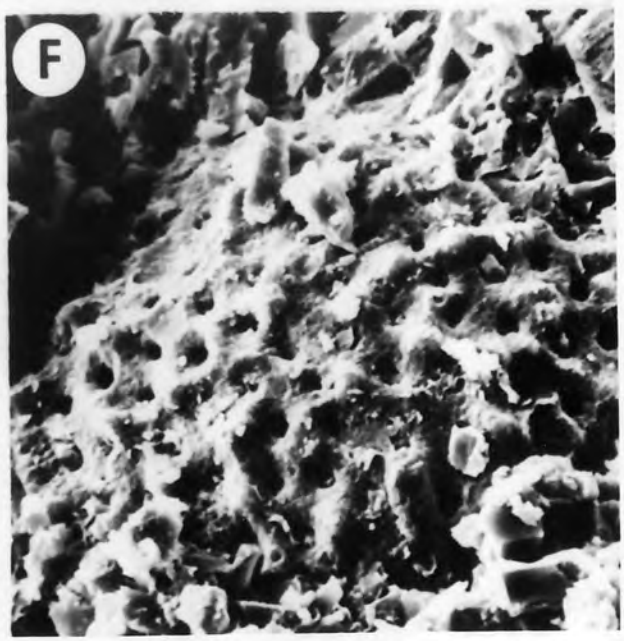

Plate 51 - Dolomite textures under SEM

A. Unorientated rhombic dolomite in a micritic matrix.
Sample N6 1755'6, Magnification X3200.

B. Growth zones of the dolomite rhomb are apparent. The dolomite is enveloped by clayey micrite.
Sample ZU-4 2661', Magnification X4000.

C. Undolomitised globogerinid in a dolomitised matrix. Sample D11 2352'6, Magnification X1500.

D. Spar-filled globogerinid in a dolomitised matrix.
Sample N6 1755'6, Magnification X1500.

E. An unaltered foraminifer in a slightly dolomitised matrix.
Sample N4 1675', Magnification X1500.

F. The matrix is a mixture of calcite spar, micrite and dolomite. In contrast to c-e, the matrix in which this foraminifer is embedded is of relatively coarse crystal size.
Sample D11 2352'6, Magnification X350.

PLATE 51

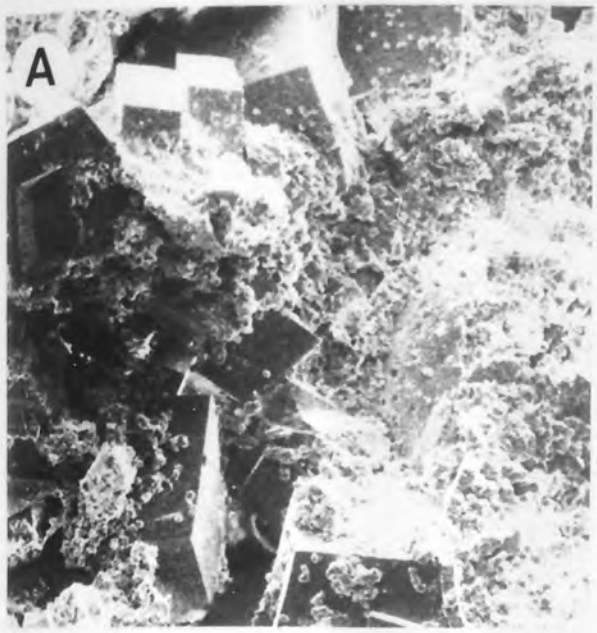

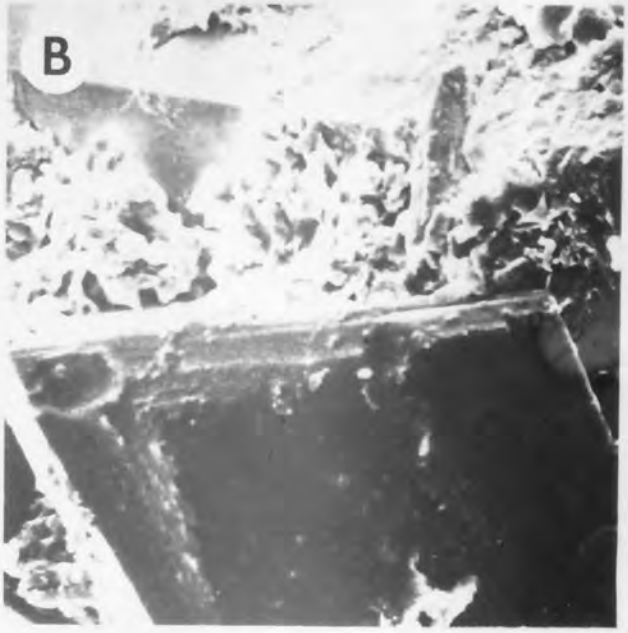

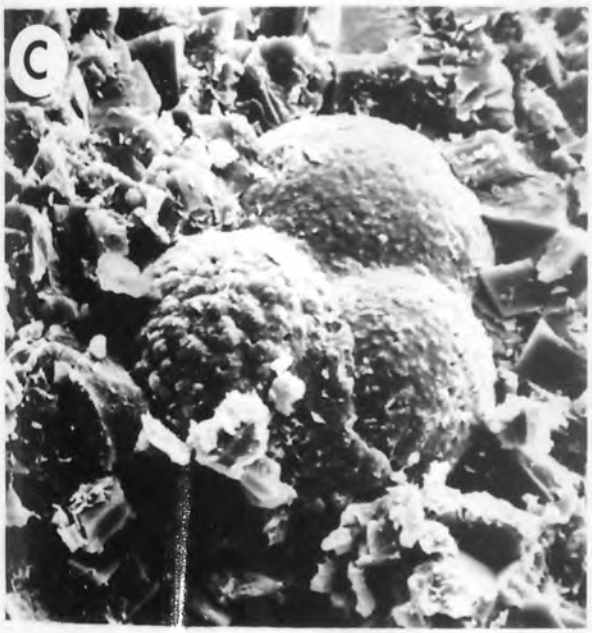

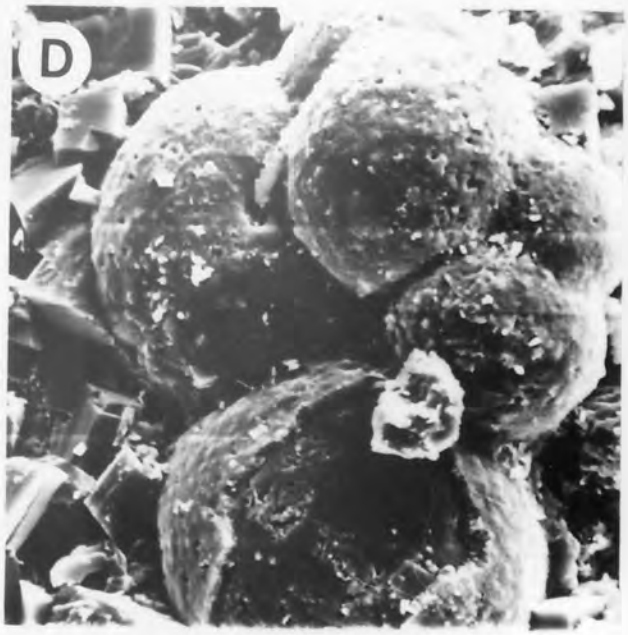

Plate 52 - Authigenic clays in dolomitised intervals, under SEM

A. Stringy authigenic illitic clays.
Sample D5 2473', Magnification X2500.

B. Similar to A. Such clays as these divide up pores, trap fine particles and impede permeability.
Sample N6 1775'6, Magnificaiton X2500.

C. Dolomite embedded in a micrite matrix.
Sample D5 2414'6, Magnification X1800.

D. Frilled ragged sheets of illitic clay.
Sample ZU4 2661', Magnification X5800.

E. Clays concentrated at the crystal boundaries of microspar. Insoluble impurities are expelled from the microspar during crystal growth and form residues around the crystal.
Sample D5 2414'6, Magnification X2000.

F. Clay rich slightly dolomitised porous limestone.
Sample D5 2410'6, Magnification X180.

PLATE 52

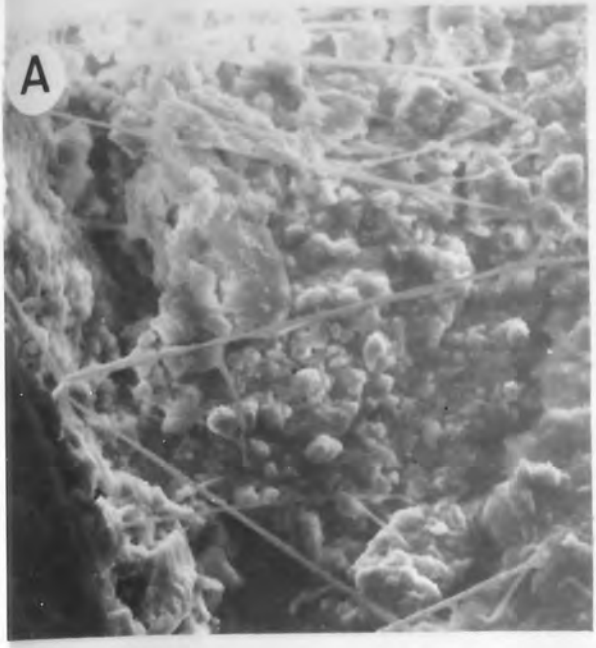

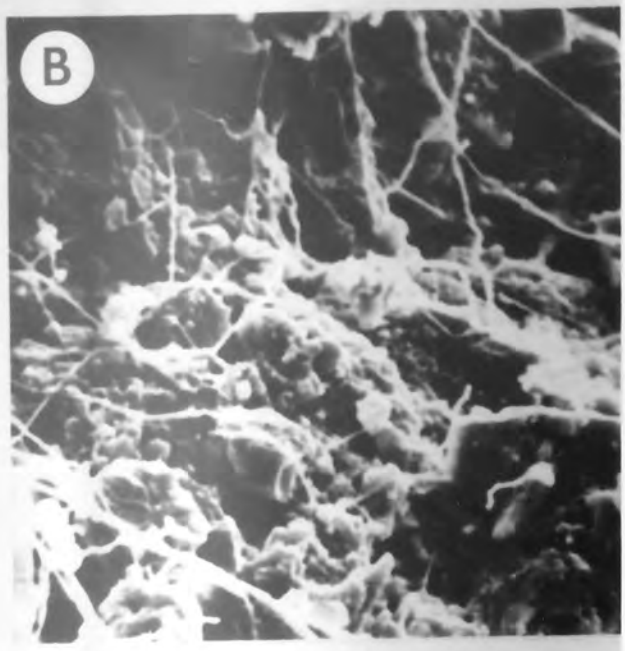

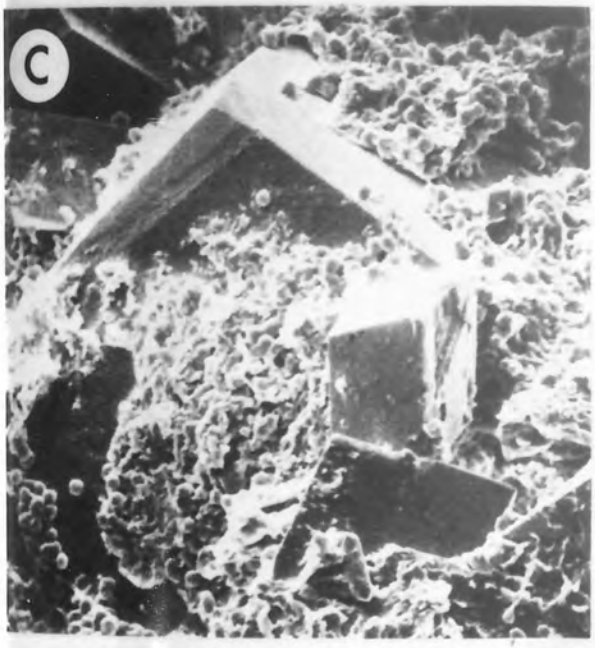

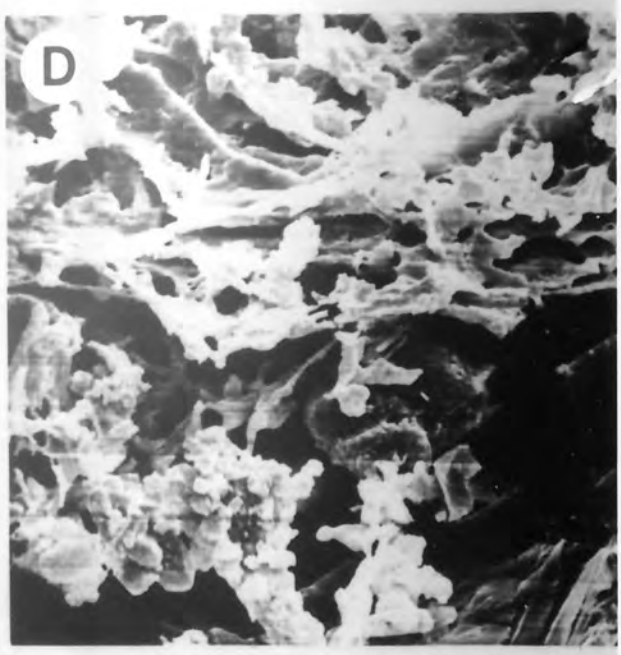

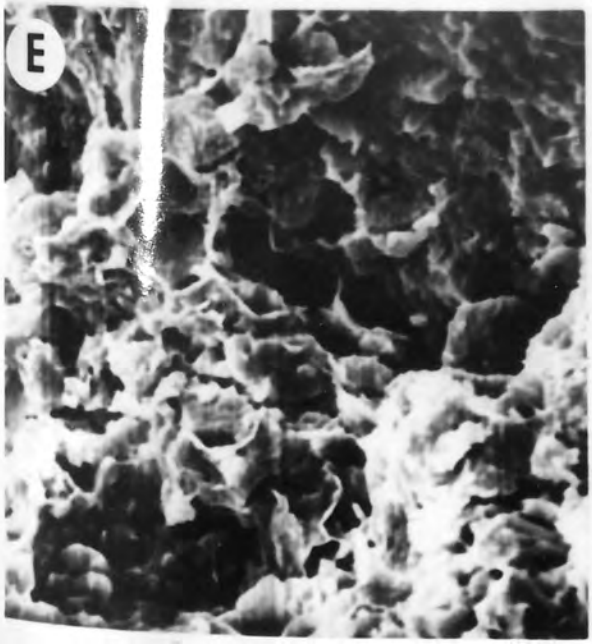

Plate 53 - Luminescent characteristics of dolomite crystals

A. Tightly interlocked hypidiotopic dolomite displaying a dull to medium bright orange core and a brightly luminescing marginal zone.
Sample ZU1 2588'4, Magnification X58.

B. Dolomite associated with leached patches. Rhombic crystals are finely zoned, alternating bright yellow-orange and medium bright orange.
Sample D5 2414'6, Magnification X58.

C. Highly porous open texture to dolomitised matrix. The rhombic crystals are slightly ragged-looking and may have suffered marginal leaching contemporaneous wiht the dissolution episode that removed the residual matrix. Micritised skeletal grains (top right) are undolomitised.
Sample ZU1 2631'9, Magnification X167.

D. Finely zoned dolomite rhombs in association with a leached interval.
Sample ZU1 2638'2, Magnification X58.

PLATE 53

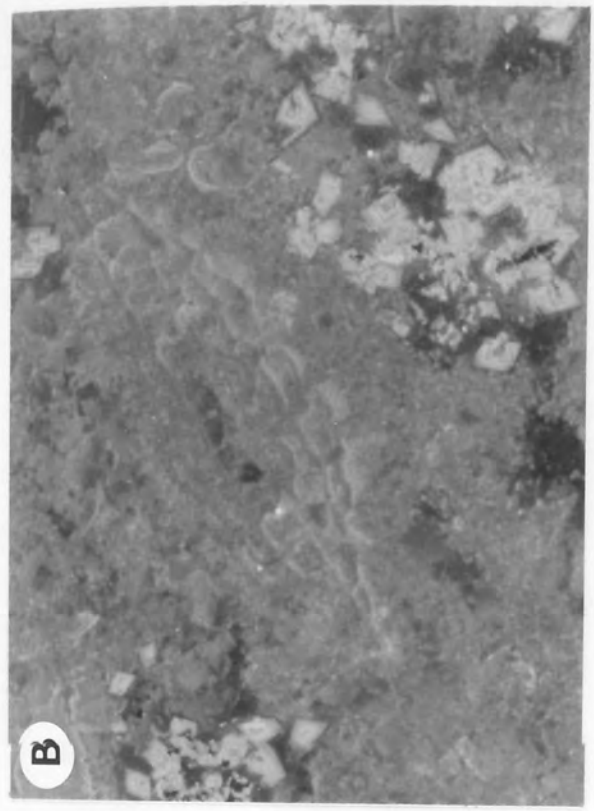

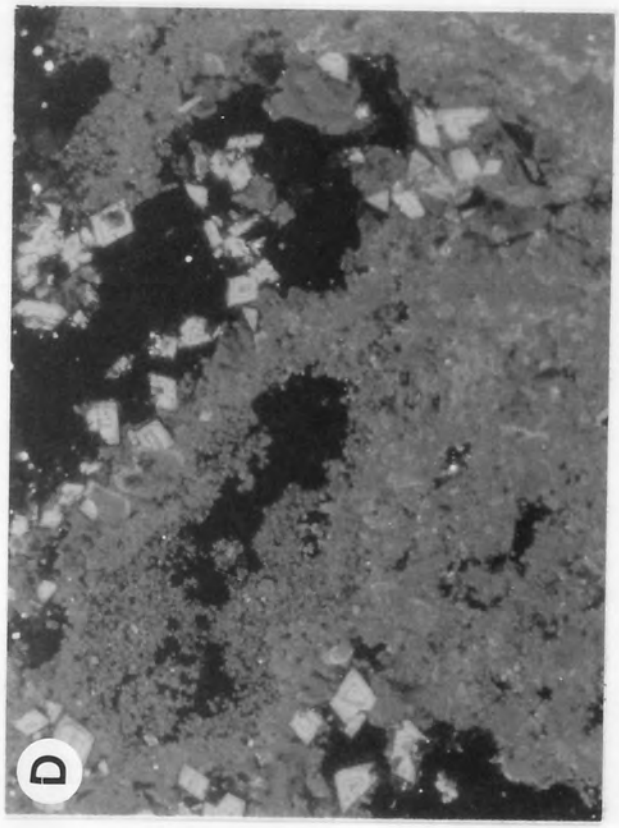

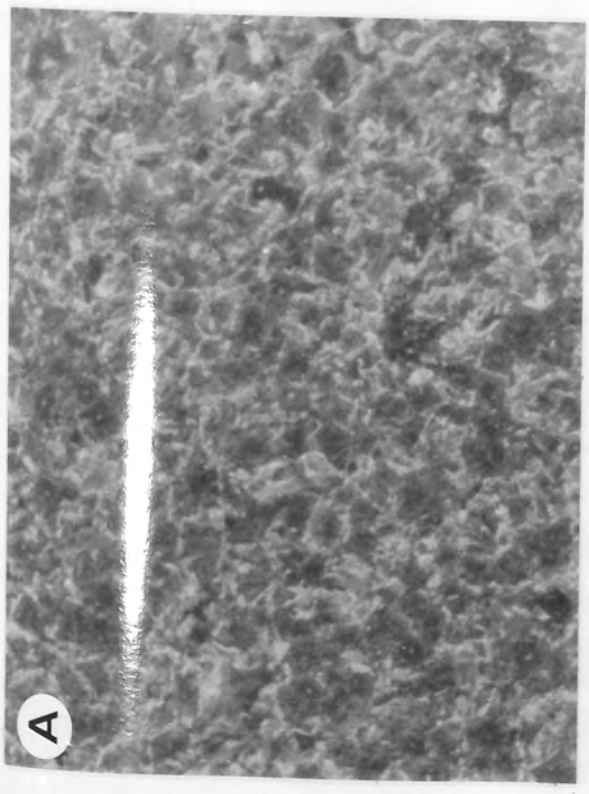

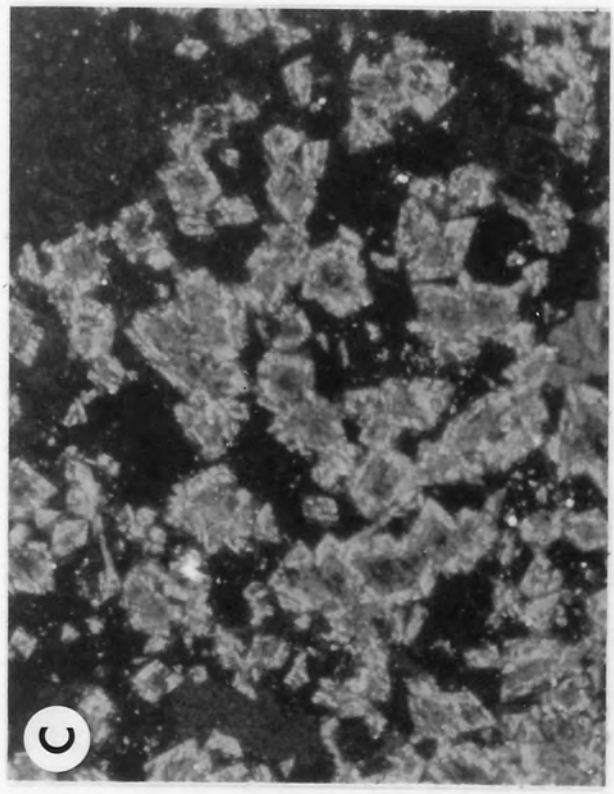

Plate 54 - Dolomite lining and replacing allochems

A. Dolomite nucleating on the boundary between the recrystallised coral and the dark slightly pelletal micrite filling intraskeletal pores. The dolomite grows preferentially into the coral.
Sample N6 1755'6, Magnification X167.

B. Dolomite concentrated on the boundary between recrystallised coral and the neomorphosed microspar. Dolomite grows both into the neomorphosed coral and microspar.
Sample N6 1755'6, Magnification X167.

C. Preferential dolomitisation of the slightly ferroan neomorphic spar. The unaggraded slightly pelletal micrite resists dolomitisation.
Sample N6 1755'6, Magnification X167.

D. Dolomite replacing ferroan spar within the coral is relatively coarse and clear compared with that replacing the micritic matrix.
Sample N6 1755'6, Magnification X167.

E. Dolomite in bored cavities within an amorphous algal fragment.
Sample Duma 5 2414'6, Magnification X58.

F. Dolomite growing within micritised allochems is coarser compared with that nucleating within the matrix.
Sample N6 1755'6, Magnification X58.

PLATE 54

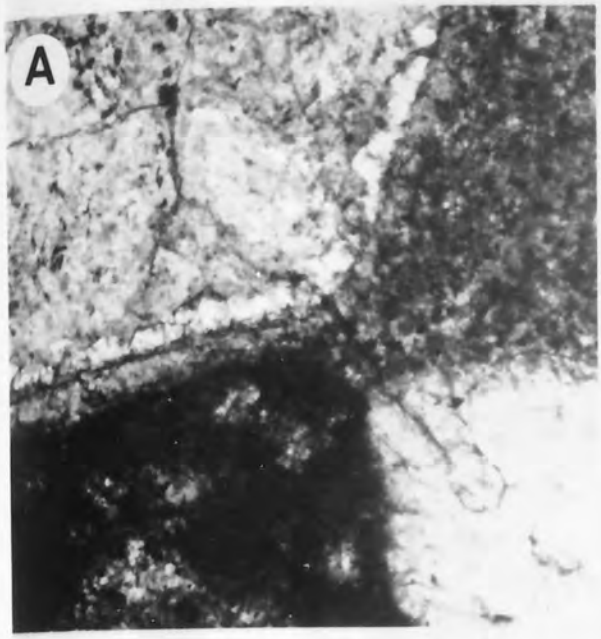

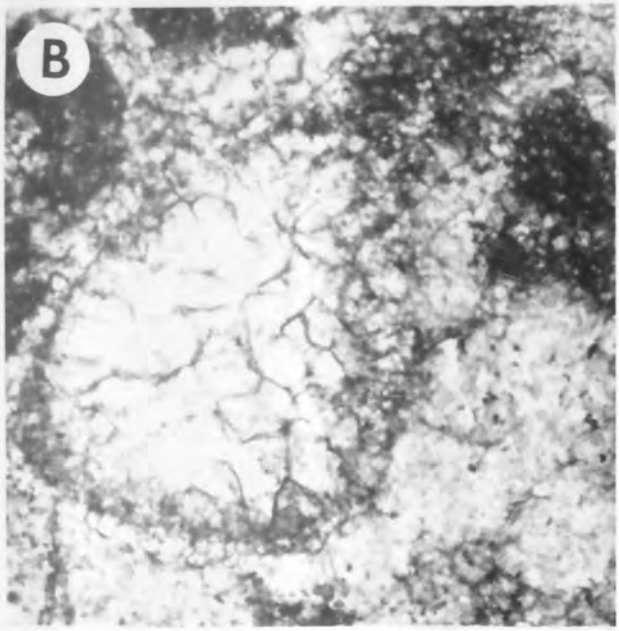

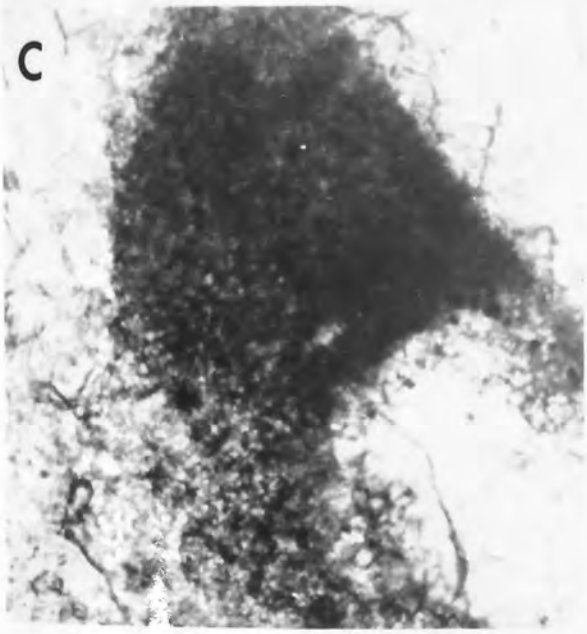

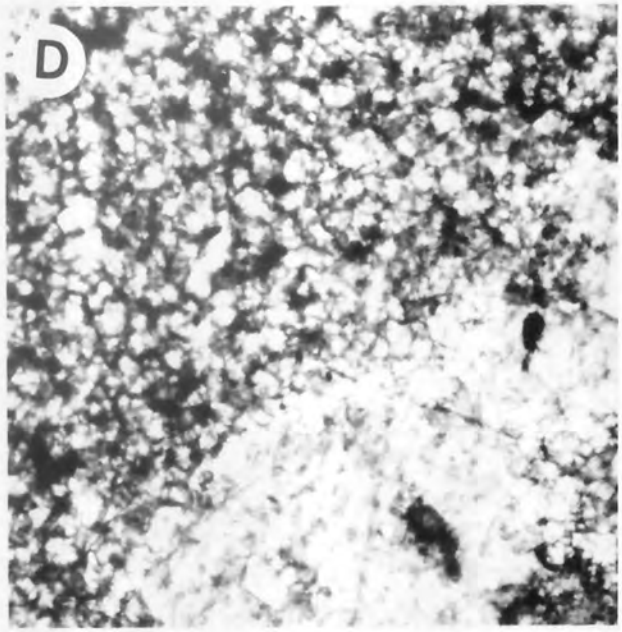

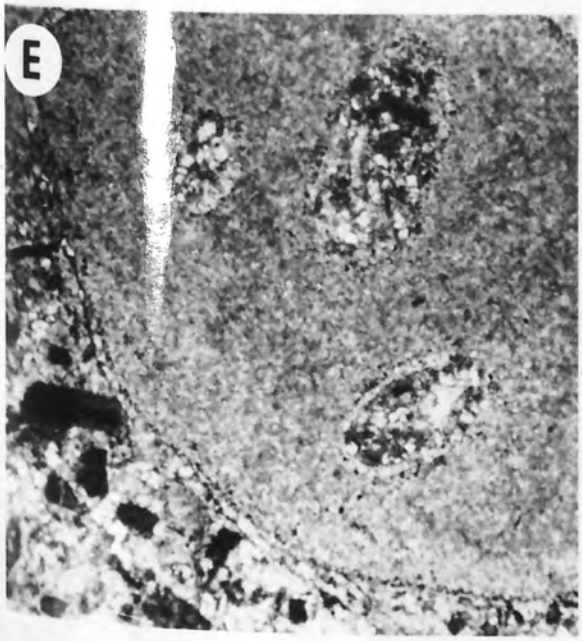

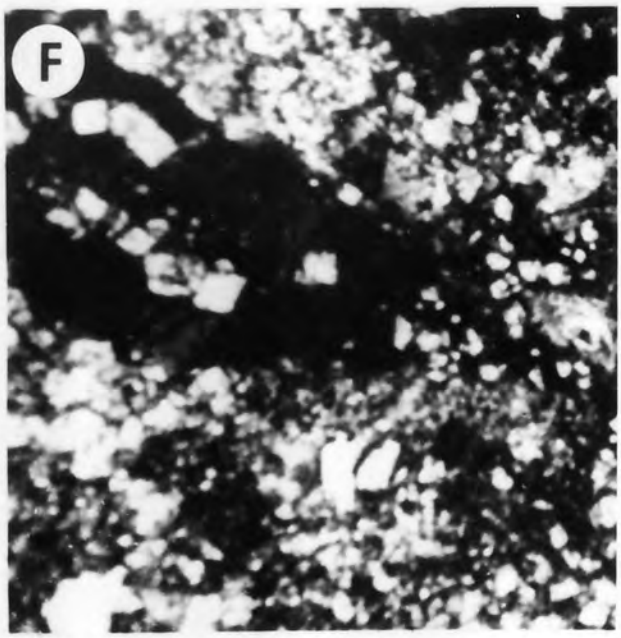

Plate 55 - Dolomitisation of allochems

A. Rhombs nucleating within a micritised skeletal fragment.
Sample N6 1755'6, Magnification X167.

B. Matrix entirely replaced by dolomite. A micritised foraminifer/algal fragment is being replaced.
Sample D11 2320', Magnification X49.

C. An impurity-rich pressure solution boundary between dolomitised limestone and neomorphic non-ferroan calcite. Rhombs encroach into the skeletal fragment at the pressure solution boundary.
Sample N6 1755'6, Magnification X58.

D. Rhombic dolomite replacing micritic matrix and nucleating within skeletal cavities (bottom left).
Sample D11 2320', Magnification X42.

E. Dolomite rimming a micritised skeletal fragment (possibly algal).
Sample D5 2473', Magnification X58.

F. Allochem enitrely replaced by rhombic dolomite. This is a very unusual texture. The matrix is a mixture of fine hypidiotopic dolomite and micrite.
Sample N4 1675', Magnification X58.

PLATE 55

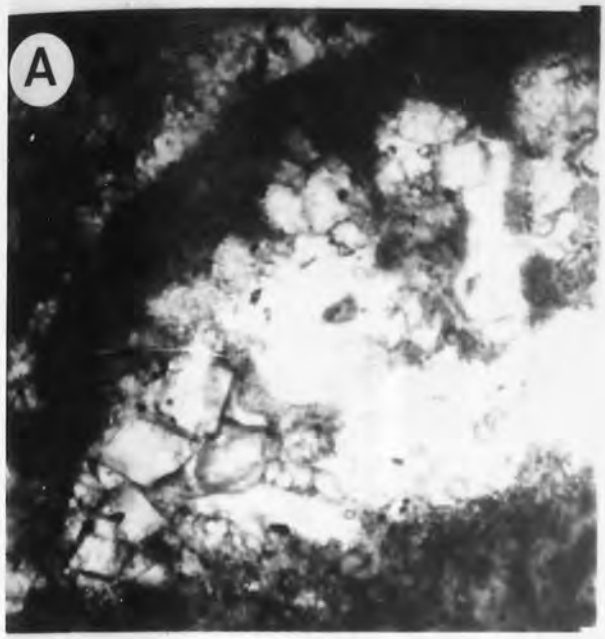

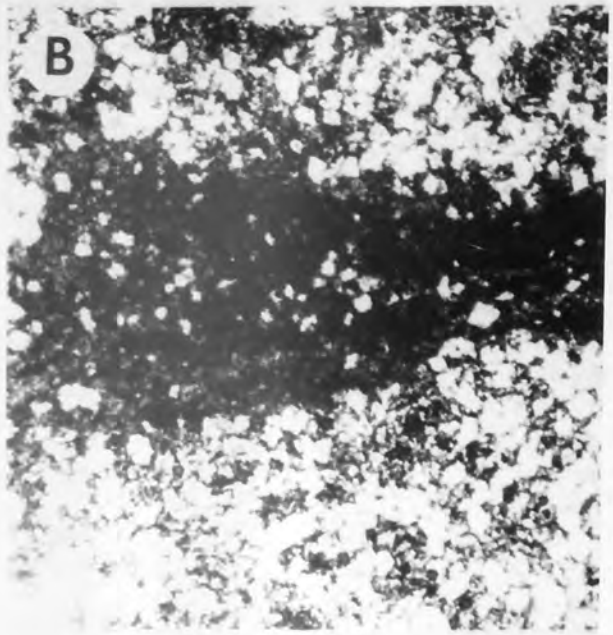

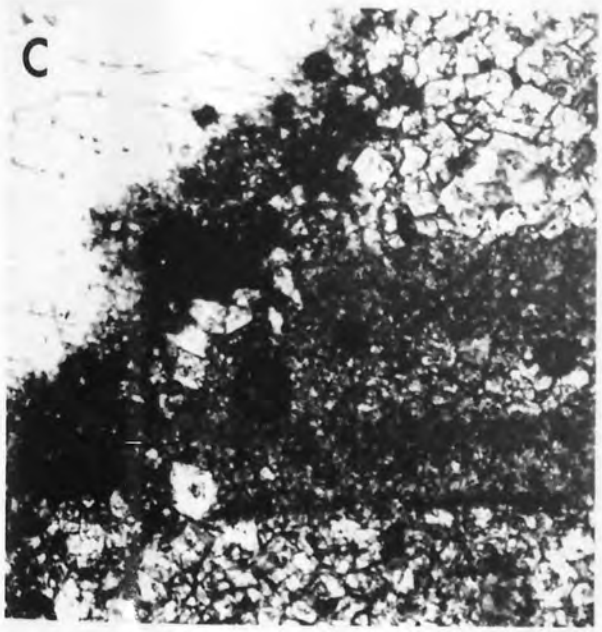

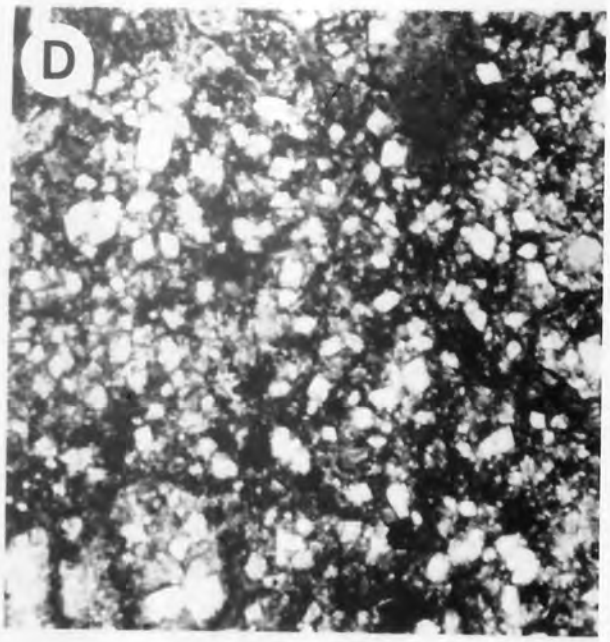

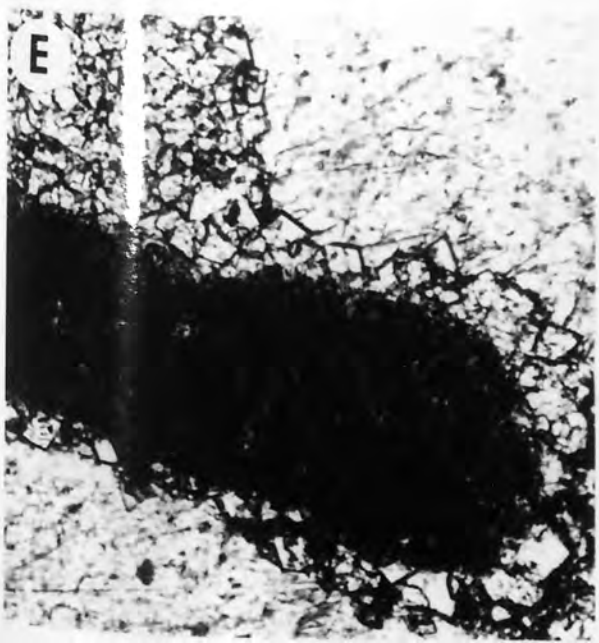

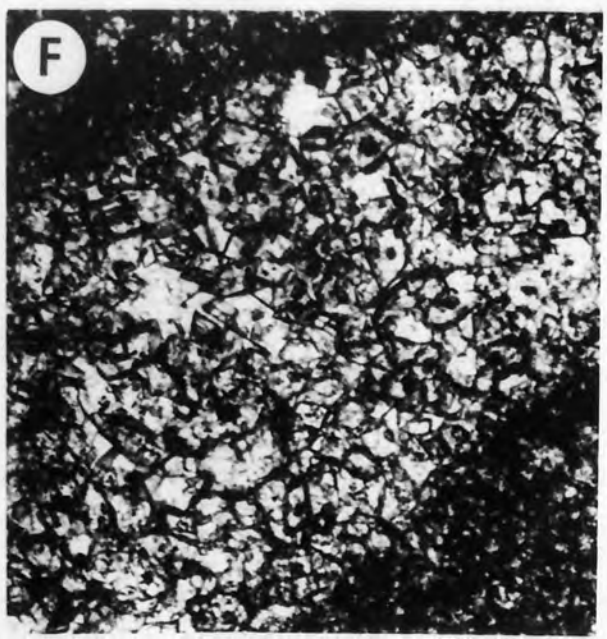

Plate 56 - Dolomite pseudomorphing selenite, and replacement of sparry calcite

A. Lozenge-shaped dolomite pseudormorphing selenite in coral mouldic porosity.
Sample ZU-1 2627'4, Magnification X42.

B. Lozenges are commonly orientated at a high angle to the margins of the pore or dessication crack in which they occur. The lozenges are enclosed within poikilotopic ferroan calcite.
Sample ZU-1 2627'4, Magnification X42.

C. Lozenge displaying an inclusion filled core.
Sample ZU-1 2627'4, Magnification X167.

D. Lozenges in dessication cracks.
Sample ZU-1 2627'4, Magnification X58.

E. Rhombic dolomite replacing bladed sparry calcite encrusted on a foraminifer. Rhombs nucleate on crystal boundaries.
Sample N6 1759'11, Magnification X167.

F. Rhombs replacing slightly ferroan neomorphic sparry calcite. Replacement initiates on the boundaries of the neomorphic crystals.
Sample N6 1759', Magnification X58.

PLATE 56

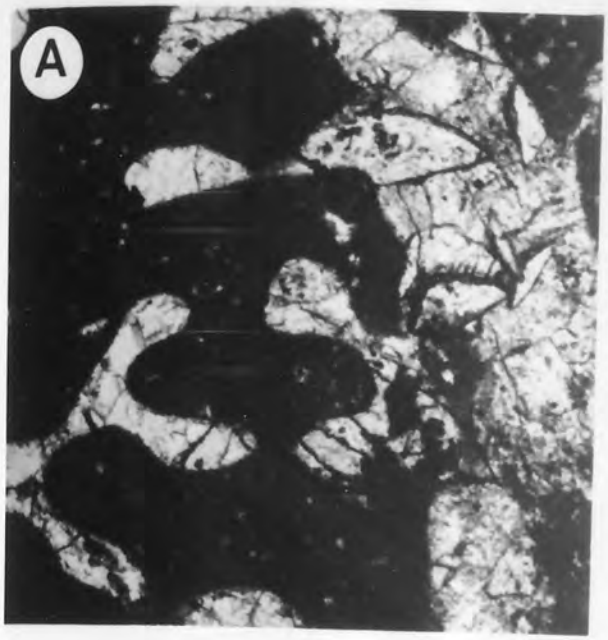

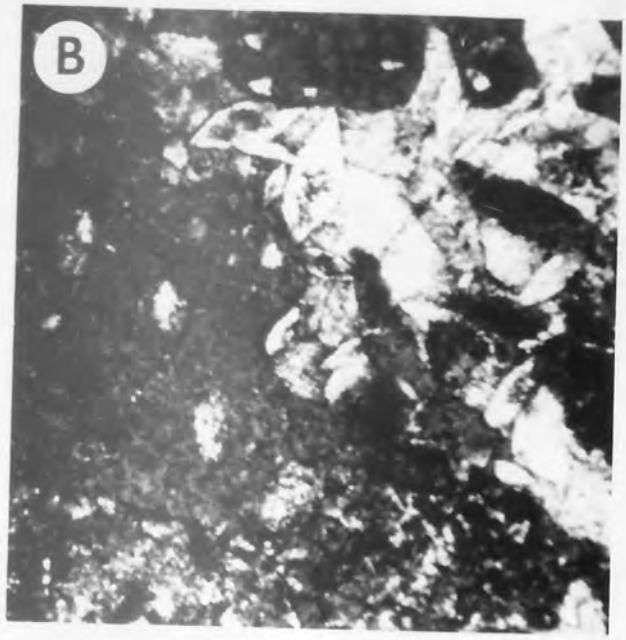

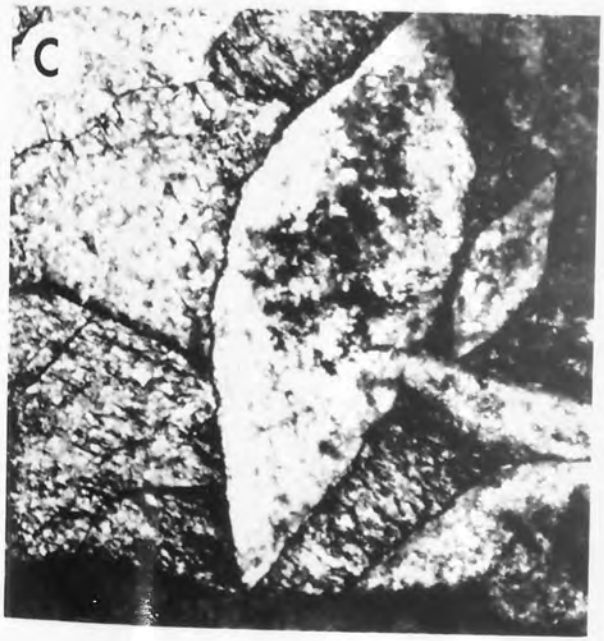

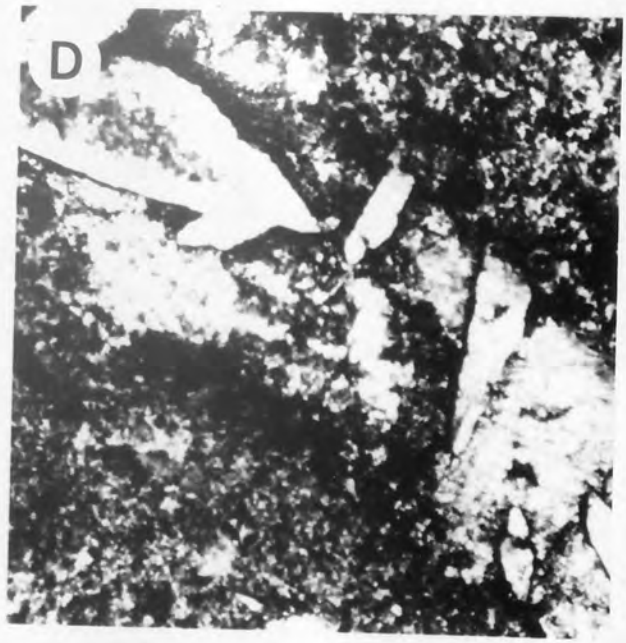

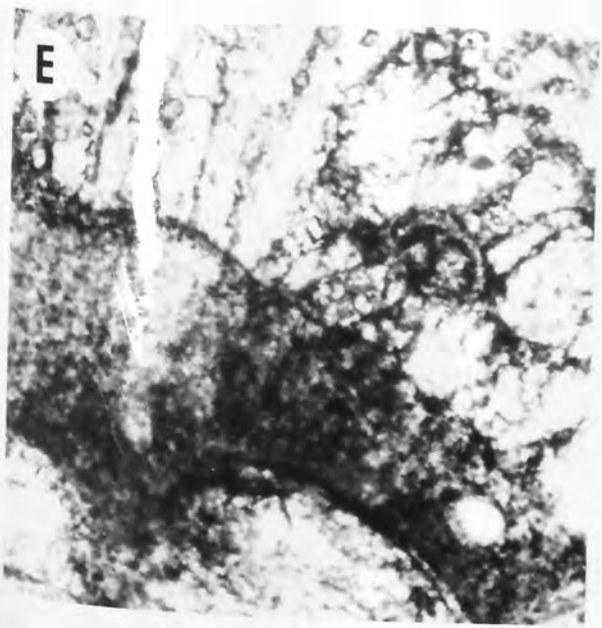

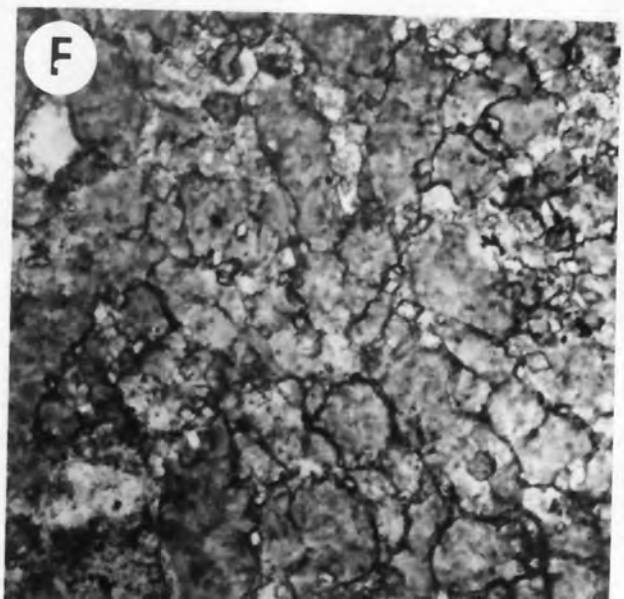

Plate 57 - Occurrence and distribution of ferroan and non-ferroan calcite

A. Slightly ferroan radiating equant-bladed cements on an echinoderm and foraminifer.
Sample N6 1759'11, Magnification X42.

B. Dolomite growing into slightly ferroan neomorphic spar. The coarse non-ferroan interstitial sparry calcite results from aggrading recrystallisation of a former micritic matrix. Granular impure microspar is visible in the tope right of the photograph.
Sample N6 1755'10, Magnification X167.

C. Mouldic pores infilled with slightly ferroan calcite. The matrix is entirely dolomitised and dolomite is visible within the calcite cement in the bottom left of the photograph.
Sample N6 1755'6, Magnification X42.

PLATE 57

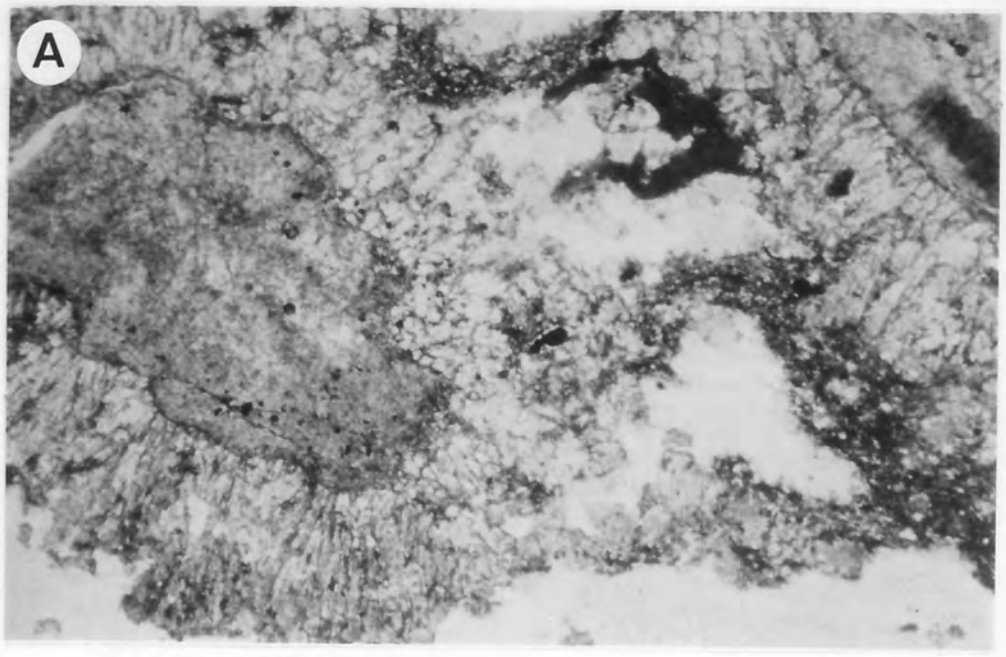

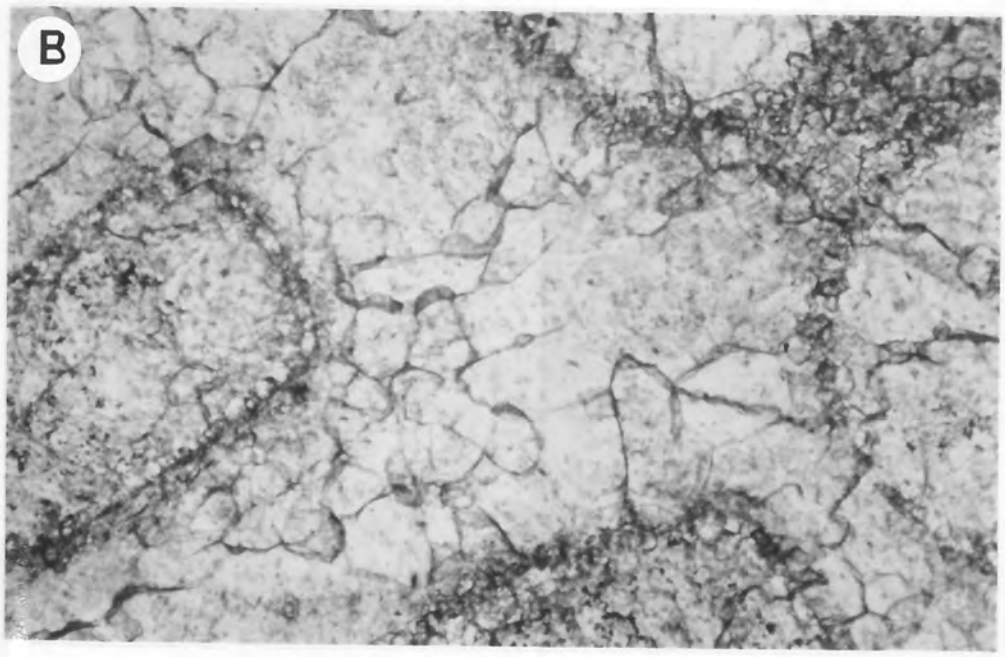

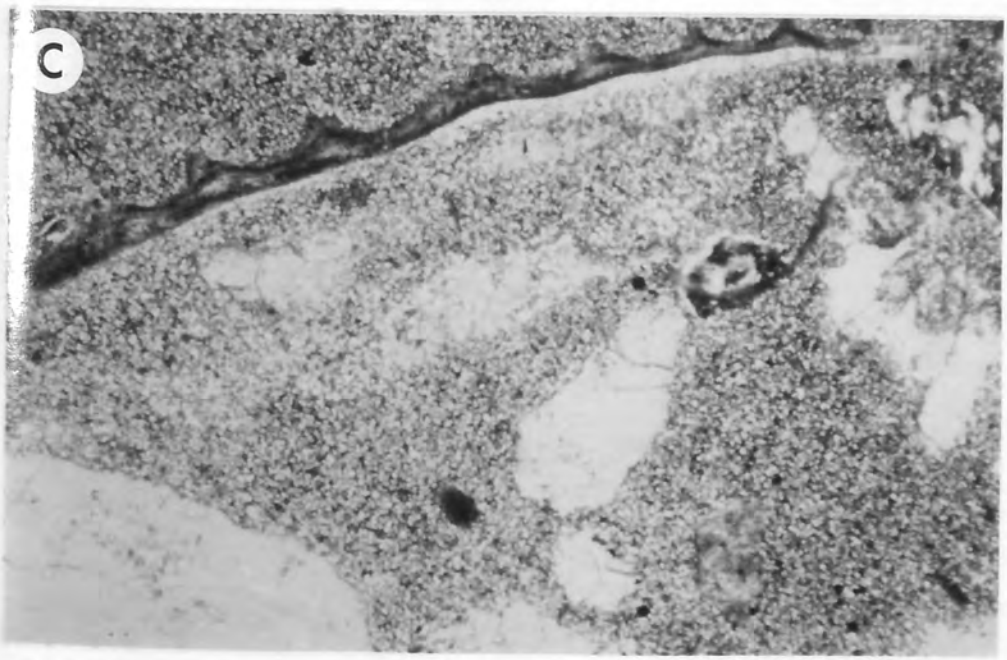

Plate 58 - Occurrence and distribution of ferroan and non-ferroan calcite

A. A thick-walled calcite-filled benthic foraminifer. The margins of the intraskeletal cavity are lined with non-ferroan calcite and this merges into ferroan calcite which comprises the remainder of the mosaic.
Sample D5 2414'6, Magnification X49.

B. Mottled rhombic ferroan calcite partly filling an extensive secondary pore network.
Sample D3 2403'6, Magnification X42.

C. Non-ferroan bladed cement on an echinoid fragment. The echinoid is ferroan calcite suggesting that the rim cement was precipitated prior to the infilling of the echinoderm micropores with ferroan calcite.
Sample D3 2390, Magnification X42.

PLATE 58

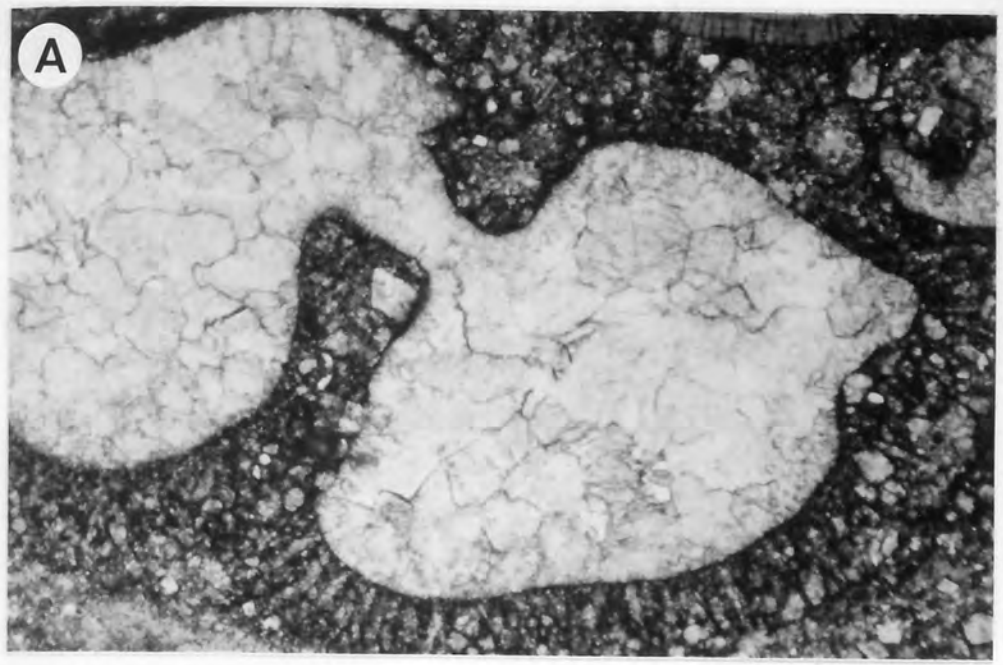

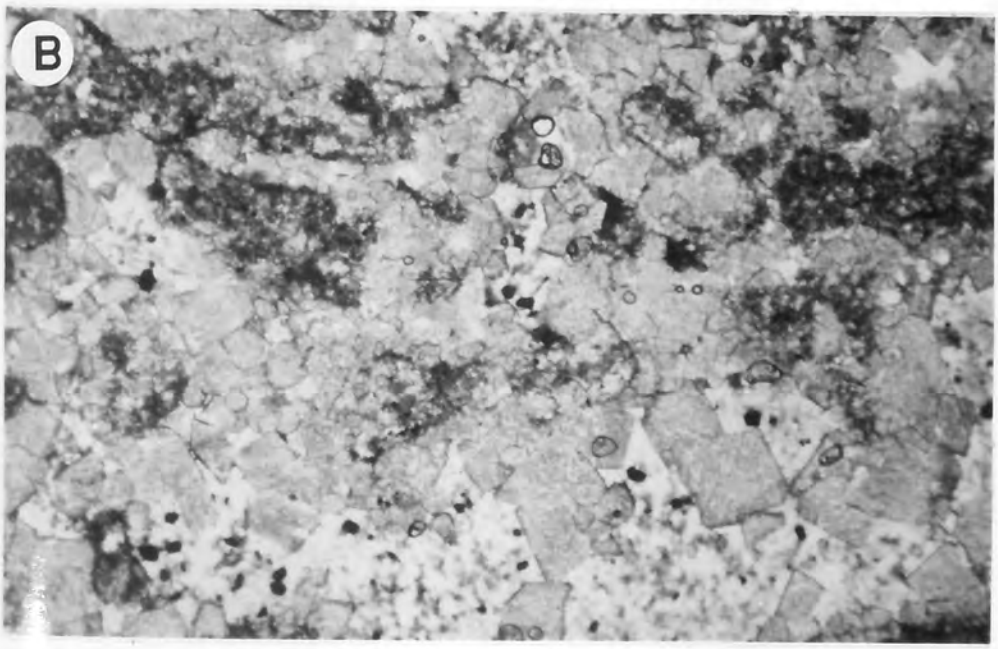

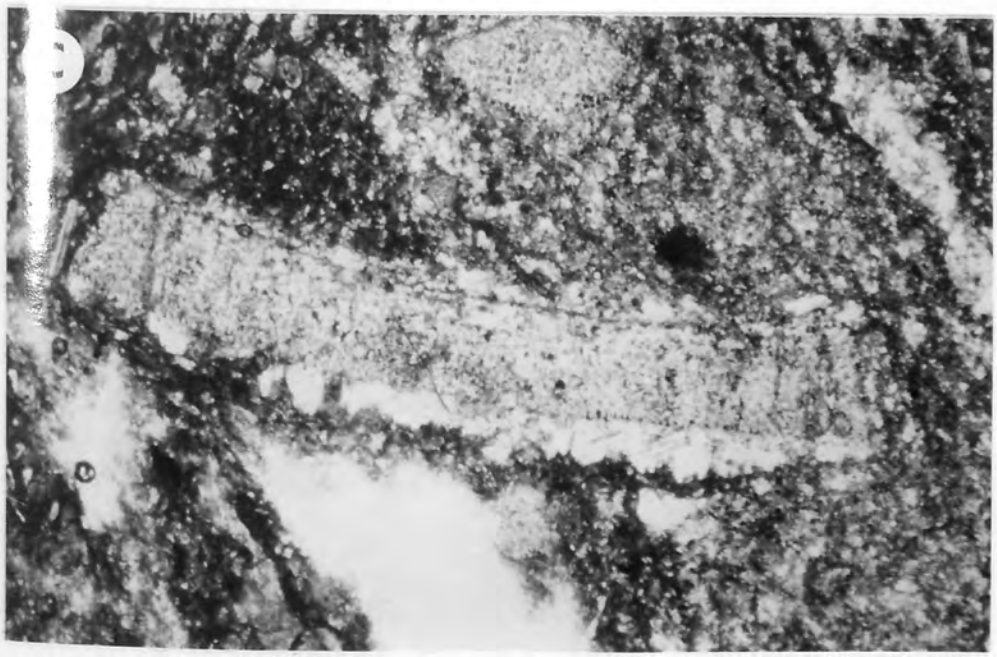

Plate 59 - Mouldic solution porosity

A. Mouldic Type II (Dodd 1966) solution porosity. The mould at the top is partly infilled with secondary calcite. The large pore (centre) may be due to plucking during thin-section preparation.
Sample D9 2288'6 Magnification X42.

B. Cellular Type II (Dodd 1966) porosity resulting from the presence originally of scattered metastable grains. Original grain type is indeterminable.
Sample D5 2403' Magnification X42

C. Isopachous poikilotopic syntaxial cement and enclosed echinoderm grain resist dissolution. The surrounding oversized pores result from enlarged mouldic. Note cement partially rimming micritised grain (top centre).
Sample D2 2803' Magnification X49

D. Filled and unfilled mouldic type II pores. The algal fragment (bottom left) is relatively insoluble.
Sample D2 2803' Magnification X42

E. Occluded mouldic solution pores. The dark grains are fragments of rhodolithic algae.
Sample D11 2334' Magnification X42.

F. Infilled solution mouldic pores.
Sample D11 2334' Magnification X42.

PLATE 59

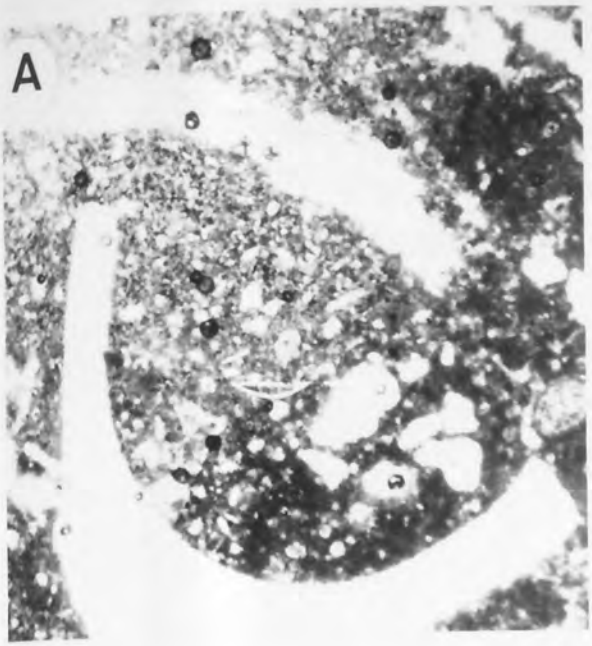

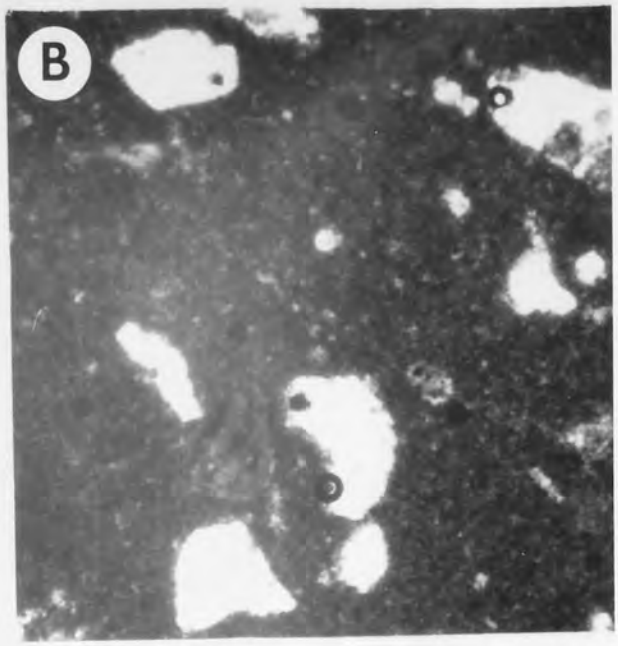

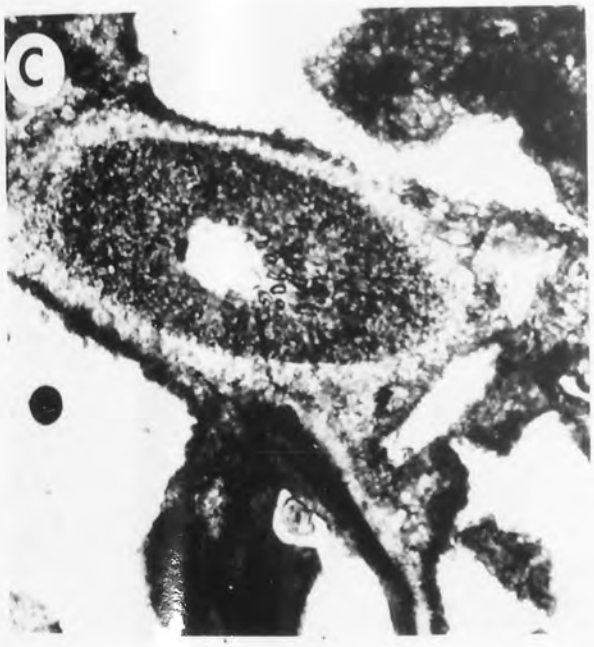

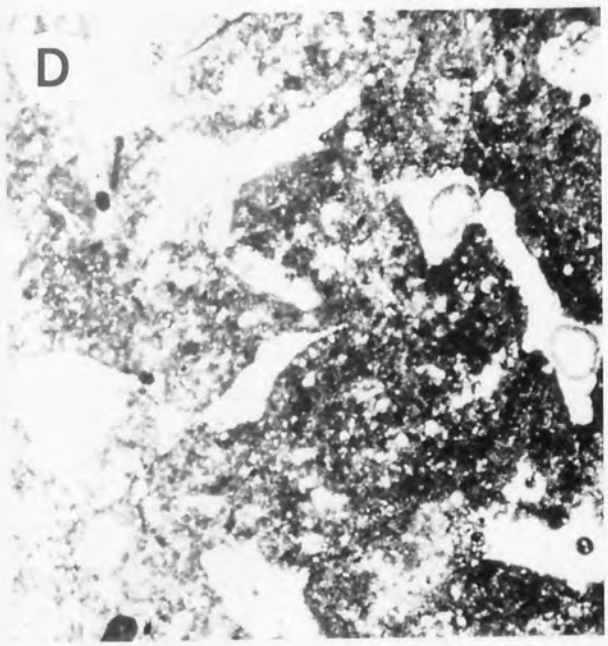

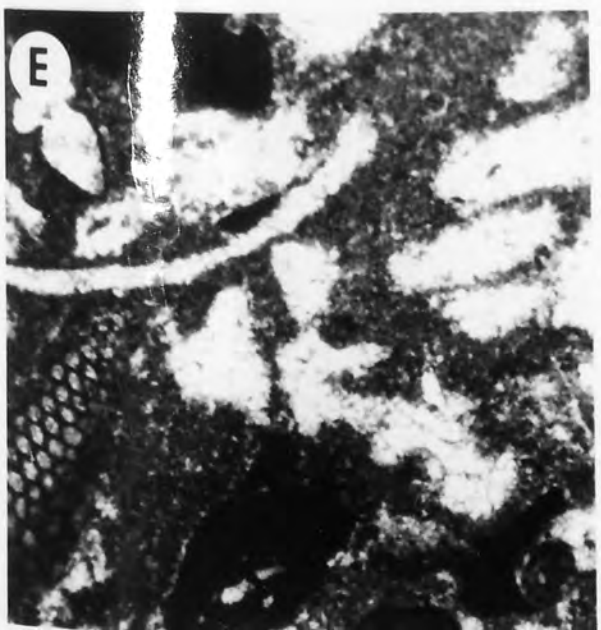

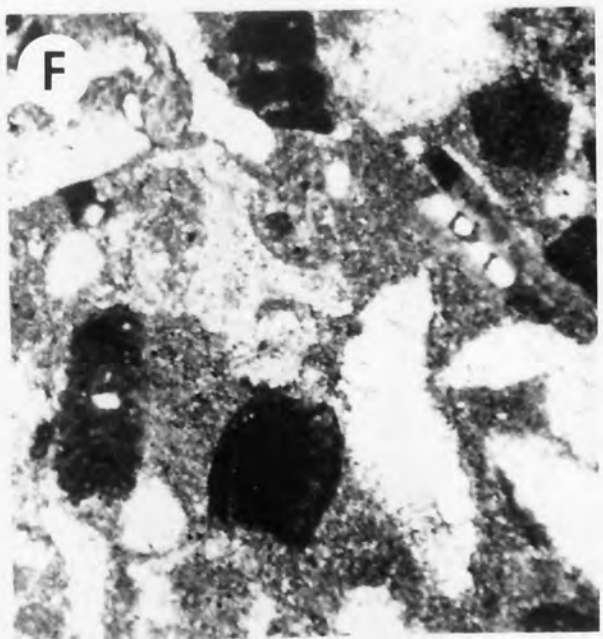

Plate 60 - Dissolution and neomorphic textures in allochems

A. Recrystallised coral. Crystals do not cross-cut the original skeletal walls. Sclerites are clearly preserved and outlined by micrite envelopes and the interstitial area is occupied by a mixture of microspar and coarse sparry calcite.
Sample D5 2529', Magnification X42.

B. Coral undergoing solution infilling.
Sample D5 2428', Magnificaiton X42.

C. Fenestrate calcitic thick-walled bryozoan encrusting a coral (not visible). The fibrous wall structure is well preserved and finely crystalline calcite within zooeicia prevents them from collapsing from overburden compaction.
Sample D11 2348', Magnification X42.

D. Solution-infill replacement of a gastropod and several unidentifiable fragments. The micrite infilling the mollusc has aggraded to microspar whilst that comprising the interstital matrix has not. The matrix micrite has a pelletal texture. Opaque grains are calcareous algae.
Sample D11 2334', Magnification X42.

E. Irregular dissolution and infilling with calcite results in a patchwork appearance. The infilling calcite is finely crystalline on the margins of pores and coarsens inwards (Bathurst, 1958 "drusy" texture).
Sample D9 2283'6, Magnification X42.

F. Coral mouldic porosity occluded by a calcite mosaic. Prior to dissolution of the original aragonite, the matrix must have been at least semi-lithified in order to support the void prior to its infilling.
Sample D9 2283'6, Magnification X42.

PLATE 60

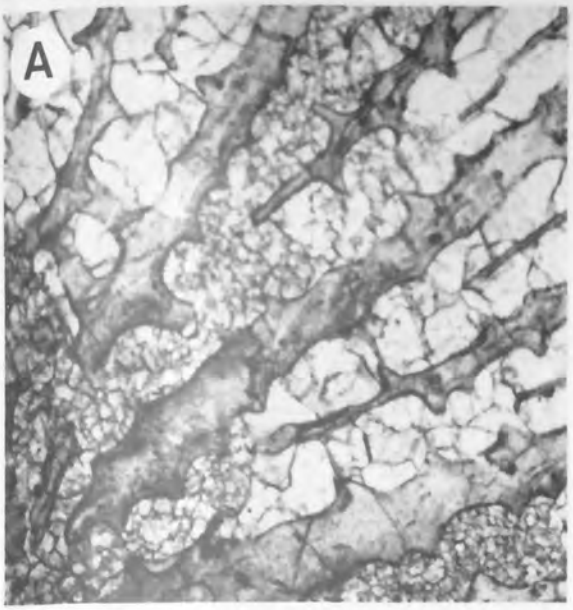

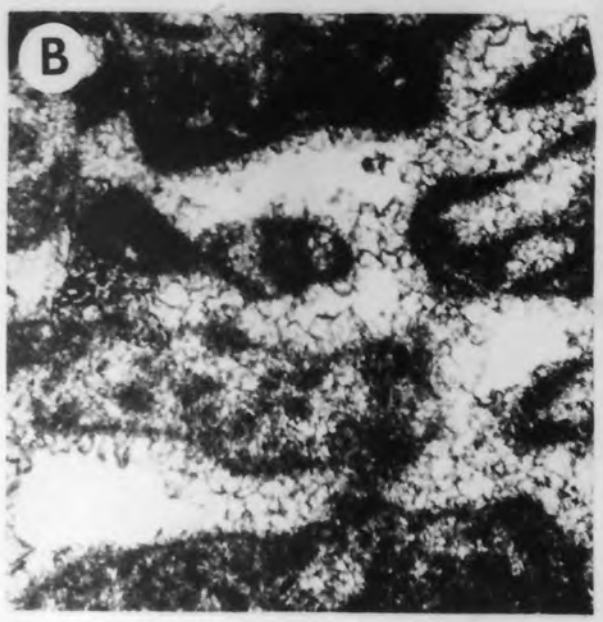

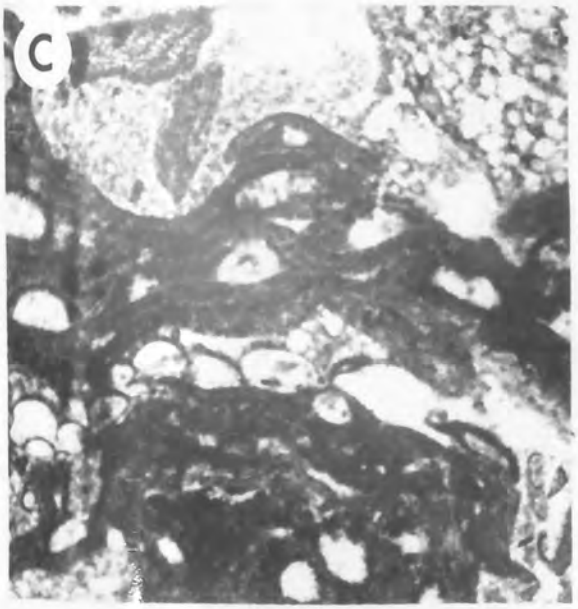

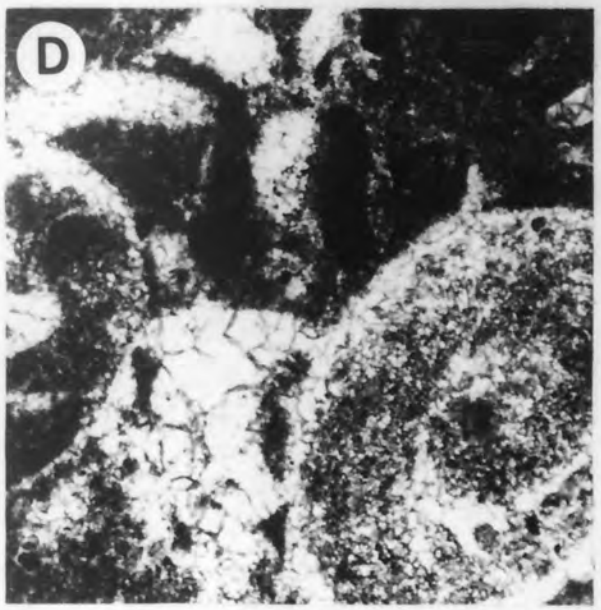

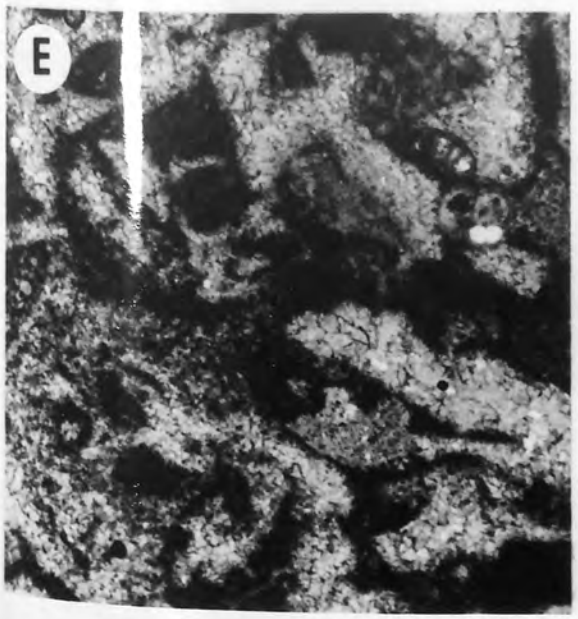

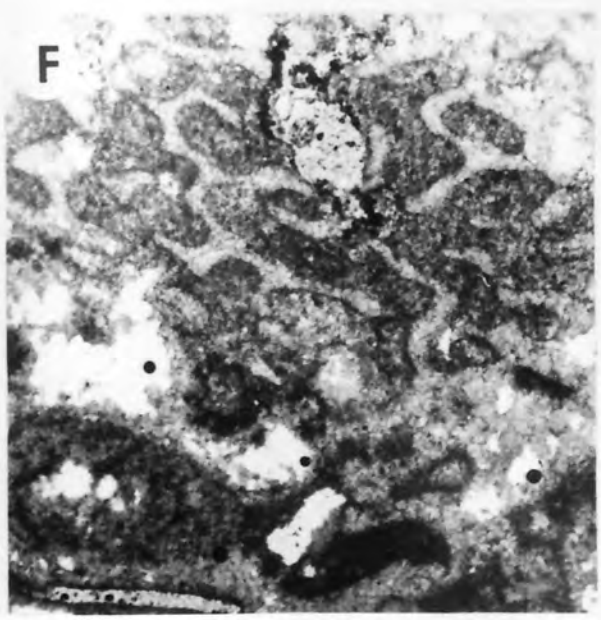

Plate 61 - Selective dissolution textures

A. Micritic envelopes remain intact in a largely recrystallised lithology. The circular cross-section may formerly have been a delicate calcisphere.
Sample D3 2403'6 Magnification X167.

B. Micrite filled coral. The coral dissolution pore has been infilled first with a crust of cement, and subsequently with equant space-filling calcite. The first generation is poikilotopic.
Sample D 2291' Magnification X58.

C. Mouldic pore occluded by cement is defined by a micrite envelope. Pores in top right and bottom left are unfilled. The foraminifera are relatively insoluble.
Sample ZU-1 2588'4 Magnification X42.

D. Intrafabric dissolution of an echinoid fragment. The dissolution porosity is partly filled with ferroan calcite on the margins of the grain.
Sample ZU-1 2587'8 Magnification X42.

E. Oil migration front corresponds with a dissolution front. Beyond the area of the stain no mouldic porosity is developed.
Sample D2 2803' Magnification X42.

F. Foraminifera are resistant to dissolution in a largely dissolved sample. Residual skeletal grains provide a delicate support.
Sample ZU-1 2617' Magnification X42.

PLATE 61

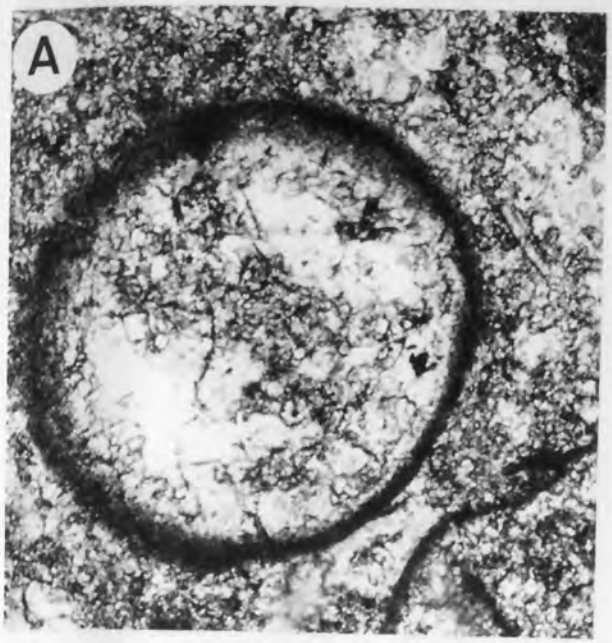

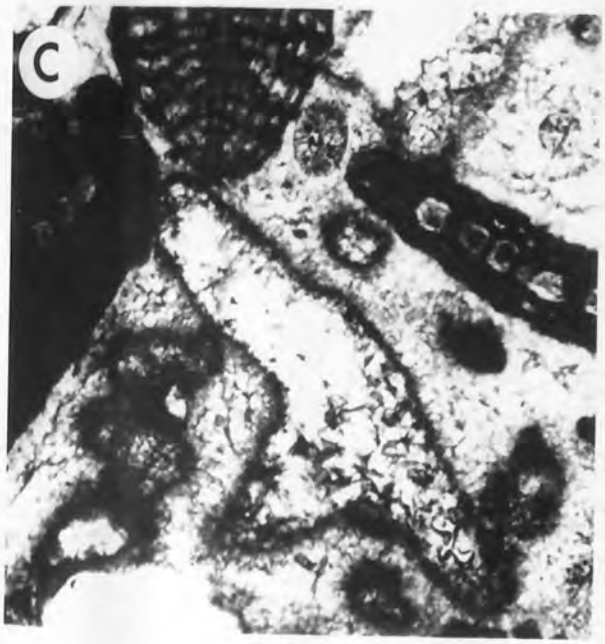

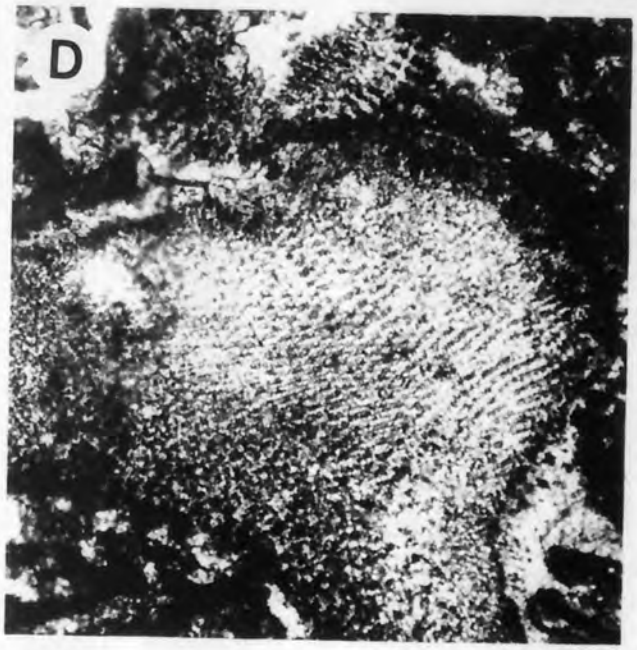

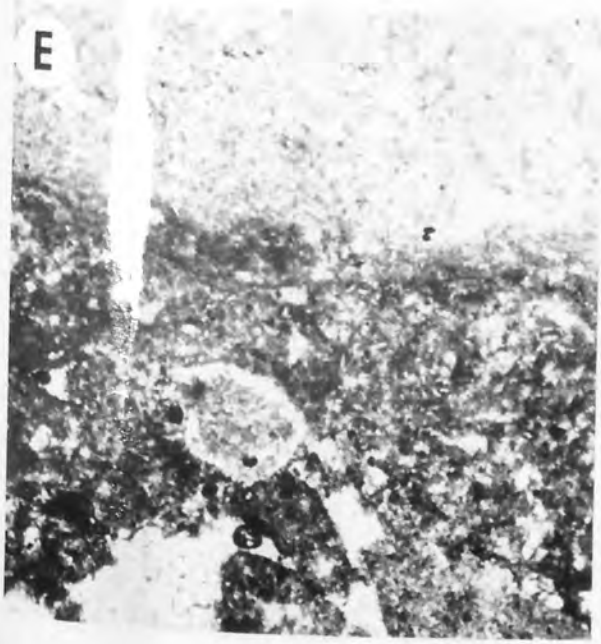

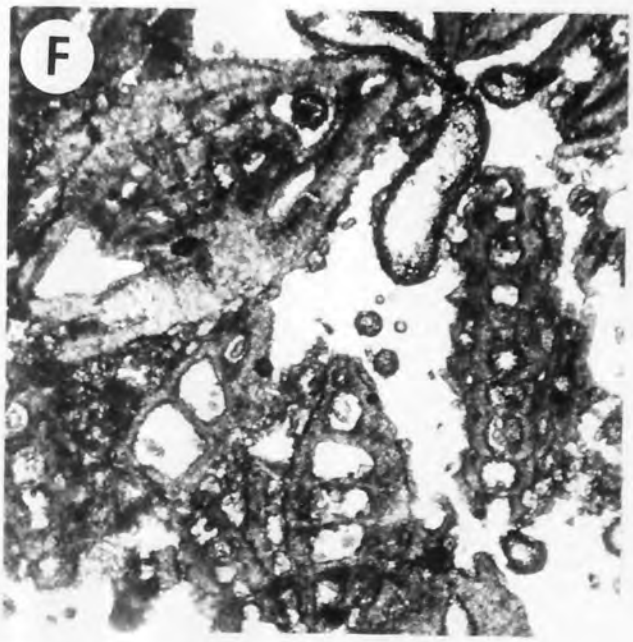

Plate 62 - Solution infilling and micrite neomorphism

A. Vuggy and mouldic pores undergoing infilling. Allochems (mainly algae) are defined by relict micrite envelopes.
Sample N4 1755'6 Magnification X42.

B. Partly occluded mouldic dissolution porosity.
Sample N6 1674' Magnification X42.

C. Fragments are partly resorbed into the matrix which is a mixture of micrite and microspar.
Sample D2 2820'6 Magnification X42.

D. Microspar grading patchily into neomorphic sparry calcite. Residual micrite is removed by dissolution. High vuggy matrix porosity, part-filled with calcite.
Sample D3 2403'6 Magnification X58.

E. Borings in intraclast.
Sample D2 2820'6 Magnification X42.

F. Obliteration of a packstone texture by recrystallisation and resorbtion of grains into the matrix. Pyrite fills some dissolution pores. The skeletal fragments are barely discernible largely through the distribution of impurities are through crystal size.
Sample D2 2815' Magnification X49.

PLATE 62

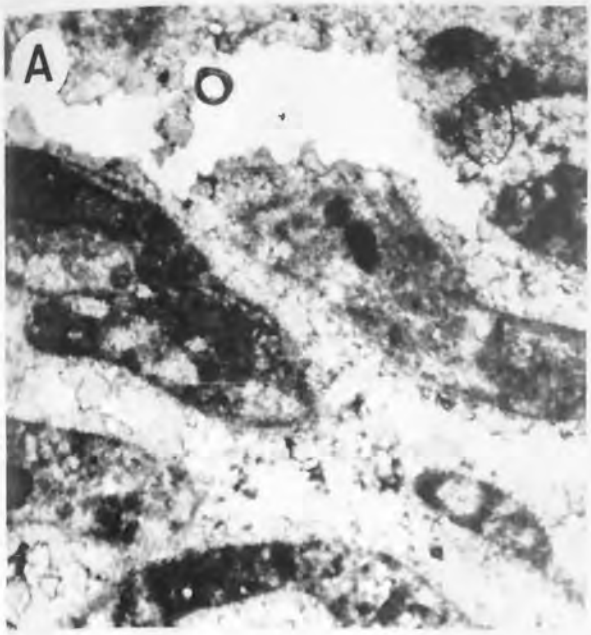

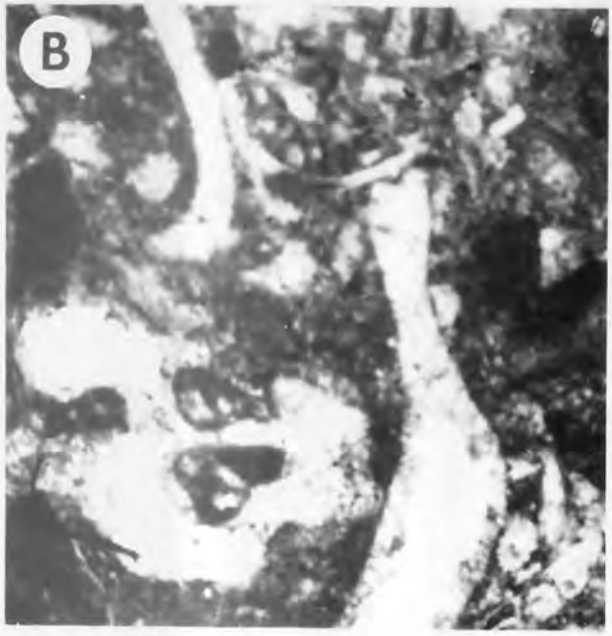

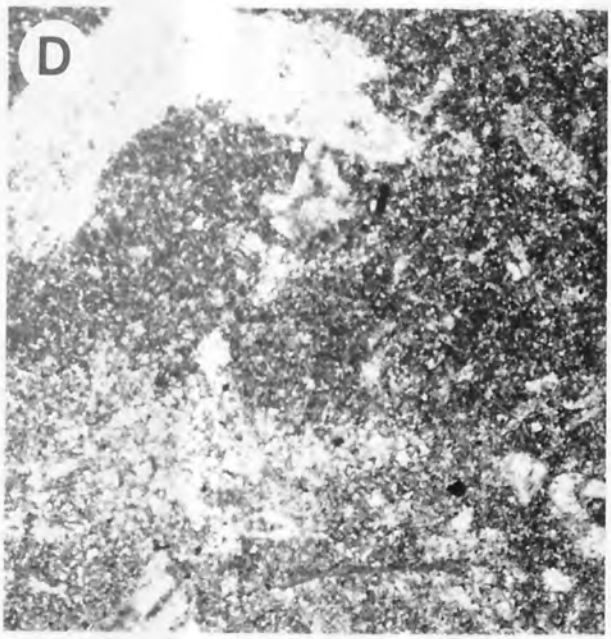

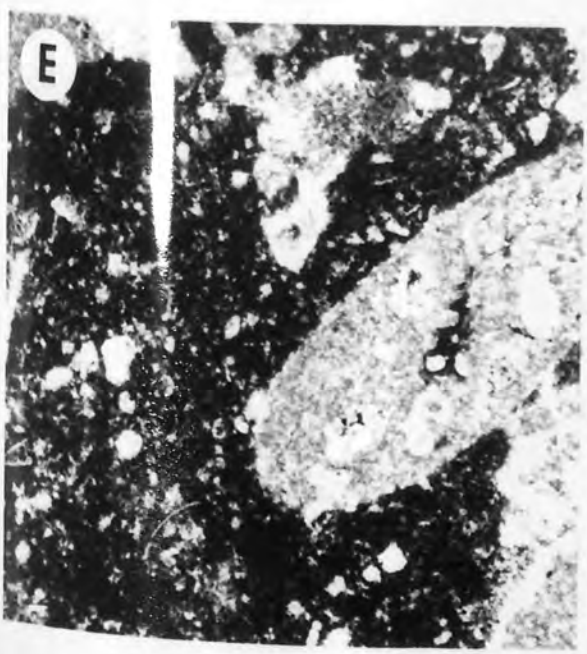

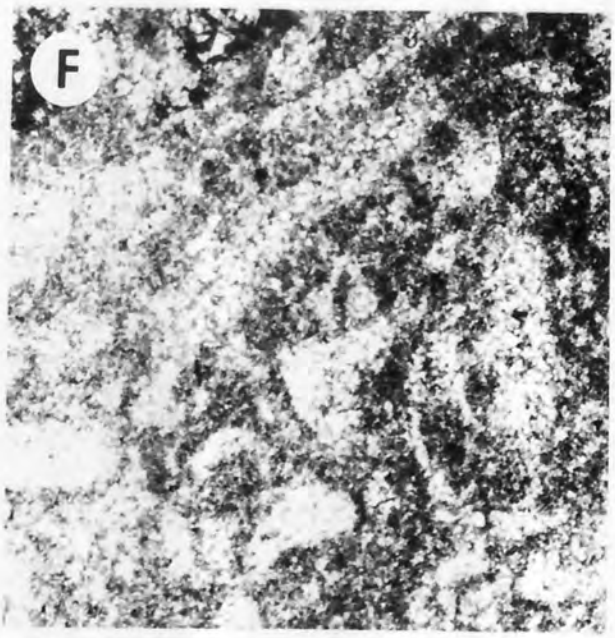

Plate 63 - Examples of pore types and compaction of lime mudstones

A. Duma 5 2492'. Numerous subhorizontal anastomosing streaks are interpreted as representing relicts of leached tabular corals.

B. Duma 11 2344'. Numerous subparallel leached tabular corals. A streaky layering results from dissolution of foliose fragments in a poorly indurated lithology.

C. Duma 5 2438'6. Leached packstone. Mouldic, vuggy and fine matrix porosity form a connected permeable network. Blotchy oil stain is restricted to the lower half of the slab.

D. Duma 5 2449'. Argillaceous impure lime mudstone-wackestone. Pale lenses are elongate unfractured delicate foraminifera.

E. Duma 11, 2351'6. Anastomosing organic-rich wispy layers at the base of the core slab may mark the incipient development of a stylolite swarm. Cream coloured foraminifera are orientated parallel to the streaky layers.

PLATE 63

E
DUMA #11
2351'6"

C
DUMA#5
2438'6"

D
DUMA#5
2449'

A
DUMA#5
2492'

B
DUMA #11
2344'

Plate 64 - Cathodoluminescence textures of micrite and neomorphic spar

A. Non-luminescent recrystallised allochems in the mottled matrix.
Sample ZU-4 2691', Magnification X58.

B. A recrystallisation front picked out sharply through differences in luminescence. The dark area to the right and bottom of the photograph is unaggraded micrite whilst the luminescing area is a mixture of microspar and residual micrite.
Sample ZU-4 2698'5, Magnification X167.

C. Appreciable differences in composition occur between the micrite matrix and the large nonluminescent irregular spar crystals. The latter appear to have grown within the matrix prior to late compaction since the spar crystals are fractured.
Sample ZU-4 2630'6, Magnification X167.

D. A recrystallisation front is clearly defined by luminescent contrasts between the nonluminescent neomorphic spar and mottled medium bright yellow-orange luminescence of unaggraded micrite.
Sample Zu-4 2630'6, Magnification X167.

PLATE 64

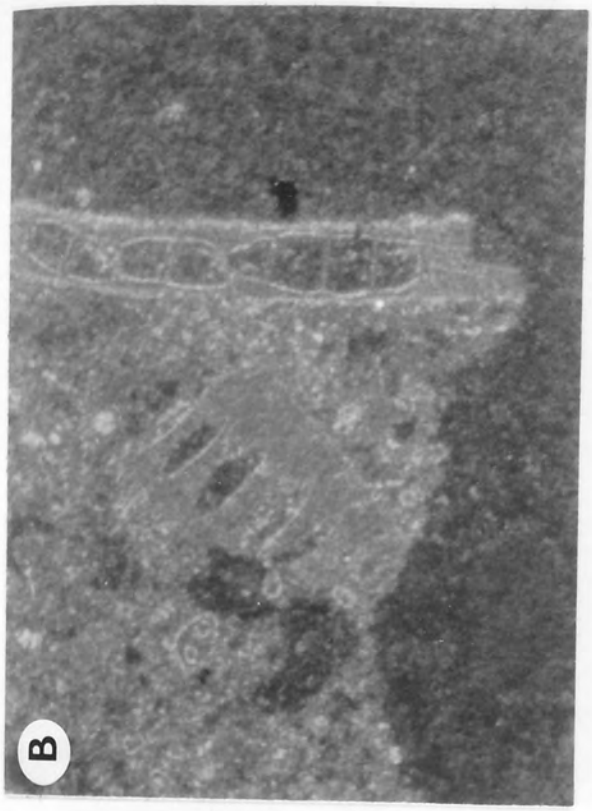

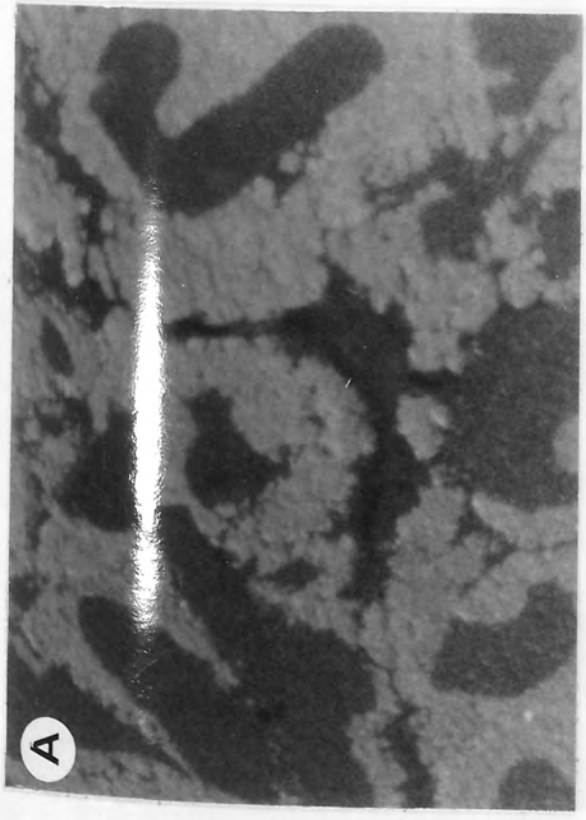

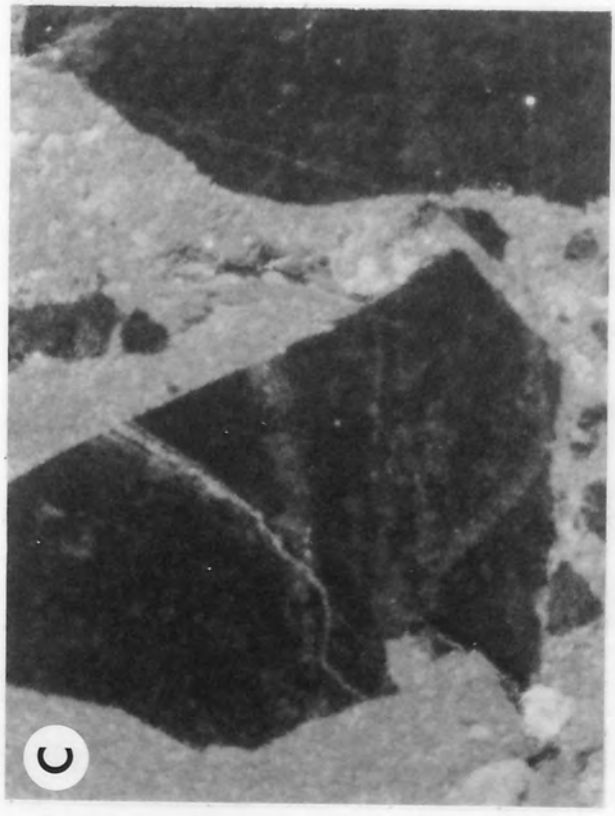

Plate 65 - Intraskeletal porosity and matrix textures under SEM

A. Course calcite cement or neomorphic calcite replacing or infilling the mouldic pore from a former allochem.
Sample D11 2345', Magnification X1500.

B. Globogerinid wall structure and intraskeletal porosity are preserved. The foraminifer is embedded in a matrix of mixed microspar and micrite.
Sample D11 2359', Magnification X3500.

C. Globogerinid embedded in an indurated microsparry matrix. Intraskeletal porosity is unfilled.
Sample N4 1755'6, Magnification X3500.

D. Highly porous unlithified mud matrix. Some of the ragged platy grains might be authigenic clays.
Sample N10 1756, Magnification X8500.

E. Nonporous interlocked fabric of fine neomorphic sparry calcite replacing the primary micrite matrix.
Sample D11 2352'6, Magnification X3500.

F. Patchily recrystallised matrix. The platy grain (centre bottom) might be a skeletal fragment.
Sample N10 1756', Magnification X3000.

PLATE 65

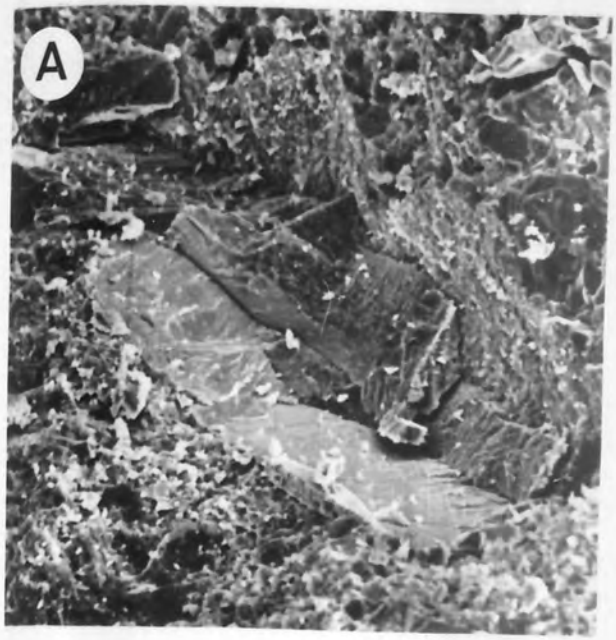

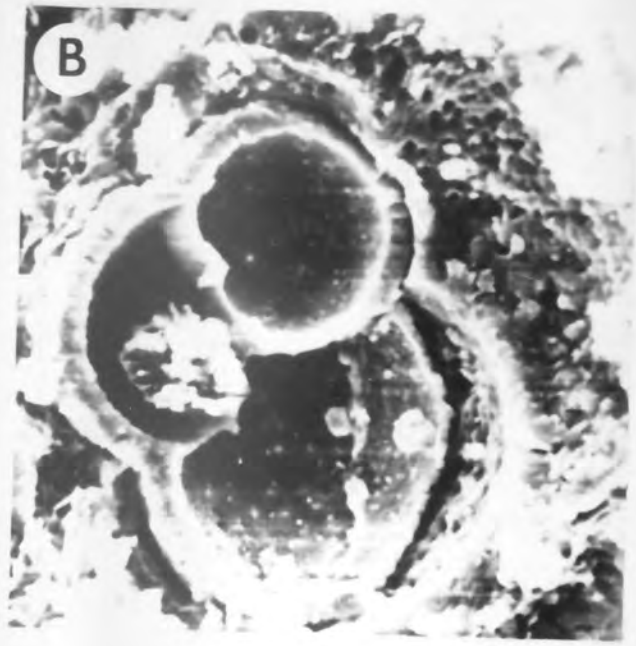

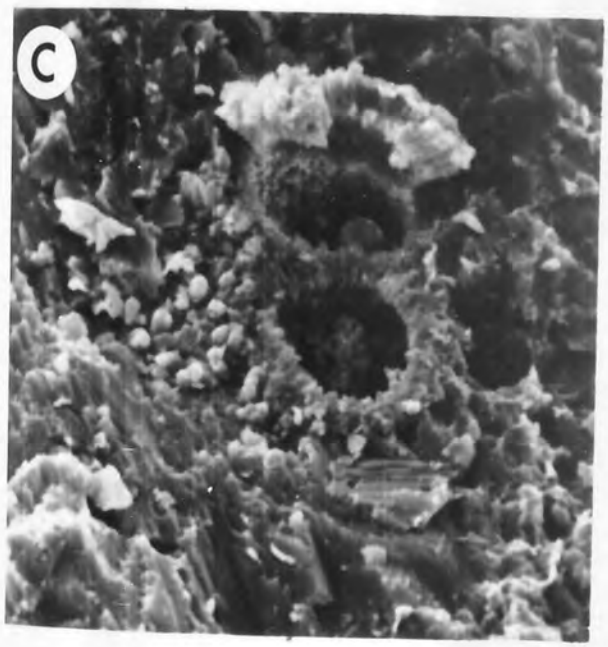

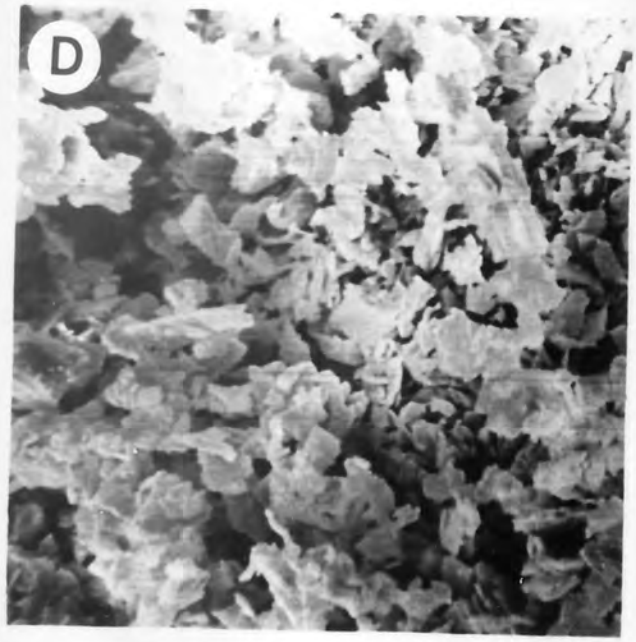

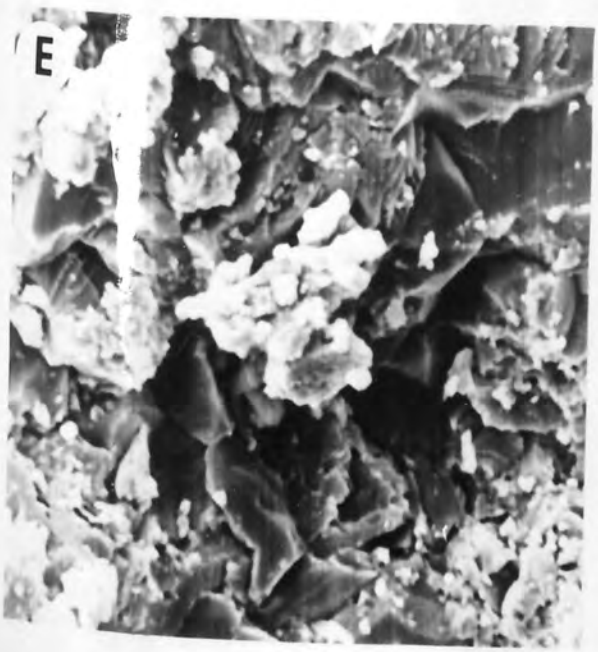

Plate 66 - Inter- and intraskeletal preo-filling calcite cement and syntaxial rims.

A. Thin syntaxial cement on an echinoderm grain in a grainstone.
Sample D11 2307', Magnification X42.

B. Irregular jagged syntaxial cement enclosing an echinoid spine. An early generation of cement was fibrous in morphology and has been recrystallised in optical continuity with the later monocrystalline cement. The early generation is preserved as inclusions. Other bioclastic grains have oily rims.
Sample N4 1675', Magnification X42.

C. The unit crystal echinoderm ossicle serves as a substrate for an overgrowth. The rim is inclusion-rich close to the host substrate.
Sample D2 2803', Magnification X42.

D. Vuggy pores are often incompletely filled, and cement crystals commonly display euhedral terminations.
Sample ZU-1 2587'8, Magnification X167.

E. Chambers of a benthic foraminifer lined with an isopachous crust of low-Mg calcite.
Sample D11 2345', Magnification X42.

F. A large serpulid tube infilled with coarse bladed radially orientated calcite.
Sample ZU-1 2638'2, Magnification X58.

PLATE 66

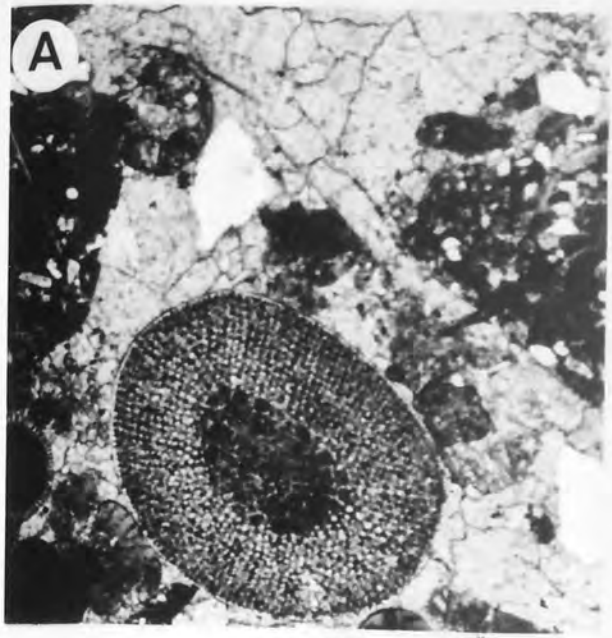

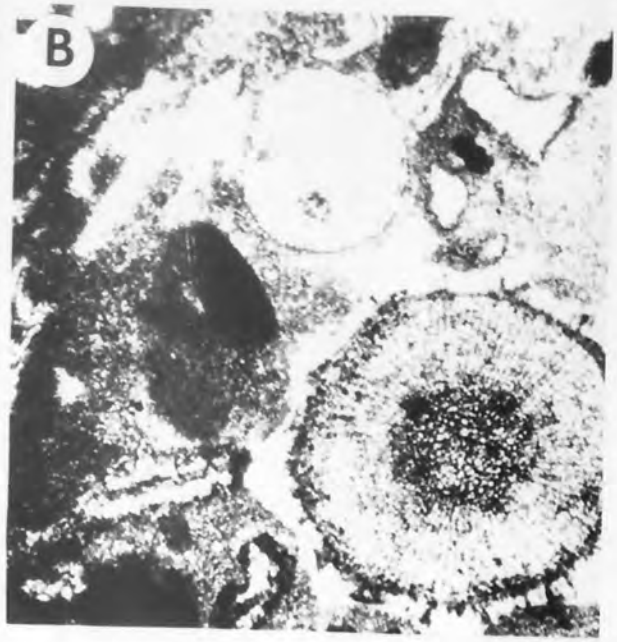

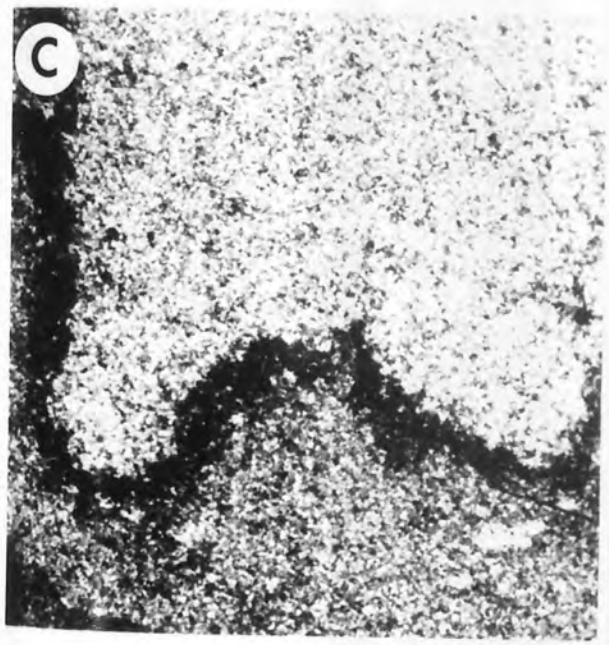

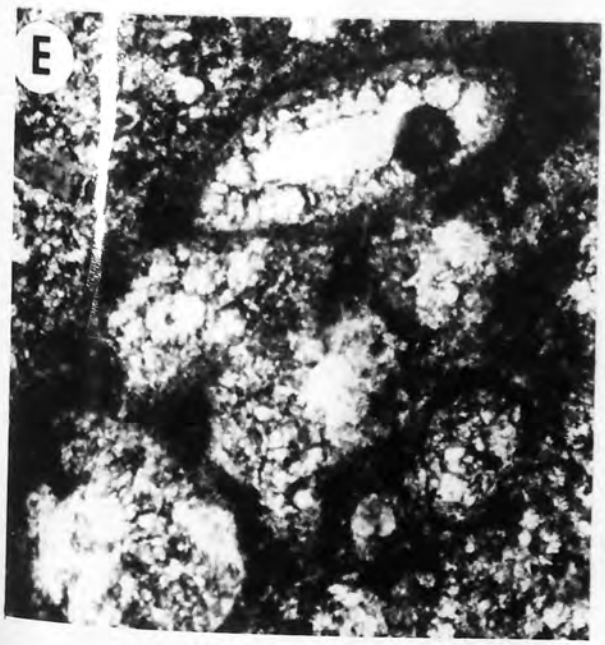

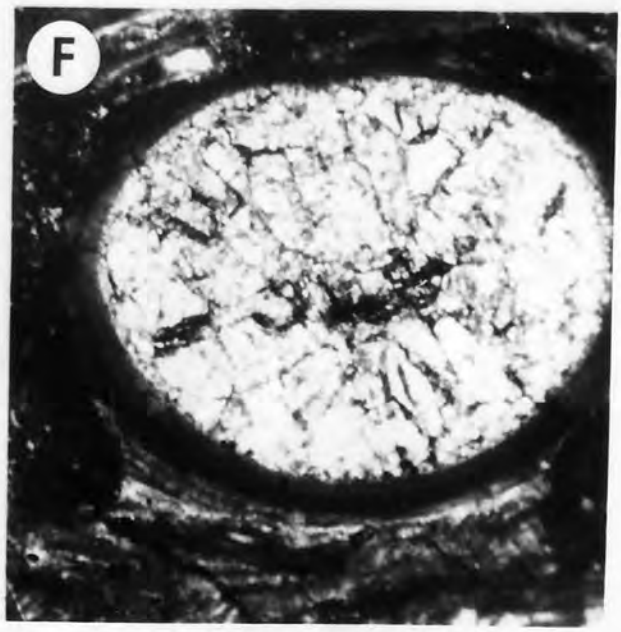

Plate 67 - Cathodoluminescence characteristics of syntaxial rims

A. Isopachous rim on an echinoid spine. The rim exhibits a thick medium bright orange inner zone and thin bright yellow-orange zone.
Sample ZU-1 2588'4, Magnification X167.

B. Core of the echinoid is cemented with brightly luminescing yellow-orange calcite and the fragment is partly surrounded by a cement rim. The boundary between non-luminescent and bright zones is transitional.
Sample D2 2803', Magnification X167.

C. Jagged bladed cement on an echinoderm plate displaying a similar zonation to that described above. Note also brightly zoned dolomite rhombs.
Sample ZU-1 2588'4, Magnification X167.

D. Thin irregular rim around an echinoid plate.
Sample D2 2803', Magnification X167.

PLATE 67

Plate 68 - SEM textures of calcite cement and microspar

A. Calcite-filled post-lithification fracture cross-cutting the finely crystalline matrix.
Sample N10 1756', Magnification X150.

B. Matrix composed of blocky interlocked calcite. Intercrystalline porosity moderate.
Sample ZU4 2589', Magnification X1800.

C. Intraskeletal pores lined with scatenohedral calcite crystals. Foraminifer is embedded in fine unaggraded micrite.
Sample ZU3 2617'3, Magnification X850.

D. Coral mouldic porosity occluded by secondary calcite. The calcite crystals are orientated at a high angle to the host substrate.
Sample N10 1756', Magnification X850.

E. Foraminifer filled with calcite cement.
Sample D5 2414'6, Magnification X1000.

F. Calcite-filled foraminifer embedded in a dolomitised micrite matrix.
Sample D5 2414'6, Magnification X850.

PLATE 68

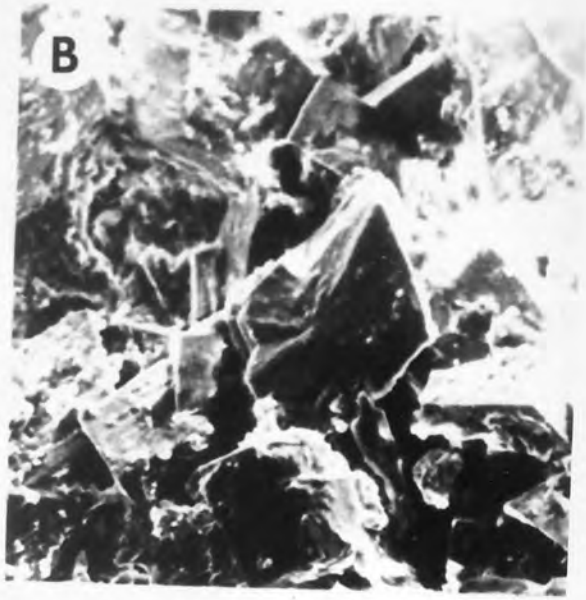

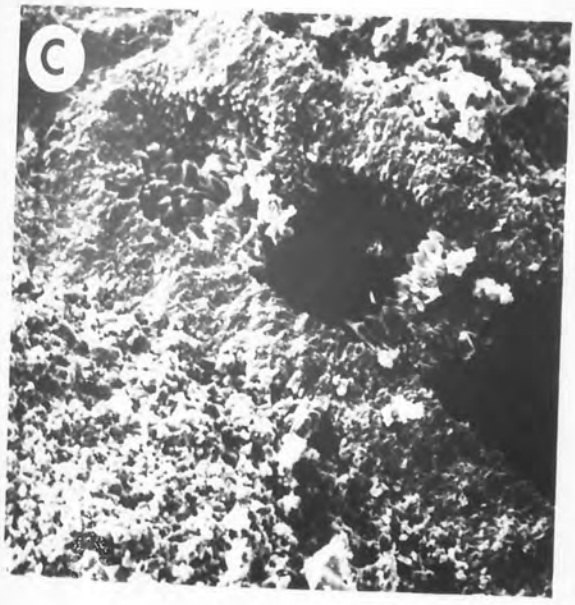

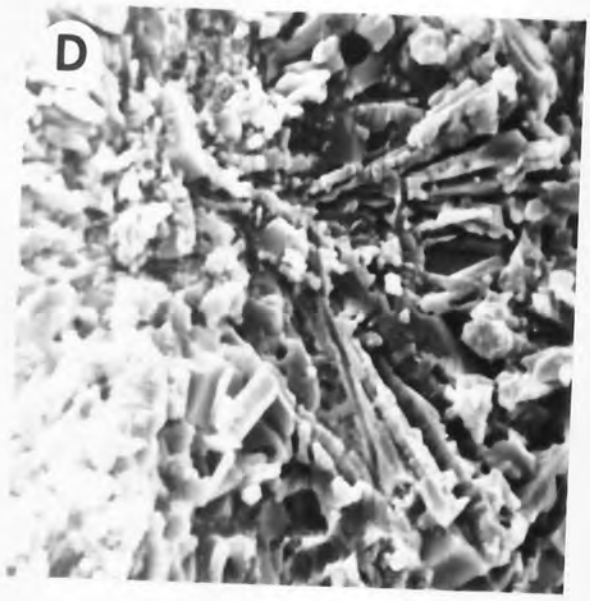

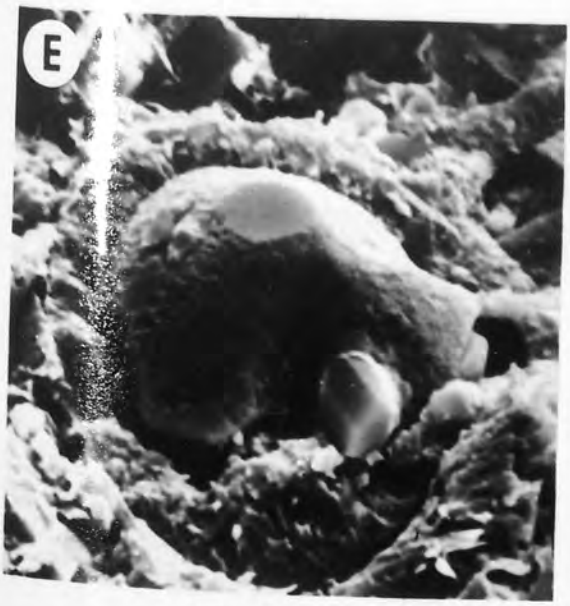

Plate 69 - Calcite occluding primary and secondary porosity

A. Calcite filled intraskeletal cavities in a benthic foraminifer.
Sample D9 2306', Magnification X42.

B. Calcite infilling intergranular porosity in a grainstone. The cellular organism at the bottom of the photograph is the benthic foraminifer Discoclycina. The dark kidney-shaped grain (centre) is a faecal pellet.
Sample D11 2307'.

C. Lepidocyclina chambers filled with calcite.
Sample D9 2306', Magnification X42.

D. Blocky low-Mg calcite partly fills chambers of a gastropod and also occludes secondary mouldic pores in the matrix.
Sample D11 2334', Magnification X42.

E. Much of the primary texture is lost through dissolution of allochems and subsequent infilling of pores with equant calcite. Minor secondary porosity remains.
Sample D11 2346'6, Magnification X42.

F. Recrystallised coral. The lower intraskeletal chambes are micrite-filled and the upper chambers occluded with calcite.
Sample D5 2475', Magnification X42.

PLATE 69

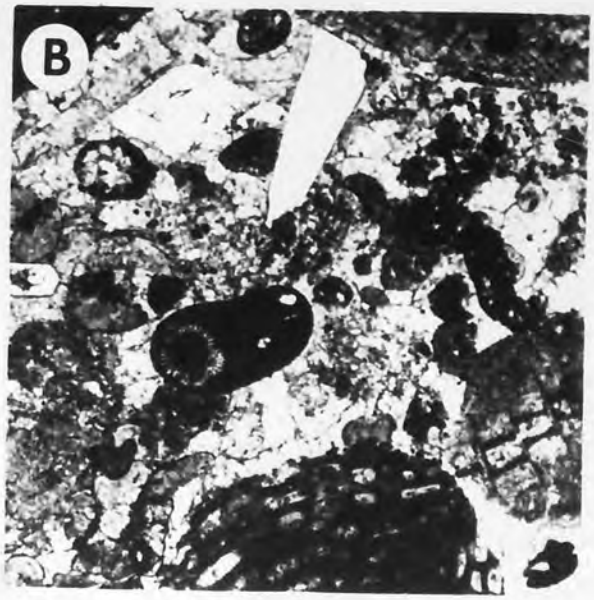

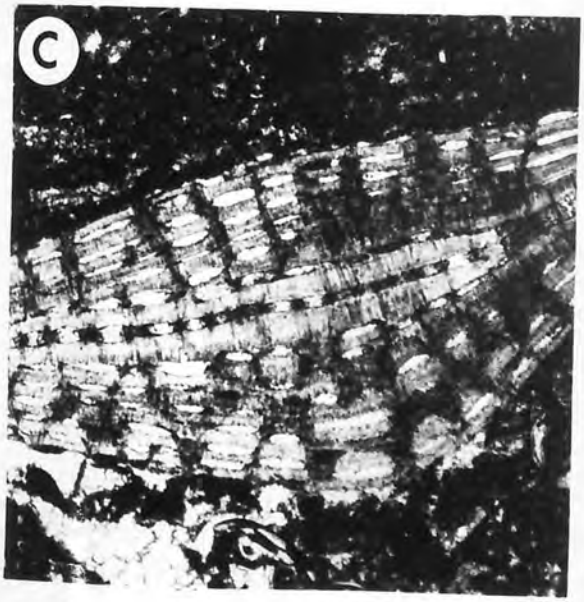

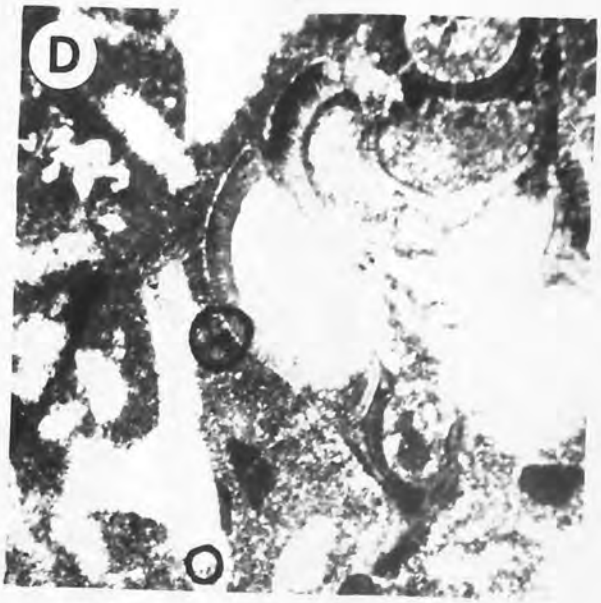

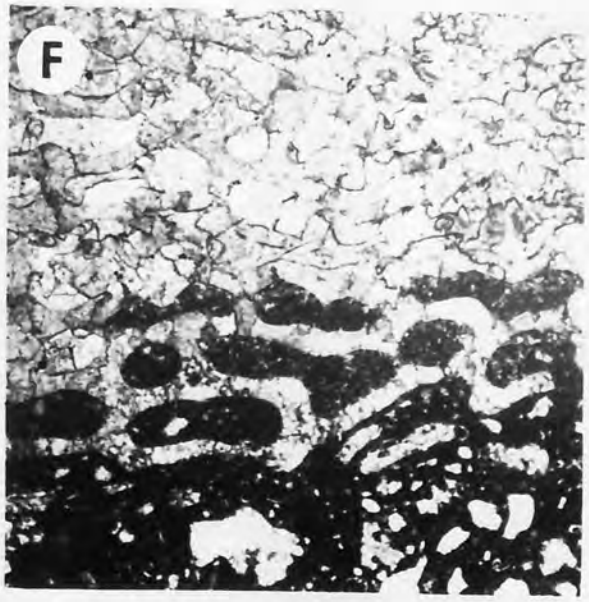

Plate 70 - Sparry calcite under SEM

A. Vuggy matrix pore partly filled with coarse calcite cement.
Sample ZU3 2855', Magnification X350.

B. A mosaic of coarse interlocked calcite replacing an allochem or filling a pore.
Sample D3 2448', Magnification X350.

C. Coarsely crystalline interlocked nonporous calcite. Note smooth conchoidal appearance and cleavage surfaces.
Sample D5 2414'6, Magnification X450.

D. Angular intercrystalline porosity in interlocking calcite.
Sample D5 2414'6, Magnification X800.

E. Boundary between the smooth surface of a calcite allochem and recrystallised matrix.
Sample ZU3 2617'3, Magnification X450.

F. Laminated fabric of an allochem (bivalve?) embedded in a finely crystalline matrix.
Sample D3 2448', Magnification X350.

PLATE 70

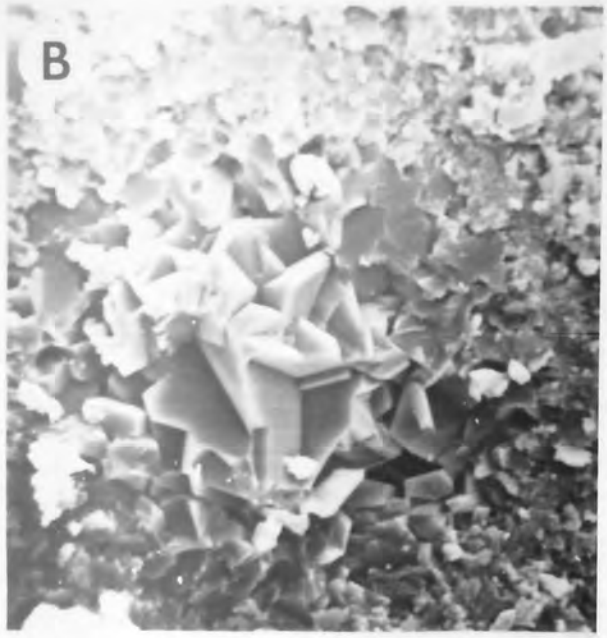

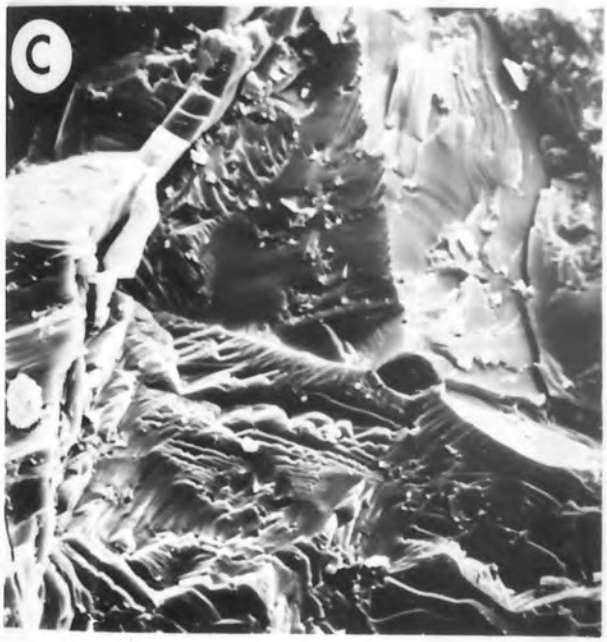

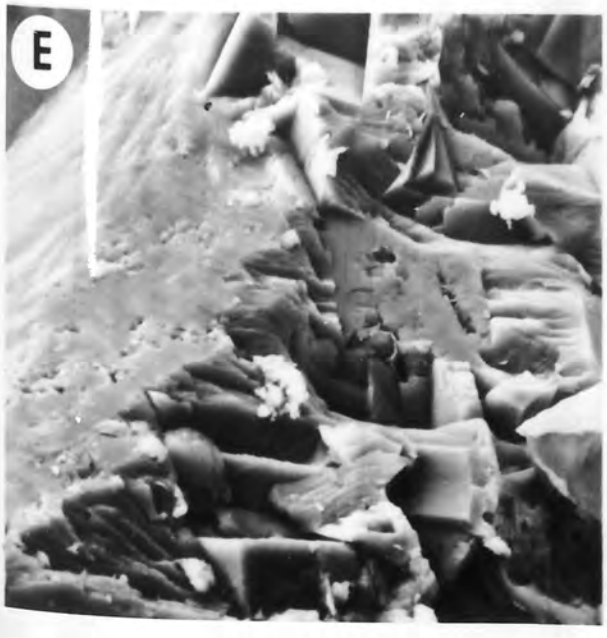

Plate 71 - Cathodoluminescene characteristics of neomorphic calcite and sparry calcite cement

A. Complex zonation of a coarse-spar crystal. Zones oscillate between bright yellow-orange luminescing calcite and non-luminescent calite. The development of incremental zones such as this indicates that this is a cement rather than a neomorphic crystal.
Sample ZU4 2679'6, Magnification X167.

B. Bright orange luminescing calcite partly filling a late fracture.
Sample ZU4 2679'6, Magnification X58.

C. Zonation of cements in a secondary pore. The first generation of cement is bladed in morphology and grades from non-luminescent at the core, to moderately brightly luminescent at the margins. The succeeding generation is coarse, equant and non-luminescent to dull-mottled.
Sample ZU4 2697', Magnification X167.

D. Mottled unzoned neomorphic spar. The bright zone lines some allochems and might be contemporaneous with the development of micrite-envelopes and associated cryptocrystalline cements in the marine environment.
Sample D2 2803', Magnification X167.

PLATE 71

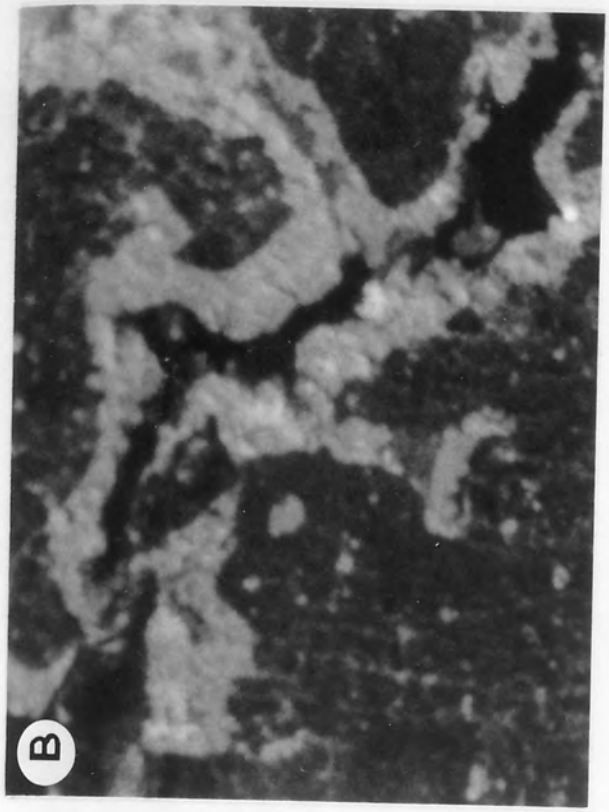

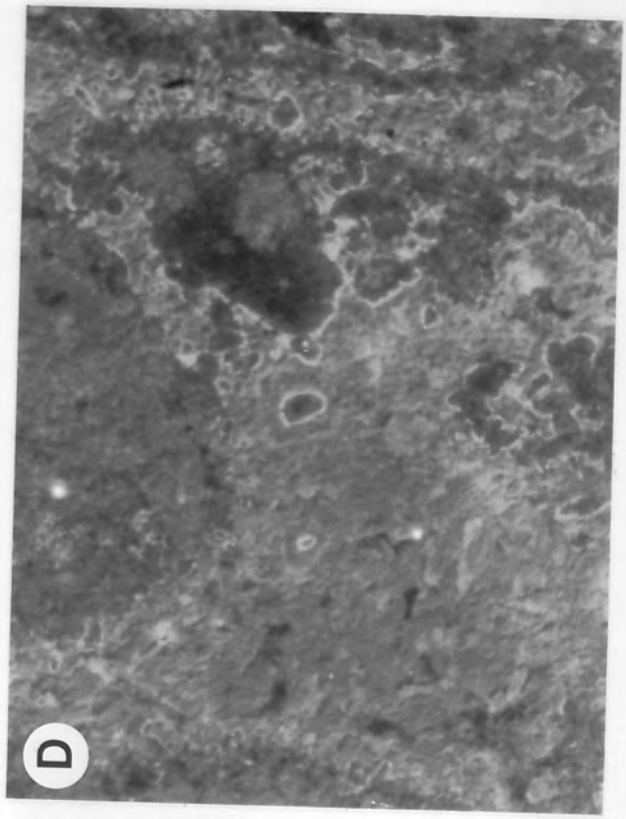

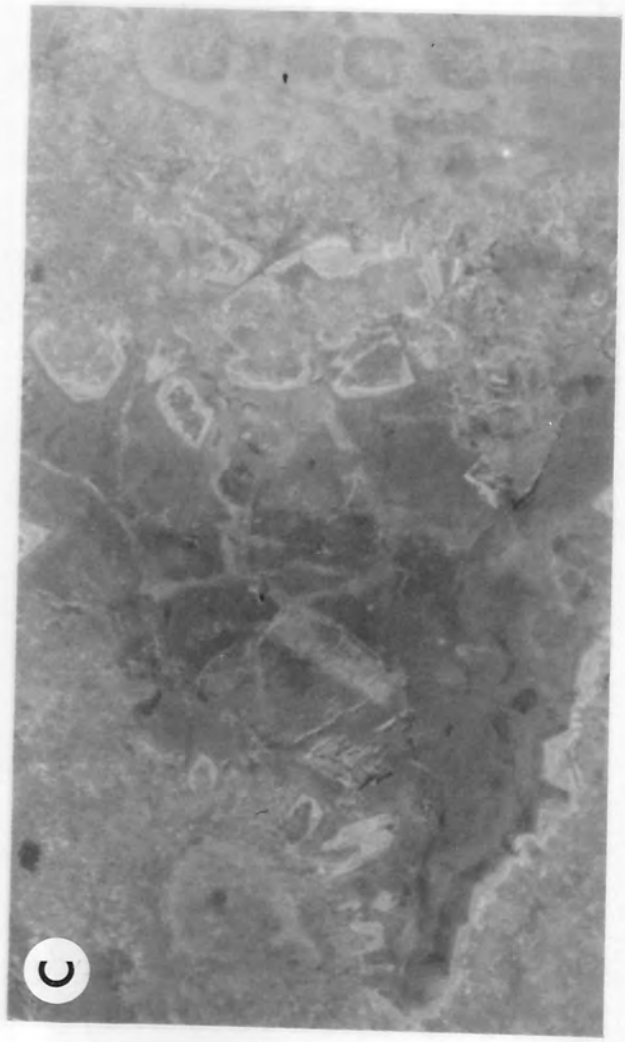

Plate 72 - Calcite cement textures and silicification

A. Calcite filled straight-sided fracture in a foraminiferal wackestone matrix. Note crystals orientated at a high angle to fracture walls.
Sample ZU3 2628'3, Magnification X42.

B. Coarse calcite mosaic occluding a late post lithification fracture.
Sample ZU4 2679'6, Magnification X42.

C. Fabric of cone-in-cone displacive calcite.
Sample D11 2359'6, Magnification X58.

D. Silica-carbonate admixture replacing a ribbon-like zone through an echinoid spine. Replaced zone is immediately to right-hand-side of centre.
Sample D5 2529', Magnification X42.

E. Pale irregularly shaped area of silica-carbonate replacement in echinoid spine. Pyrite grains are concentrated around the rim of the grain.
Sample D11 2346'6, Magnification X42.

F. Silica-carbonate admixture replacing part of the skeletal material and chambers of a benthic foraminifer.
Sample D5 2438'6, Magnification X42.

PLATE 72

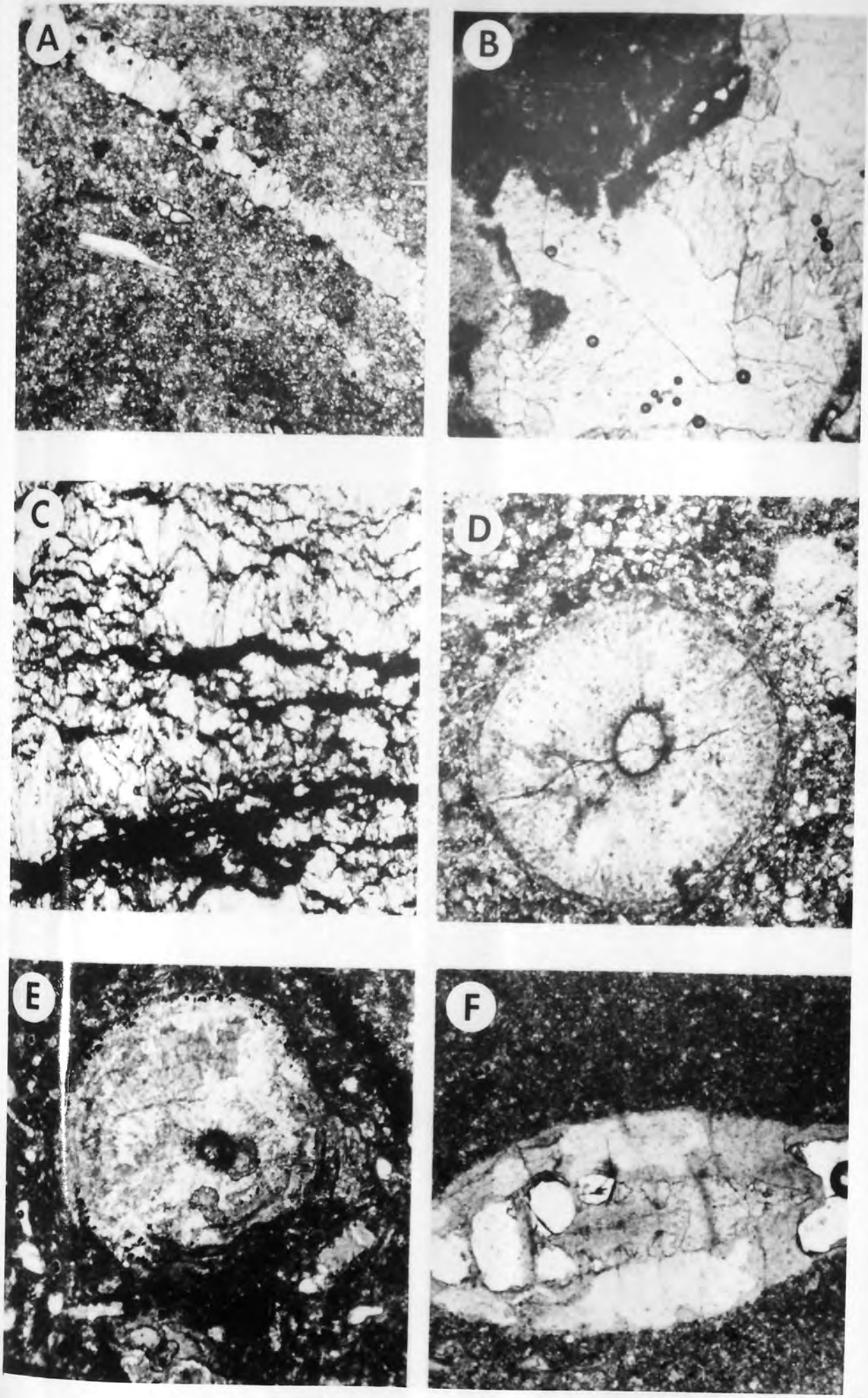

Plate 73 - Silicification textures

A. Chalcedony rosette within a benthic foraminifer.
Sample D5 2438'6, Magnification X42.

B. Spherical rosettes of chalcedony replacing the margins of an echinoderm spine.
Sample D5 2403', Magnification X42.

C. Benthic foraminifer replaced by chalcedonic quartz. The replacement does not cross cut the outer wall of the allochem.
Sample D5 2438'6, Magnification X42.

D. Chalcedony replacing echinoderm spines. Pyrite is associated with the silicification and grows parallel to the radial fabric of the chalcedony.
Sample D5 2403', Magnification X42.

E. Etched grain of quartz sand. The margins of the quartz and thin zones of weakness are replaced by granular calcite.
Sample D11 2307', Magnification X42.

F. Abundant detrital quartz silt in a packstone.
Sample N5 1923'7, Magnification X42.

PLATE 73

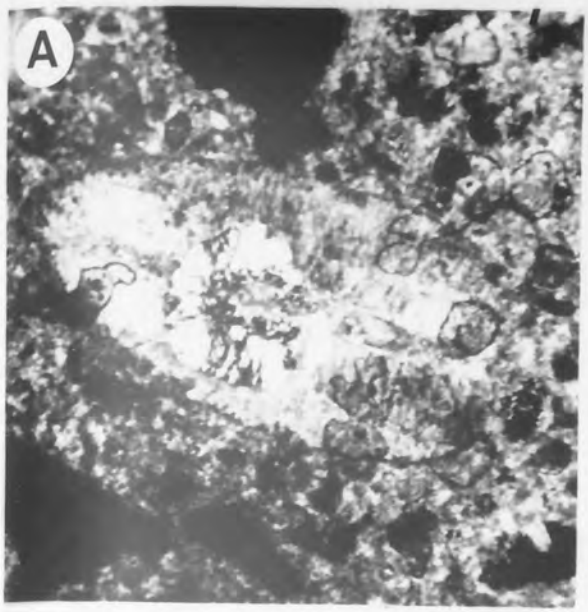

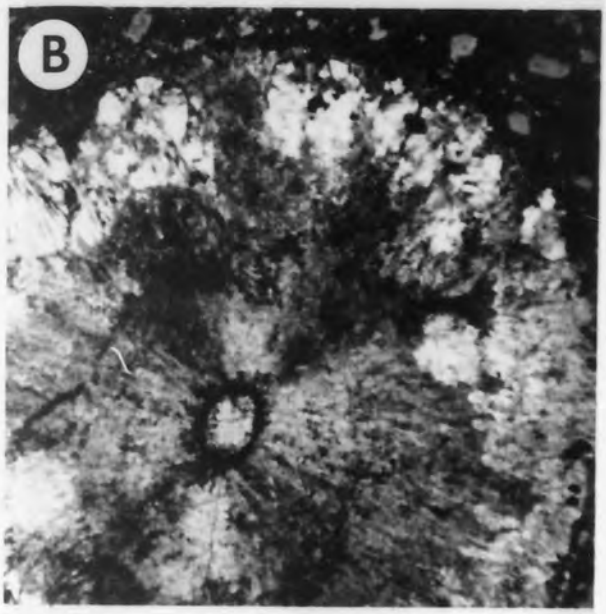

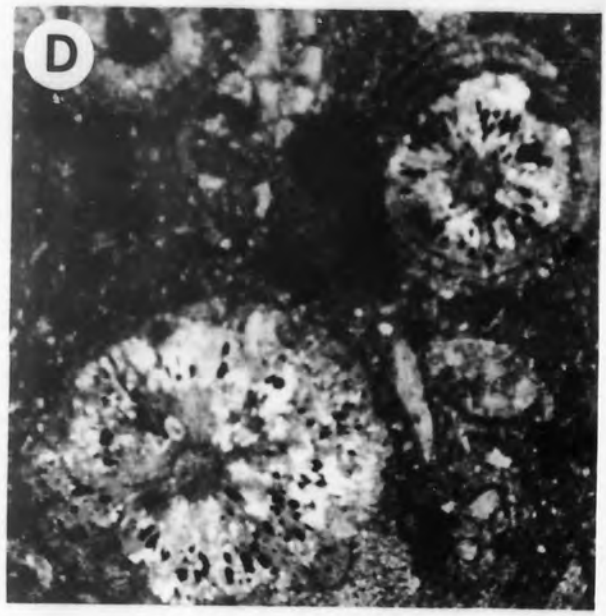

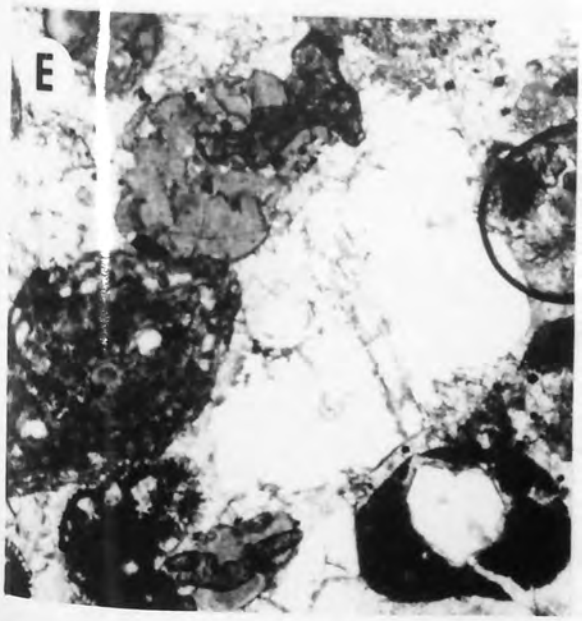

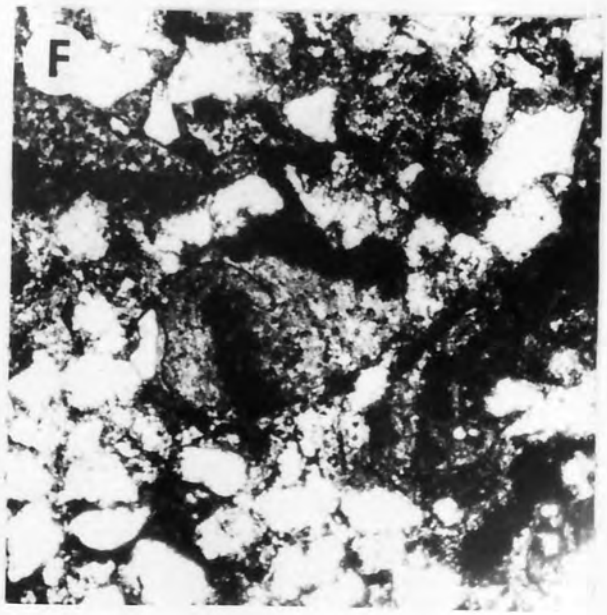

Plate 74 - Textures associated with pyrite growth

A. Pyrite partly replacing a skeletal fragment.
Sample D5 2403', Magnification X42.

B. Pyrite concentrated around the periphery of an echinoid spine cross-section. Pyrite is also concentrated in the central cavity.
Sample D2 2820'6, Magnification X42.

C. Small pores in an echinoid plate filled with pyrite. The syntaxial cement surrounding the plate is also poikilotopic.
Sample D9 2283'6, Magnification X49.

D. Pyrite filling the intraskeletal porosity in a recrystallised coral fragment.
Sample D2 2802', Magnification X42.

E. Clusters of pyrite replacing a recrystallised bivalve.
Sample ZU-3 2628'3, Magnification X42.

F. Pyrite growing in association with a pressure solution microstylolite. Note the euhedral pyrite on extreme right of photograph.
Sample D2 2835', Magnification X42.

PLATE 74

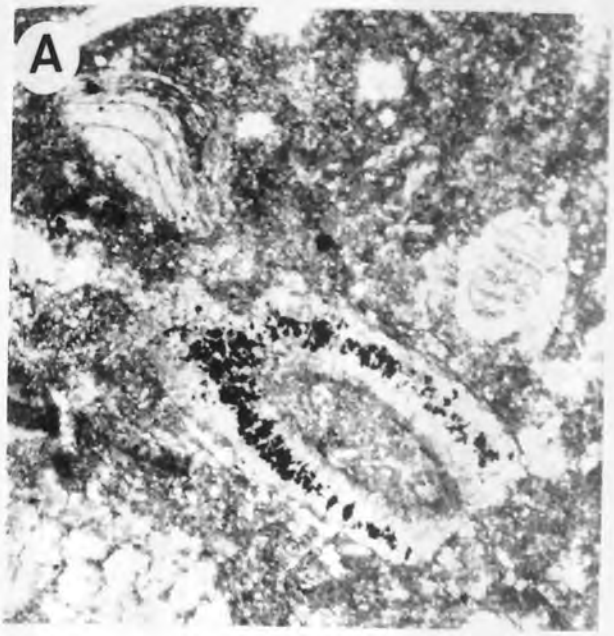

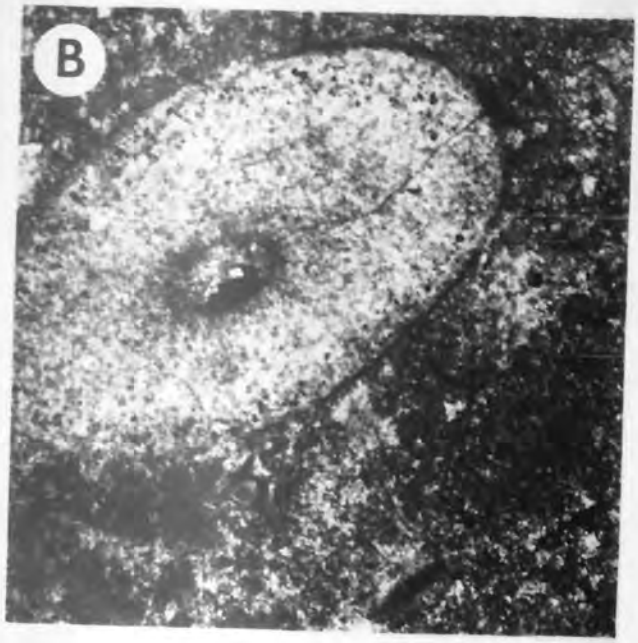

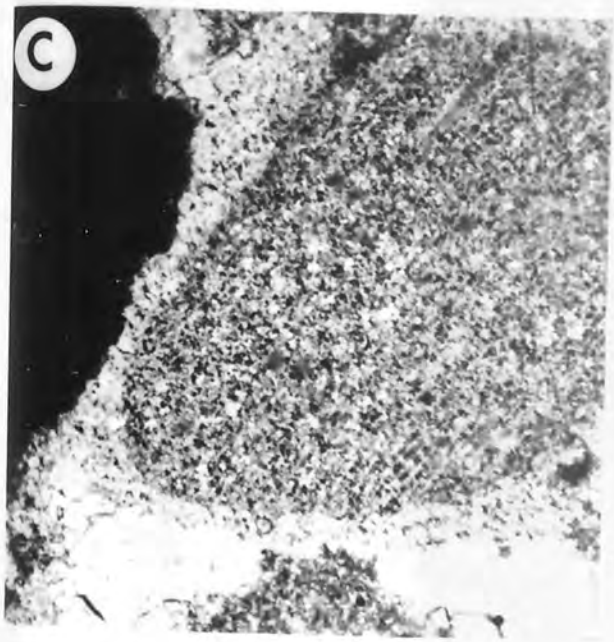

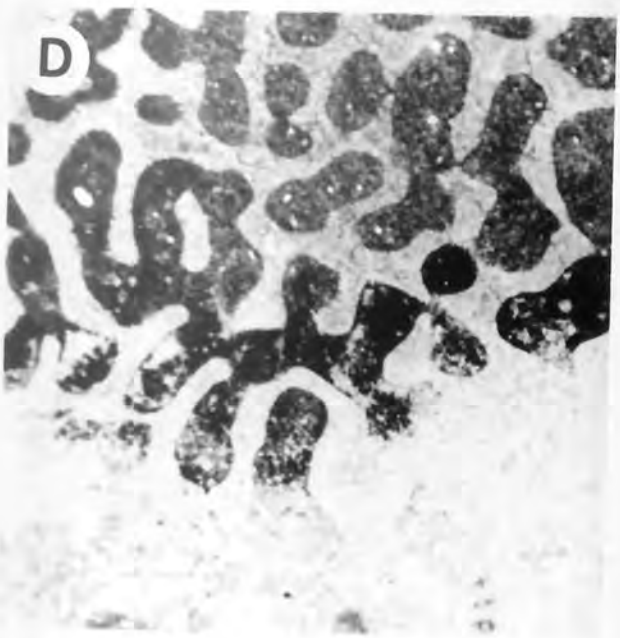

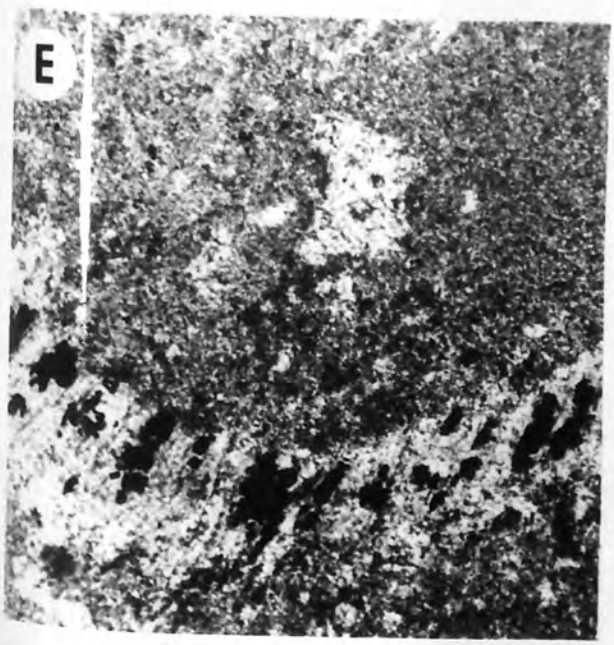

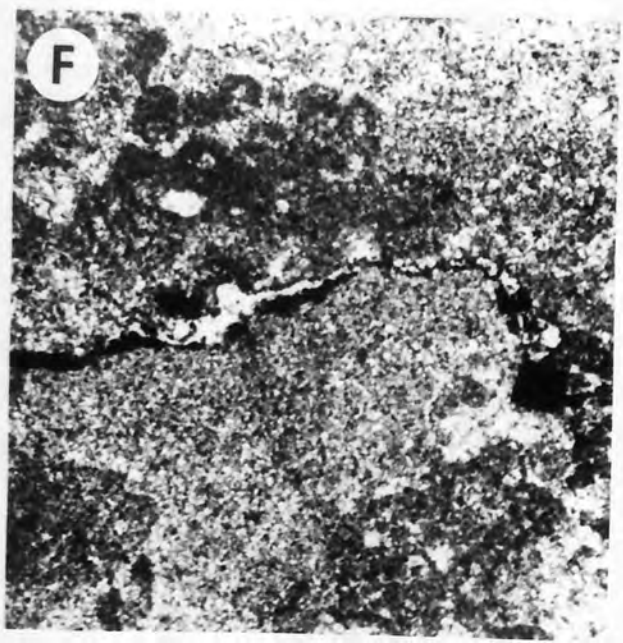

Plate 75 - Compactional features

A. Microfractures in an echinoid spine.
Sample D2 2803', Magnification X42.

B. Crushed echinoid spine in a porous dolomitised matrix which exhibits no clear evidence of compaction.
Sample D5 2414'6, Magnification X49.

C. Prelithification fracture in an echinoid spine does not continue into the relatively ductile matrix. Fracture is partly filled with non-ferroan calcite.
Sample D5 2421', Magnification X42.

D. Fenestrate bryozoan with a calcite filled vertical boring in top right of photograph. The zooecia in the upper part of the bryozoan are more flattened than those in the lower part which are spar-filled.
Sample D5 2473', Magnification X49.

E. Chemical compaction between an echinoderm fragment and Discocyclina.
Sample D3 2403'6, Magnification X42.

F. Minor displacements along early in situ prelithification fractures in Lepidocyclina. The fractures are filled with ferroan calcite.
Sample D3 2415', Magnification X42.

PLATE 75

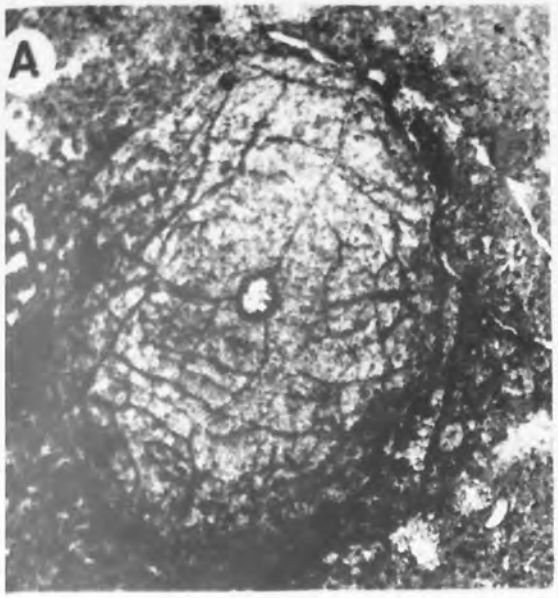

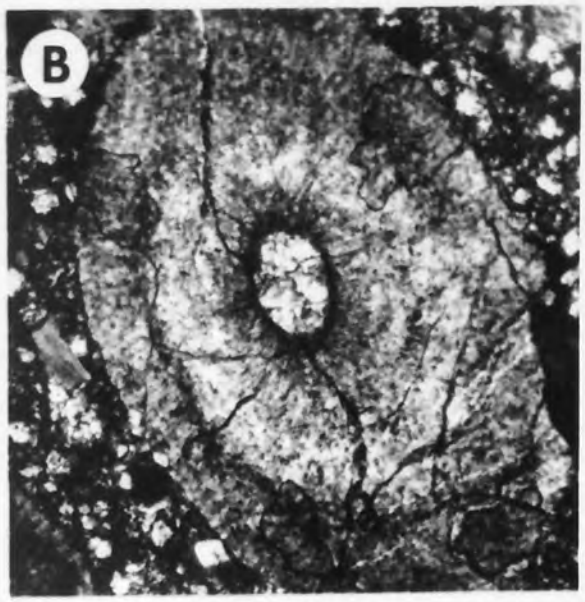

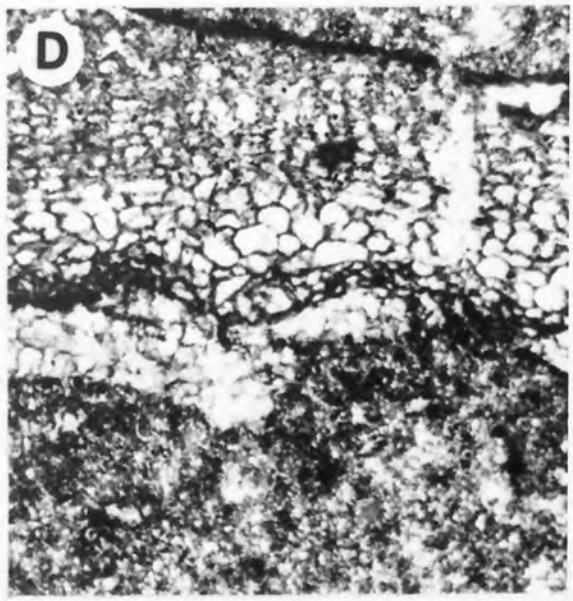

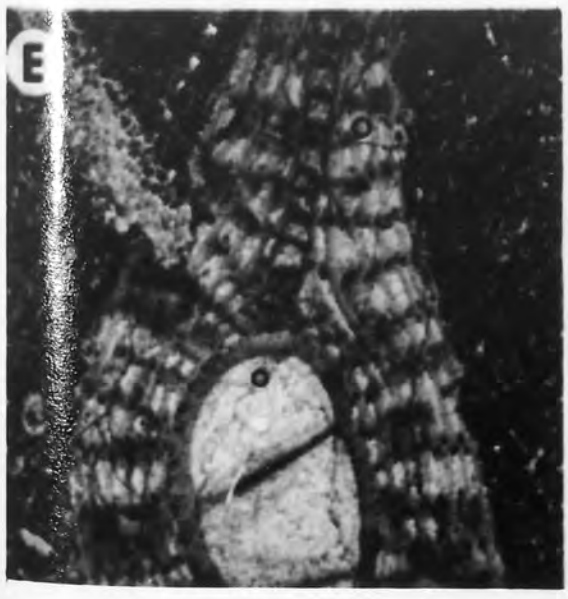

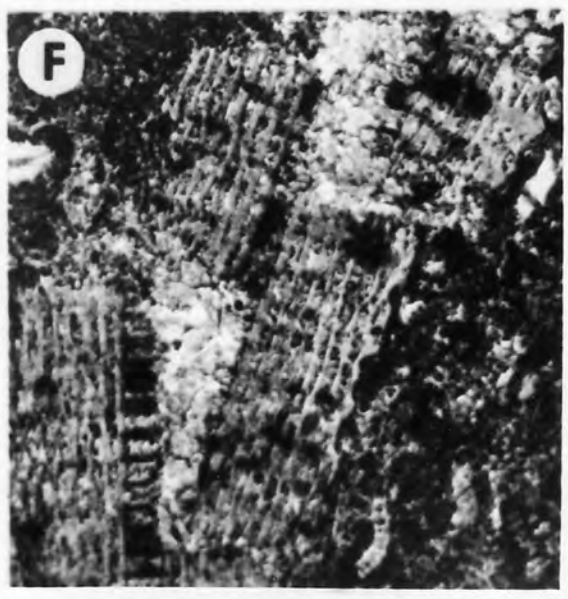

Plate 76 - Fracturing, pressure solution and hydrothermal alteration

A. Prelithification crushing of a foraminifer. The fracture is filled with ferroan calcite which subsequently underwent dolomitisation.
Sample ZU-1 2597'9, Magnification X42.

B. A sharply defined post lithification fracture in a micritic lithology. Crystals are elongated at a high angle to the fracture walls.
Sample D2 2815', Magnification X49.

C. Stylolitic contact between two foraminifera.
Sample ZU-1 2597'9, Magnification X42.

D. A high amplitude pressure solution stylolite.
Sample, D11 2348', Magnification X42.

E. Dolomite. Intercrystalline porosity is almost entirely occluded through compaction. Crystals are welded together along microstylolitic contacts.
Sample ZU-4 2661', Magnification X42.

F. Texture of hydrothermally altered rock. The large pale grains are barytes and the dark grains a mixture of sulphides, predominantly pyrite.
Sample ZU-3 2859'3, Magnification X42.

PLATE 76

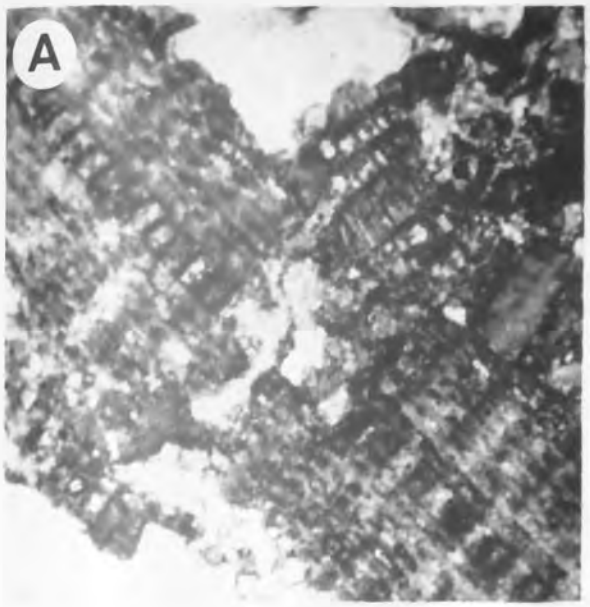

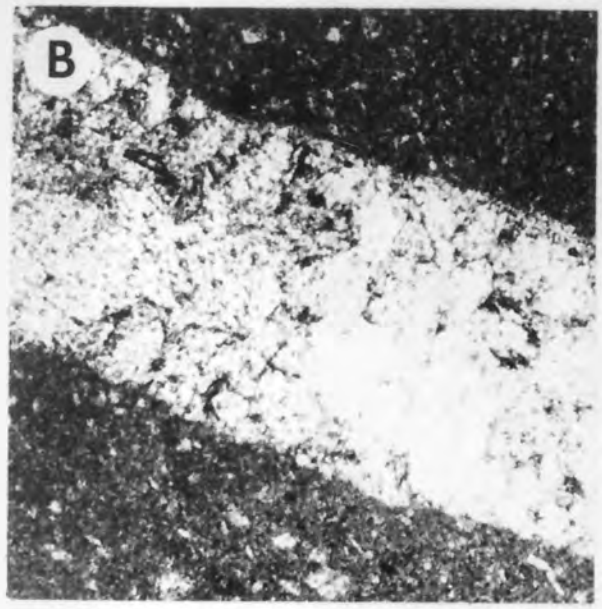

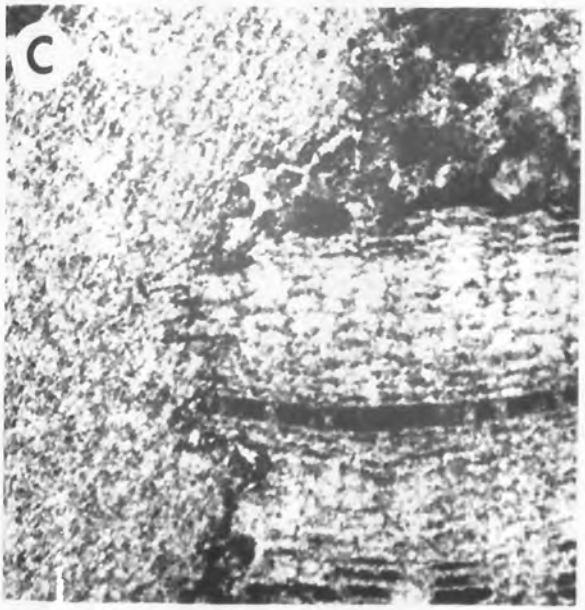

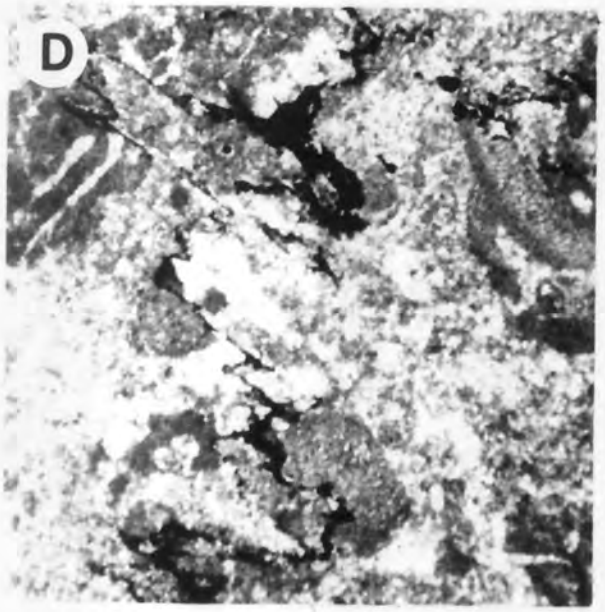

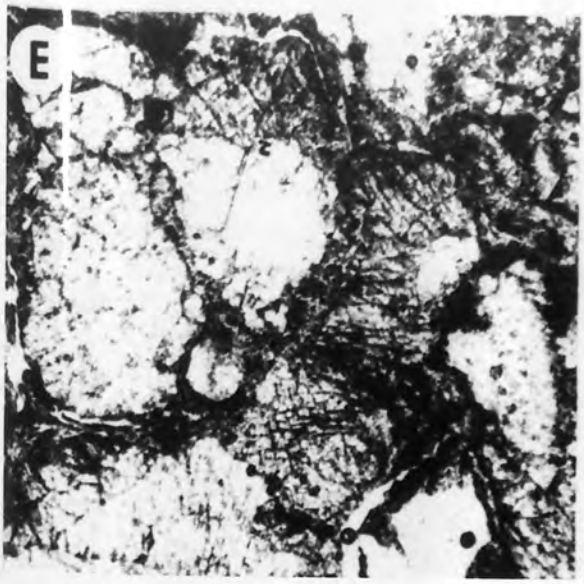

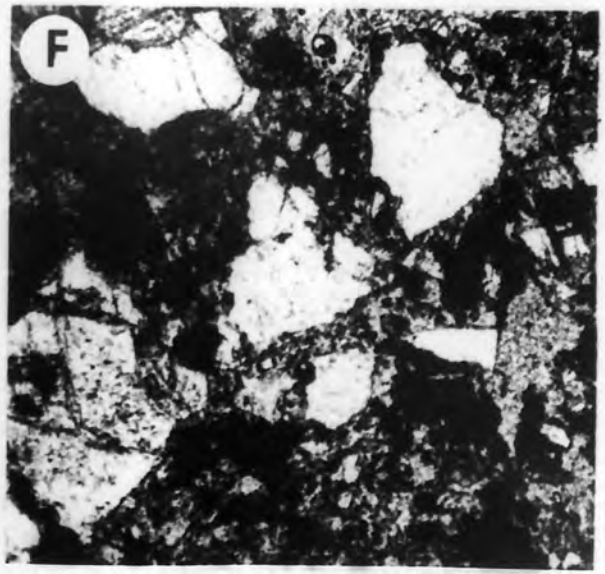

Plate 77 - Diagnetic Fabrics

A. A distinct crust of relatively inclusion-free calcite adjacent to algal and mollusc fragments suggests the original presence of an early metastable rim cement. Sample D5 2421. Bar represents 0.5 mm.

B. The crystals fringing the mollusc retain an elongate character and long exes lie at a high angle to the host substrate. Sample D5 2421. Bar represents 0.2 mm.

C. The dark fractured fragment is encrusted with a fibrous rim cement. Subsequent to the precipitation of the fibrous cement, dissolution or removal of whatever the dark rim enclosed, and compaction of hte unlithified sediment resulted in deposition of an echinoderm grain within the empty chamber and breakage of the brittle enclosing walls. At a later stage the fibrous cement was engulfed by non-ferroan calcite whilst the residual porosity within the void was occluded by an echinoderm over growth. Sample D11 2307. Bar represents 0.5 mm.

D. Early dedolomitisation. Dolomite rhombs are ragged in appearance due to the marginal etching by low-Mg calcite. Sample D11 2320. Bar represents 0.5 mm.

E. Close-up of dolomite rhomb showing inclusions of low-Mg calcite. Sample D11 2320. Bar represents 0.2 mm.

F. Silicified valve in a highly leached matrix. Apart from the dark brown algal fragments, there is no evidence of unsilicified allochems supporting the suggestion that the secondary dissolution pores were generated subsequent to or contemporaneous with silicification. Sample D5 2529. Bar represents 0.5 mm.

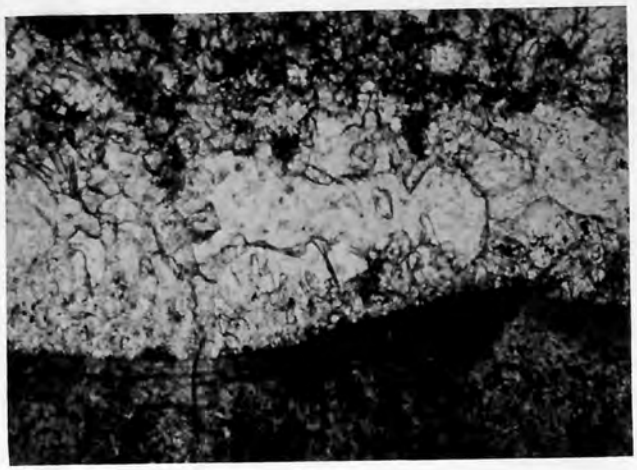

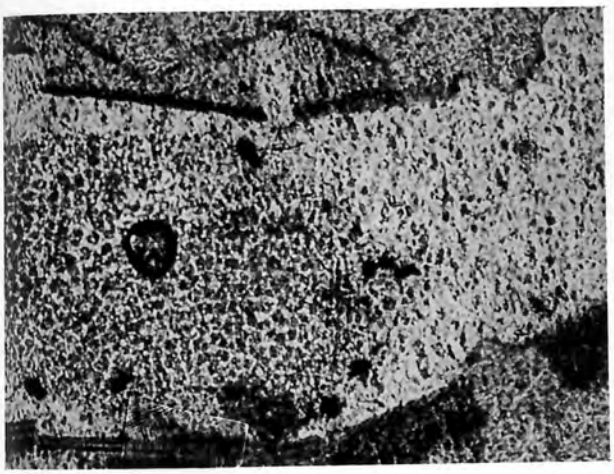

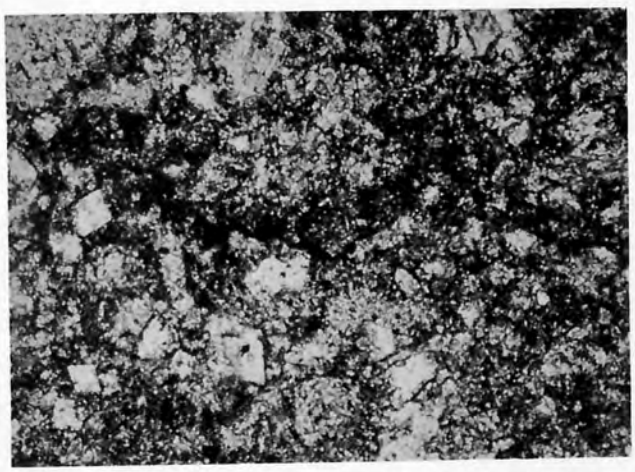

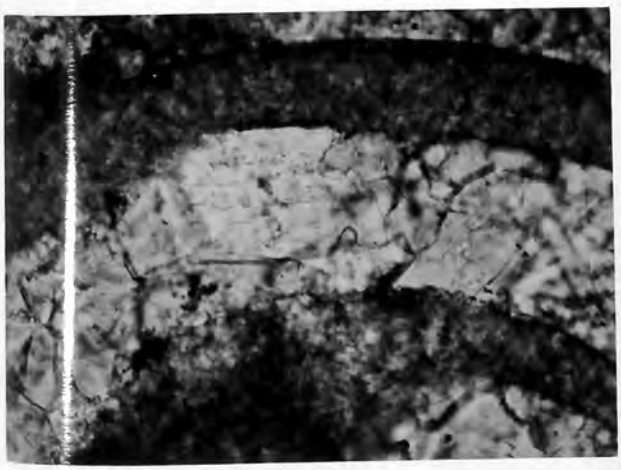

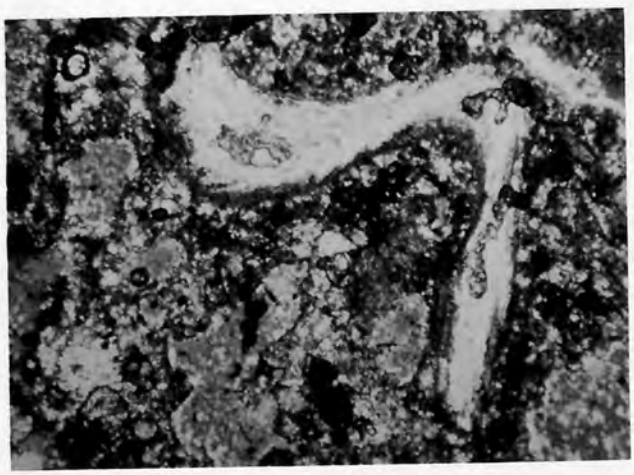

APPENDICES

(1-4)

APPENDIX 2a

List of Miocene Wells and Core Samples

ZU-3	2595'6, 2617'3, 2628'3, 2637', 2689'10, 2855', 2856'6, 2859'9
ZU-4	2584'4, 2585'3, 2586'11, 2599', 2620'6, 2625'6, 2627', 2630'6, 2636'5, 2648', 2657'9, 2661', 2679'6, 2691', 2698'5, 2699'7
ZZZ-2	C2B1, 2654', 2666', 2678', 2680', 2683'9, 2686'3
ZU-1	Thin sections only. Core not logged.
Duma-3	2390'6, 2393', 2403'6, 2406'5, 2410'6, 2415, 2418'5, 2433'7, 2436'7, 2439'4, 2448', 2451', 2456'6, 2457'6, 2472'4
Duma-2	2791'11, 2793'6, 2797', 2798'6, 2802'2, 2803', 2805', 2815', 2820'6, 2835', 2835'8
Duma-5	2403', 2414'6, 2421', 2428', 2438'5, 2438'6, 2440'6, 2465', 2473', 2475', 2496'3, 2526'5, 2529'
Duma-11	2307', 2320', 2334', 2345', 2348', 2349', 2352'6, 2359'6

Duma-9	2283'6, 2288'6, 2291', 2296'6, 2297', 2298'2, 2306'
Nurbani-4	C1T, 1675', 1737', 1755'6
Nurbani-5	1898', 1902'6, 1906', 1922', 1923'6, 1923'7
Nurbani-6	1754', 1755'6, 1755'10, 1759', 1759'11, 1782'
Nurbani-10	1756', 1786'6, 1809', 1835'

APPENDIX 2b

Localities of Miocene Outcrop Samples

A. Rajamandala Formation; Bandung Area

A ridge of the Rajamandala limestone crops out south of the Cianjur-Bandung and Padalarang-Bandung Roads. Gunung Hawu and Gunung Pabeasan are accessible from the Sukadara cement works on the main Bandung-Cianjur road. A gravel track winds to the summit of Gunung Hawu and from there one can walk to Gunung Pabeasan. The Citatah Quarry is located 5 km west of the Sukadara cement works on the same road. Tagog Apu is accessible from Cibogo Quarry, 7 km east of Citatah on the Bandung-Padalarang Road.

B. Rajamandala Formation; Sukabumi Area

The Nagrahu Quarry approximately 250 m. south of Cibatu village provides good exposures of the Rajamandala limestones of Gunung Karang. The unmetalled road to the quarry leads off the main Sukabumi-Pelabuhan Ratu road (where there is a sign reading PROYEK SEMEN POCOLAN, P.T. TENJOJAYA). Approximately 1 km. further along the main road and due east of the Nagrahu Quarry, the Karang Berlian and Bintang Quarries are found. Karang Berlian has outcrops of recrystallised limestone and Gunung Walat quartzite. A winding track leading off the main road immediately before the bridge over the Ciheulung river, runs through the Bintang cement works and into the hills. Batuasih Marls crop out in banks along the roadside.

Approximately 800 m. beyond the Karang Berlian Quarry on the

Cipatat-Pelabuhan Ratu road, turn off at the "Semen Cibinong" sign to find exposures of Gunung Walat quartzite.

C. Parigi Formation, Cibinong Quarry, West Java

The quarry is located 20 km ENE of Bogor and is found by taking the Cibinong exit off the Jakarta-Bogor toll road and driving east for 6 km. The exposures sampled are in the Narogong complex of the cement works. The quarry area is 800 hectares.

D. Sengkang Basin Limestones, South Sulawesi

Between Enrekang and Rantepao, outcrops sampled were exclusively roadside cuttings. Only one detour from the main Enrekang-Rantepao road was made, that being at Cake where a rough winding track runs eastwards to steep cliffs of limestone which are 1.5 km east of the main route.

At Tanrutedong the limestones were sampled along the banks of the Bila river where it runs through this sediment. Access to this area is difficult. The road between Barruka and Tanrutedong requiring a four-wheel drive vehicle. Exposures here are small, scattered and poor.

The reef mounds visited all lie eitherside of a rough unmetalled track which runs between T'chipi and the main Bone-Ujung Lomaru route. This too requires four-wheel drive. The Ujung Lomaru outcrop is found at a road cutting beside the bridge to the east of the village.

The Wattansoppeng-Ompo road runs through limestone outcrop and

many small exposures are easily accessible in roadside cuttings. Four kilometres south of Wattansoppeng, a track leads off to the left (eastwards) to quarry exposures which are found approximately 3 km along this road.

APPENDIX 3 : KEY TO LITHOLOGICAL SYMBOLS

LITHOLOGY & RECOVERY

- L Lime mustone
- W Wackestone
- P Packstone
- G Grainstone
- A Boundstone
- Fr Framestone
- Fl Floatstone
- R Rudstone
- C Claystone
- O Coal
- No recovery
- Rubbly recovery

SEDIMENTARY STRUCTURES

- flat lamination
- buckled lamination
- nodular bedding
- wavy bedding
- inclined bedding
- graded bedding
- deflected bedding
- parting
- mud lenticle
- bored surface / grain
- burrow
- birdseye or pseudobirdseye mottling
- bioturbation

FRACTURE PRESSURE SOLUTION & HYDROCARBON STAIN

- ° open fracture
- • filled fracture
- × partly open fracture
- microstylolite
- microstylolite swarm
- solution seam
- solution seam swarm
- heavy oil stain
- moderate
- light
- clean

LITHOLOGIGAL CONTACT

---- gradational

—— sharp

GRAIN SIZE

mud-silt

fine coase sand

gravel

ALLOCHEMS

coral branched massive

coral foliose

mollusc

benthic foram

planktic foram

alga

intraclast

indeterminate

wood fragment

rhodolith

echinoid grain

MISCELLANEOUS

cone-in-cone

g glauconite

q quartz

t undifferentiated impurities